National Aeronautics and Space Administration

README Document for

Microwave Limb Sounder (MLS) Level-2 Version 2.2 & Version 1.5 Diagnostic Products:

ML2DGG: Geophysical Parameter Grid
ML2DGM: Miscellaneous Grid

Prepared by Young-In Won, GES DISC
Last revised, August 27, 2008

Revision History

Revision Date	***Changes***	***Author***
7/24/2008	Initial version	Young-In Won
08/04/2008	Revised to combine version 1.5 & 2.2	Young-In Won
08/12/2008	Revised to add MLS2DGM	Young-In Won
08/22/2008	Revised to modify the introductory part	Young-In Won
08/27/2008	Revised according to tester's recommendation	Young-In Won
07/21/2009	Removed reference to retired WHOM search engine	Randy Barth

Table of Contents

Revision History *2*

Table of Contents *3*

1. Introduction *4*

1.1 Brief background **4**

1.2 Instrument Description **4**

1.3 Brief background on algorithm **5**

2. Data Organization *6*

2.1 File naming convention **6**

2.2 File Format **6**

3. Data Contents *7*

4. Options for Reading Data *8*

4.1 Command line tools **8**

h5dump **8**

4.2 GUI tools **8**

4.3 Read software in C, Fortran and IDL **8**

5. Data Services and Interpretation *9*

5.1 Aura MLS File Service **9**

5.2 Interpretation and Screening **9**

6. More Information *10*

6.1 Web resources for Aura MLS data users: **10**

6.2 Point of Contact **10**

7. Acronyms *11*

1. Introduction

1.1 Brief background

This document applies to the Aura Microwave Limb Sounder (MLS) Level-2 Diagnostic products.

Use of MLS diagnostic data requires detailed knowledge of the instrument and its inner workings. Users need to consult with relevant members of the MLS Science Team (http://mls.jpl.nasa.gov/data/overview.php) and also encouraged to download copy of Data Quality Documentation (http://mls.jpl.nasa.gov/data/v2-2_data_quality_document.pdf) and Supplement to Version 1.5 Level 2 Data Quality Document (http://mls.jpl.nasa.gov/data/v1-5-supplement-29jul05b.pdf, which is appended to this README. Please check for the latest version) before using the data.

The separate README file for Level 2 standard atmospheric products has detailed information on Level 2 data in general.

Version 2.2 data of Aura MLS are available from begin of mission (August 2004) to current. Previous version 1.5 data, which span the time period from Aug. 8 2004 to Feb. 28, 2007, are still available.

Table 1. Basic characteristics of the MLS L2GP data.

Latitude extent	-82° to 82°N
Longitude extent	-180° to 180°E
Horizontal resolution	varies with parameters
Temporal resolution	1 file per day

1.2 Instrument Description

The Earth Observing System (EOS) Microwave Limb Sounder (MLS) is one of four instruments on the NASA's EOS Aura satellite, launched on July 15th 2004. Aura is in a near-polar 705 km altitude orbit. As Earth rotates underneath it, the Aura orbit stays fixed relative to the sun; to give daily global coverage with ~14 orbits per day. Aura is part of NASA's A-Train group of Earth observing satellites. These satellites fly in formation with the different satellites making measurements within a short time of each other.
The Aura MLS measures thermal emission from broad spectral bands centered near 118, 190, 240 and 640 GHz, and 2.3 THz Emission are measured continuously (24 hours per day) by 7 microwave receivers (2 each at 118 and 2250 GHz) using a limb viewing geometry which maximizes signal intensities and vertical resolution. MLS is

radiometrically calibrated after each 25 second limb scan. Design lifetime is 5 years of continuous operation.

MLS makes measurements of atmospheric composition, temperature, humidity and cloud ice that are needed to (1) track stability of the stratospheric ozone layer, (2) help improve predictions of climate change and variability, and (3) help improve understanding of global air quality. MLS observes thermal microwave emission from Earth's 'limb' (the edge of the atmosphere edge) viewing forward along the Aura spacecraft flight direction, scanning its view from the ground to ~90 km every ~25 seconds.

1.3 Brief background on algorithm

The user is encouraged to read the following documents for details on algorithms.

- **An Overview of the EOS MLS Experiment**
  http://mls.jpl.nasa.gov/data/eos_overview_atbd.pdf
- **EOS MLS Retrieval Process Algorithm Theoretical Basis**
  http://mls.jpl.nasa.gov/data/eos_algorithm_atbd.pdf
- **Precision Estimates for the Geophysical Parameters**
  http://mls.jpl.nasa.gov/data/eos_precision_atbd.pdf

2. Data Organization

2.1 File naming convention

The Level-2 Diagnostics products are named in accordance to the following convention:

MLS-Aura_L2<*product1*>-<*product2*>_V02-2*_cxx_<*yyyy*>d<*ddd*>.<*format*>

For example:
MLS-Aura_L2GP-DGG_v02-23-c01_2008d182.he5
MLS-Aura_L2AUX-DGM_v02-23-c01_2008d152.h5

Where:

- **Product1** = GP : Geophysical Parameter Grid
  AUX: Miscellaneous Grid
- **Product2** = DGG : Geophysical Parameter Grid
  DGM : Miscellaneous Grid
  Cloud : Miscellaneous Grid specific to cloud
- **V02-2* =** algorithm version identifier, made up of major version, minor version (V01-5* for version 1.5)
- **cxx =** file cycle number
- **yyyy** = four digit calendar year
- **ddd** = day number in the year (001=January 1)
- **format** = he5 (HDF-EOS5) for DGG
  h5 (HDF5) for DGM (including Cloud)

The MLS diagnostic products are stored as individual swaths and as with the standard products, these swaths also contain Status and Quality information, but no column abundances are produced for these products.

2.2 File Format

Aura MLS Level-2 Geophysical Parameter Grid products (ML2DGG) are stored in the Hierarchical Data Format-Earth Observing System (HDF-EOS5) Swath format, while Level-2 Miscellaneous Grid products (ML2DGM) are stored in HDF5. HDF-EOS5 format is an extension of the HDF5 format (developed by NCSA) to meet the needs of EOS data products.

3. Data Contents

Details on the parameters contained within Aura MLS Level-2 Diagnostic parameters are found on the "Supplement to Version 1.5 Level 2 Data Quality Document" (http://mls.jpl.nasa.gov/data/v1-5-supplement-29jul05b.pdf, which is appended to this README) and from "An Overview of the EOS MLS Experiment" (http://mls.jpl.nasa.gov/data/eos_overview_atbd.pdf)

The bulk of geophysical diagnostic products are similar to the standard products, in that they represent vertical profiles of retrieved species abundances. However, the information on these diagnostic products has typically been obtained from a different spectral region than that used for the standard products. Further information should be directed to the MLS science team (http://mls.jpl.nasa.gov/data/overview.php). No documentation for diagnostic products of version 2.2 is available yet.

Table 2. Level 2 Diagnostic Data Products
(from An Overview of the EOS MLS Experiment)

product	summary description	daily volume /Megabytes
ML2DGG L2GP-DGG	'geophysical diagnostic quantities': various diagnostics pertaining directly to the MLS geophysical data products, and generally on a grid similar (or idential) to that of the geophysical data products. See Table 8-7 for a summary description of the contents.	~300
ML2DGM L2AUX-DGM	'minor frame diagnostic quantities': various diagnostics that are on a minor frame grid. These include such items as tangent pressure, 'chi-square' describing various fits to the measured radiances, number of radiances used in various retrieval phases, etc.	~800
ML2DGM L2AUX-cloud	Values for 'cloud-induced radiances' inferred for selected spectral channels. These are differences from the estimated clear-sky radiances.	~100

4. Options for Reading Data

The HDF Group provides various utilities for viewing the contents of HDF files and extracting the raster, binary, or ASCII objects (see http://hdf.ncsa.uiuc.edu/products/index.html)

4.1 Command line tools

h5dump

The **h5dump** enables the user to examine the contents of an HDF5 file and dump those contents, in human readable form, to an ASCII file or binary.

```
h5dump options filename
```

```
Options/Arguments:
-h  or  --help          Print a usage message and exit.
-B  or  --bootblock     Print the content of the boot block.
                        (This option is not yet implemented.)
-H  or  --header        Print the header only; no data is displayed.
-A                      Print the header and value of attributes;
-i  or  --object-ids    Print the object ids.
-r  or  --string        Print 1-bytes integer datasets as ASCII.
 -V  or  --version      Print version number and exit.
```

The following website (http://hdf.ncsa.uiuc.edu/HDF5/doc/RM/Tools.html#Tools-Dump) provides more detailed information.

H5ls also lists contents of HDf5 file.

4.2 GUI tools

The HDFView (http://hdf.ncsa.uiuc.edu/hdf-java-html/hdfview/) is a visual tool for browsing and editing NCSA HDF4 and HDF5 files and is available for various platforms (Windows 98/NT/2000/XP, Solaris, Linux, AIX, Irix 6.5, MacOSX).

Users, especially **those who are not familiar with Unix/Linux environment** are strongly encouraged to use **HDFView** for a quick access to data contents.
There is also an optional plug-in for handling HDF-EOS data files, which you can download from: http://opensource.gsfc.nasa.gov/projects/hdf/hdf.php

4.3 Read software in C, Fortran and IDL

Aura MLS science team provides number of reader software and format converters written in C, IDL, and FORTRAN programming language. You can download them from GES DISC web site: http://disc.sci.gsfc.nasa.gov/Aura/tools.shtml.

5. Data Services and Interpretation

5.1 Aura MLS File Service

GES DISC has a search engine called Mirador (http://mirador.gsfc.nasa.gov) that allows users to limit the number of files for download by specifying appropriate temporal and spatial constraints. The total download size can be further reduced by choosing a spatial subsetting within Mirador.

For data access and related services, check the following web site.
http://disc.sci.gsfc.nasa.gov/Aura/data_access.shtml

5.2 Interpretation and Screening

Detailed information on data quality can be found in EOS MLS Supplement to version 1.5 Level 2 data quality and description document (**http://mls.jpl.nasa.gov/data/v1-5-supplement-29jul05b.pdf**).

6. More Information

6.1 Web resources for Aura MLS data users:

NASA/JPL:

- MLS Main Page: http://mls.jpl.nasa.gov/
- MLS Data Documentation: http://mls.jpl.nasa.gov/data/datadocs.php
- Data Validation : http://mls.jpl.nasa.gov/data/validation.php

NASA/GSFC:

- MLS Data Support Main Page: http://disc.gsfc.nasa.gov/Aura/
- MLS Products & Data Access: http://disc.gsfc.nasa.gov/Aura/MLS/
- MLS Documentation: http://disc.gsfc.nasa.gov/Aura/documentation/
- Data can also be obtained from Giovanni (online visualization and analysis tool): http://gdata1.sci.gsfc.nasa.gov/daac-bin/G3/gui.cgi?instance_id=mls
- MLS FAQ (from Giovanni): http://disc.sci.gsfc.nasa.gov/techlab/giovanni/G3_manual_Chapter_11_MLS.shtml

6.2 Point of Contact

URL	http://disc.gsfc.nasa.gov/	
Contact	Name	GES DISC HELP DESK SUPPORT GROUP
	Email	help-disc@listserv.gsfc.nasa.gov
	Phone	301-614-5224
	Fax	301-614-5268
	Address	Goddard Earth Sciences Data and Information Services Center, Code 610.2 NASA Goddard Space Flight Center, Greenbelt, MD, 20771, USA

7. Acronyms

DAAC Distributed Active Archive Center
DISC Data and Information Services Center
ECMWF European Centre for Medium Range Weather Forecasts (UK)
ECS EOSDIS Core System
EDOS Earth Observing System Data and Operations System
EOS Earth Observing System
EOSDIS Earth Observing System Data and Information System
ESDT Earth Science Data Type
EU Engineering Unit
FOV Field of View
GES Goddard Earth Sciences
GES DISC Goddard Earth Sciences Data and Information Services Center
GSFC Goddard Space Flight Center
HDF Hierarchical Data Format
HDF5 Hierarchical Data Format Version 5.X
HDF-EOS Hierarchical Data Format for the EOS mission
HIRDLS High Resolution Dynamics Limb Sounder
L1A Level 1A Data
L1B Level 1B Data
L2 Level 2 Data
L3 Level 3 Data
LGID Local Granule Identification
Limb sounding A horizon-looking observation technique that uses a distant objects sun, start, or a sensor on another satellite in a different Earth orbit
MCF Metadata Configuration File
MLS Microwave Limb Sounder
MW Microwave
NASA National Aeronautics and Space Administration
OMI Ozone Monitoring Instrument
TES Tropospheric Emission Spectrometer
NCEP National Centers for Environmental Prediction
NESDIS National Environmental Satellite, Data and Information Service
NOAA National Oceanic and Atmospheric Administration
PGE Product Generation Executive
PGS Product Generation System
PREPQC NCEP quality controlled final observation data
QA Quality Assessment
RTA Radiative Transfer Algorithm
SPS Science Processing System
URL Universal Reference Link
VIS Visible
WMO World Meteorological Organization

JPL D-32382

Earth Observing System (EOS)

Microwave Limb Sounder (MLS)

Supplement to version 1.5 Level 2 data quality and description document.

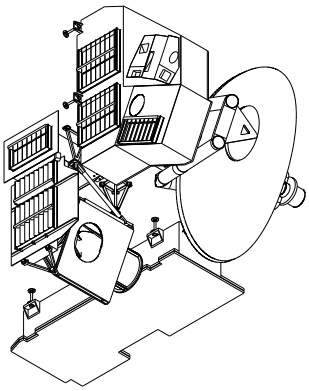

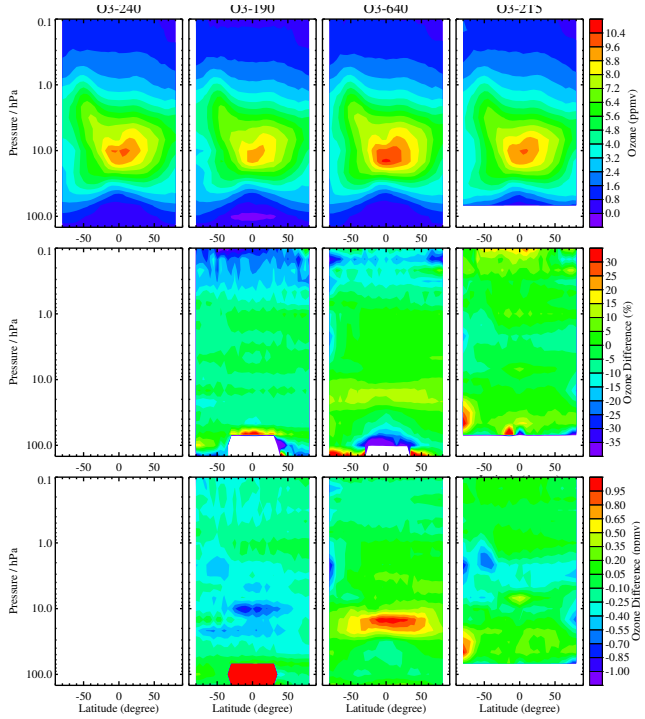

Nathaniel J. Livesey, William G. Read, Mark J. Filipiak, Lucien Froidevaux, Robert S. Harwood, Jonathan H. Jiang, Carlos Jimenez, Herbert M. Pickett, Hugh C. Pumphrey, Michelle L. Santee, Michael J. Schwartz, Joe W. Waters, and Dong L. Wu

Version 1.51
July 29, 2005

Jet Propulsion Laboratory
California Institute of Technology
Pasadena, California, 91109-8099

Contents

A Results for 'diagnostic' products **1**
A.1 Introduction . . . 1
A.2 190 GHz methyl cyanide . . . 3
A.3 190 GHz chlorine monoxide . . . 7
A.4 190 GHz nitric acid . . . 11
A.5 240 GHz nitric acid . . . 15
A.6 640 GHz nitric acid . . . 19
A.7 Diagnostic cloud products . . . 23
A.8 190 GHz nitrous oxide . . . 27
A.9 Ozone diagnostic products . . . 31
A.10 Temperature from various retrieval phases . . . 49

Acknowledgment

This research was carried out at the Jet Propulsion Laboratory, California Institute of Technology, under a contract with the National Aeronautics and Space Administration.

Appendix A
Results for ‘diagnostic’ products

A.1 Introduction

In this appendix, we detail the quality of selected ‘diagnostic products’ from v1.5 in a similar manner to the discussion of the ‘standard products’ in chapter 3.

The MLS diagnostic products are stored as individual swaths (named, e.g., `O3-190`) in the L2GP *Diagnostic products Geophysical Grid* (DGG) file named as described in section 1.3, with the letters `DGG` used for `<product>`. As with the standard products, these swaths also contain `Status` and `Quality` information. However, no column abundances are produced for these products. Further diagnostics in the DGG and other files are beyond the scope of this document.

A.2 190 GHz methyl cyanide

Swath name: `CH3CN-190`

Contact: Nathaniel Livesey, **Email:** `<livesey@mls.jpl.nasa.gov>`

As with the standard CH_3CN product, the 640 GHz product is not appropriate for scientific use. This is mainly due to the persistent large negative bias in the data.

Simulations

The simulation studies summarized in Figures A.1 and A.2 indicate that biases of as high as 100 pptv on average (∼200%) are to be expected in this product in the lower stratosphere. Biases of order 100% are expected in the upper stratosphere.

Vertical resolution

The averaging kernels shown in Figure A.3 indicate that the 640 GHz CH_3CN product has a vertical resolution of 6 km in the lower stratosphere, worsening to 10 km in the upper stratosphere.

Early results

640 GHz MLS observations show very unrealistic values of CH_3CN (when compared to expectations). Average abundances of as high as 330 pptv are seen in the lowermost stratosphere (where 10 – 30 pptv are generally expected). Persistent average values of −30 to −20 pptv are seen in the upper stratosphere.

Data screening

Do not use: The v1.5 640 GHz CH_3CN data should not be used in scientific studies.

Artifacts

As discussed above, the 640 GHz CH_3CN product displays significant biases that preclude its use in scientific studies.

Priorities for future versions

Improvements to radiance fits and other products in the 640 GHz spectral region should lead to improvements in the CH_3CN product from this radiometer. However, its improvement is not in itself a priority concern for the immediate future.

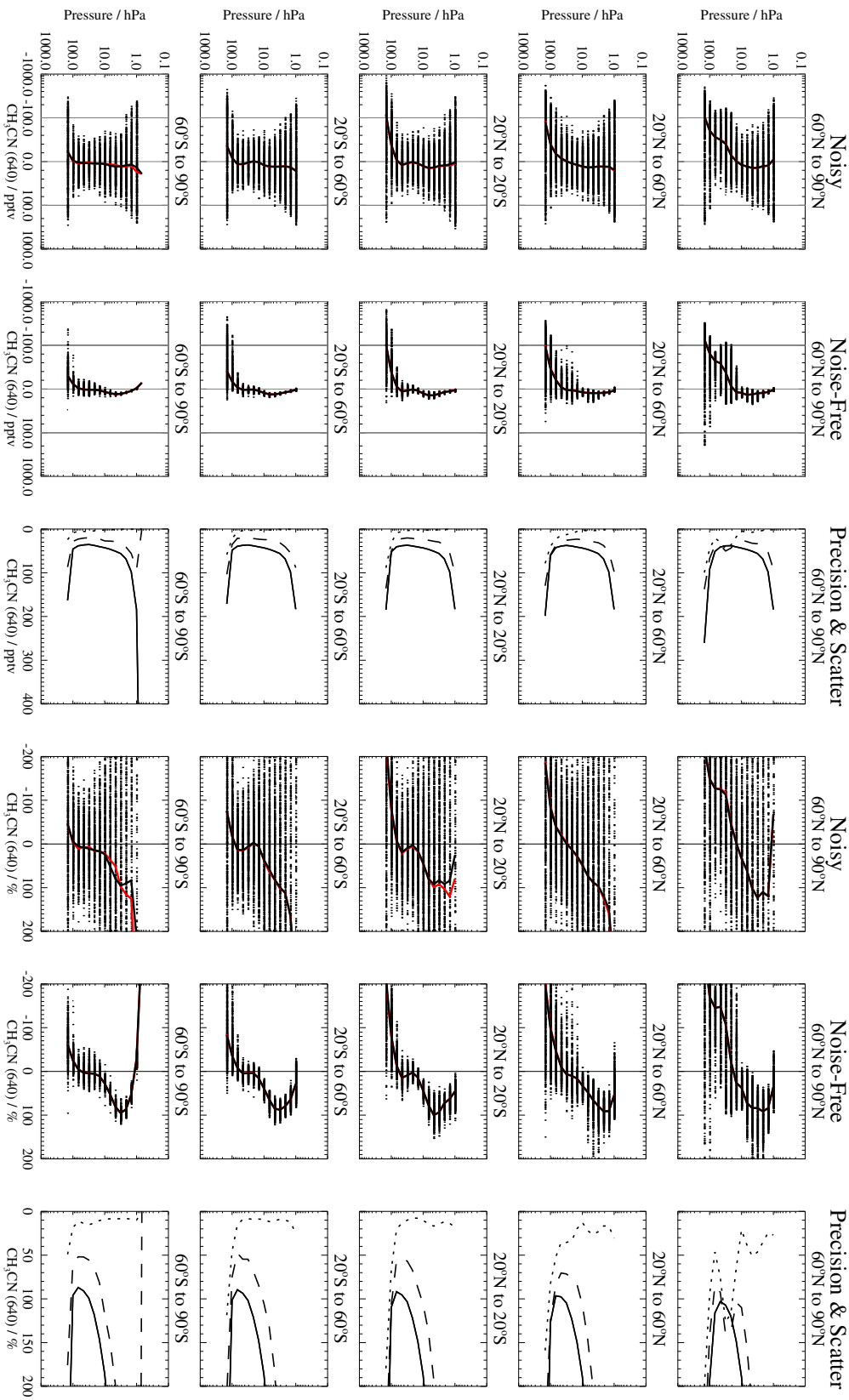

Figure A.1: A summary of the v1.5 data quality for 640 GHz CH_3CN for the `1996d051` test data set. Each row of panels represents a broad latitude bin. The first two columns columns show the differences between the retrieved 640 GHz CH_3CN and the true CH_3CN as a function of pressure, for the noisy and noise free case, along with a solid line which shows the median bias. The median bias of the `Status=0` profiles (i.e., those not significantly affected by clouds) is shown in red. The third column shows the mean estimated precision of 640 GHz CH_3CN (solid line), and the rms scatter about the mean bias in the noisy (broken line) and noise free (dotted line) cases. The remaining three columns show the same information as in the first three columns in the form of a percentage of the true values.

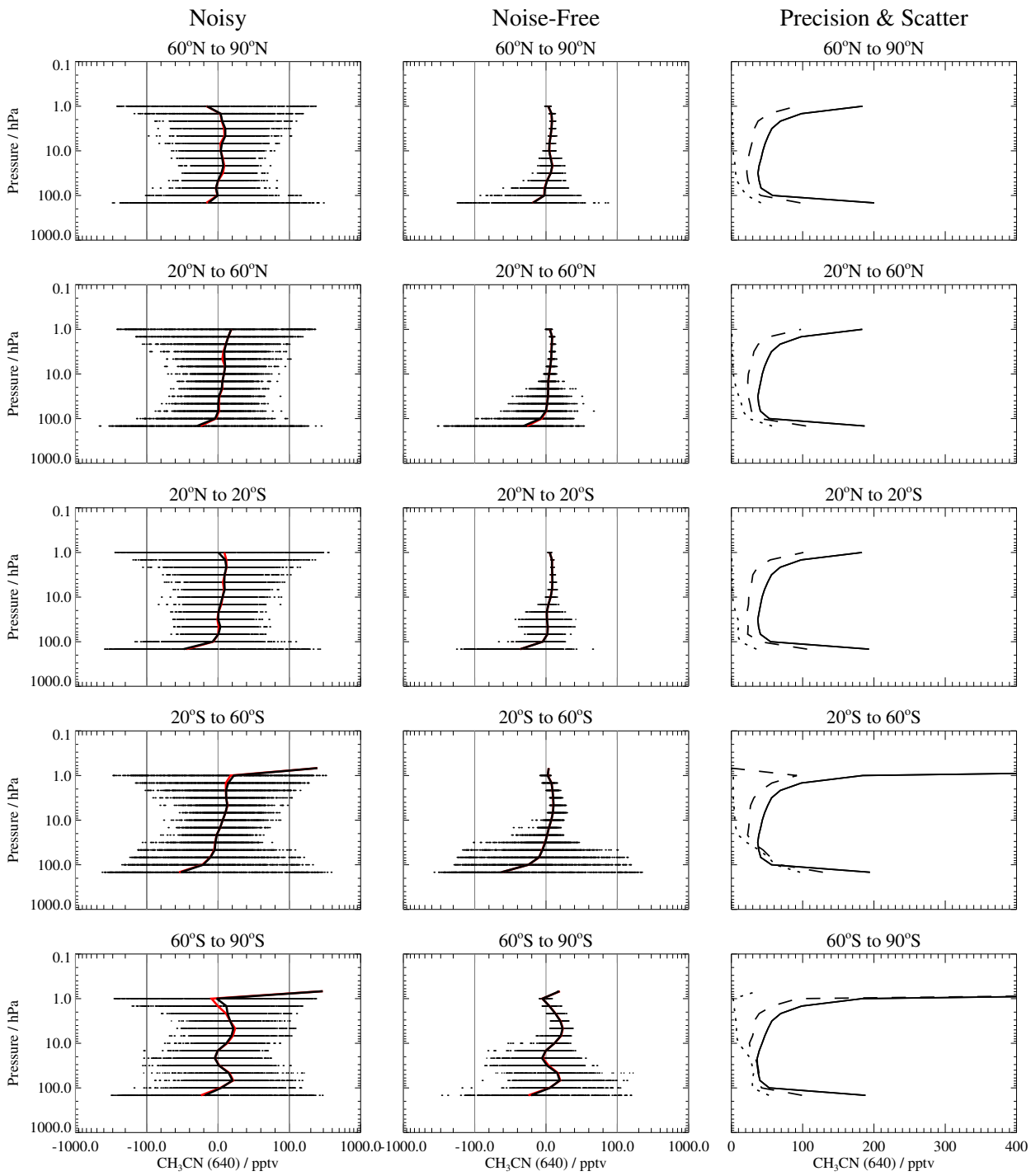

Figure A.2: A summary of the v1.5 data quality for 640 GHz CH_3CN, as for figure A.1 but for the `2000d276` test data set. The percentage plots are omitted here as the 'true' values are zero.

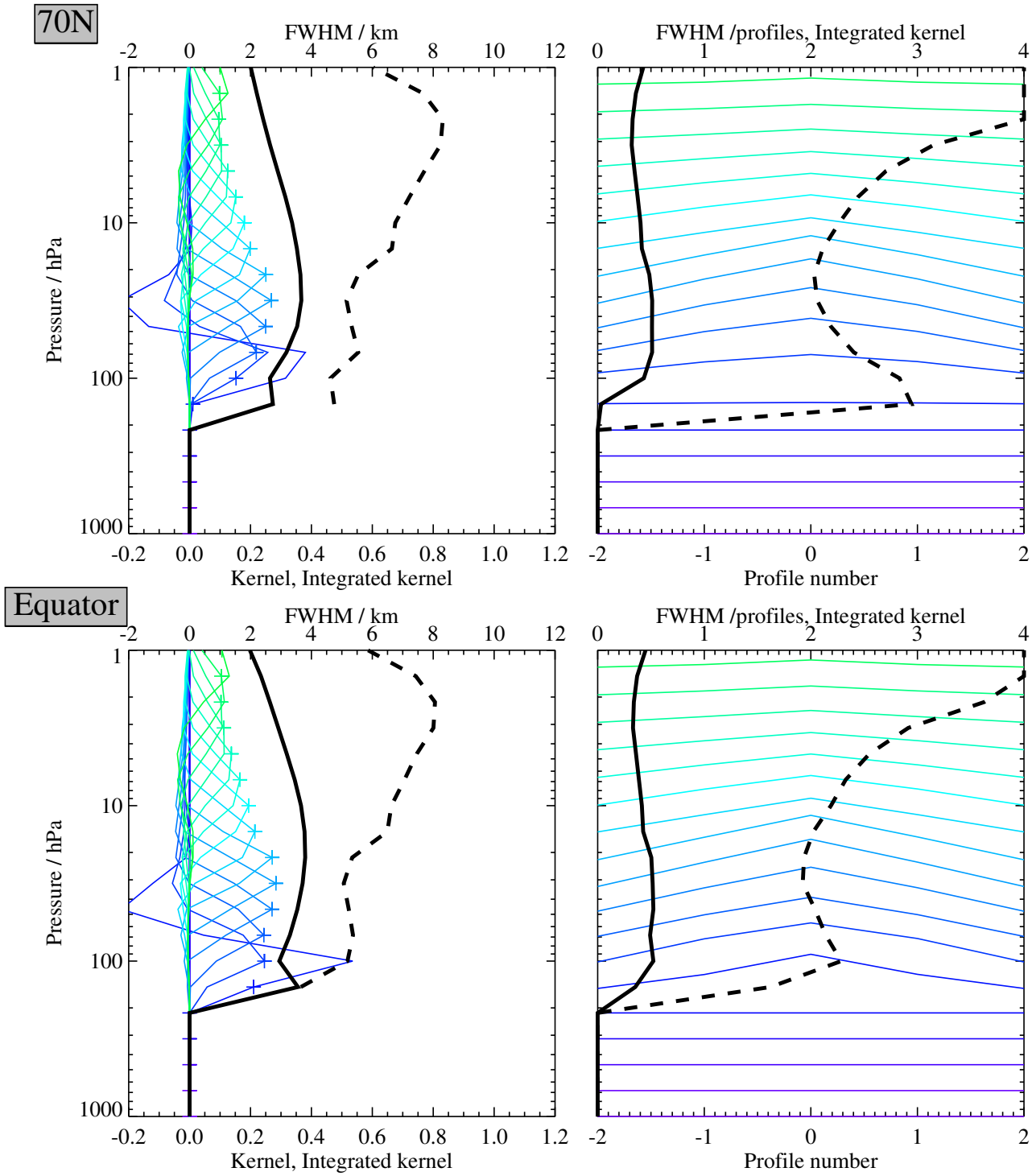

Figure A.3: The left hand plots show the vertical averaging kernel for 640 GHz CH_3CN for the `1996d051` test data set. The colored lines denote the averaging kernels for individual retrieved surfaces (denoted with the matching color + symbols). The thick solid black line shows the integrated area under each colored line. The thick dashed black line denotes the vertical resolution (full width at half maximum) approximately scaled into kilometers. The right hand plots show the horizontal averaging kernels in a similar manner, where the profiles are spaced at 1.5° great circle angle (approximately 165 km).

A.3 190 GHz chlorine monoxide

Swath name: `ClO-190`

Useful range: 100 – 1 hPa

Vertical resolution: 4 to 7 km

Contact: Michelle Santee, **Email:** `<mls@mls.jpl.nasa.gov>`

Although there are no serious issues with the `ClO-190` data, the standard product for ClO is taken from the Core+R4 (640 GHz) retrieval because of its better spatial (horizontal and vertical) resolution and precision.

Simulations

ClO is strongly diurnal in the lower stratosphere; day-night differences can be used to reduce systematic effects in the measurements from 100 to 10 hPa. Simulations (see Figures A.4 and A.5) show residual average biases in these differences (indicating systematic errors that cannot be eliminated by taking day-night differences) as large as 0.1 ppbv in the winter polar regions. Elsewhere, residual average biases are less than 0.04 ppbv (often considerably so).

Vertical resolution

Based on Figure A.6, the `ClO-190` vertical resolution varies with altitude, from ∼4 km at 100 hPa to more than 7 km near the top of the profile.

Early results and validation

The estimated single-profile precision reported by the Level 2 software is ∼0.2 – 0.3 ppbv over most of the vertical range, degrading to 0.7 ppbv at 1 hPa. The observed scatter in the data, evaluated in a 20°-wide latitude band centered around the equator where natural variability is expected to be small in the lower stratosphere, suggests a measurement precision of 0.15 – 0.3 ppbv throughout the profile. Thus the precision of the `ClO-190` data is slightly worse than that of the standard ClO product. Time series of daytime, nighttime, and day-night difference values from almost nine months of version 1.5 data have been examined in 5°-wide equivalent latitude bands between 87.5°S and 87.5°N on the 660, 580, 520, 460, and 410 K potential temperature surfaces (corresponding to pressure levels of 22, 32, 46, 68, and 100 hPa, respectively). Based on this analysis, persistent systematic biases are largely absent in the `ClO-190` data; however, taking day-night differences in the lower stratosphere effectively eliminates the small (∼0.1 – 0.2 ppbv) biases that are present at some latitudes and seasons.

Artifacts

There are no known significant artifacts in the `ClO-190` data.

Priorities for future data version(s)

None in particular.

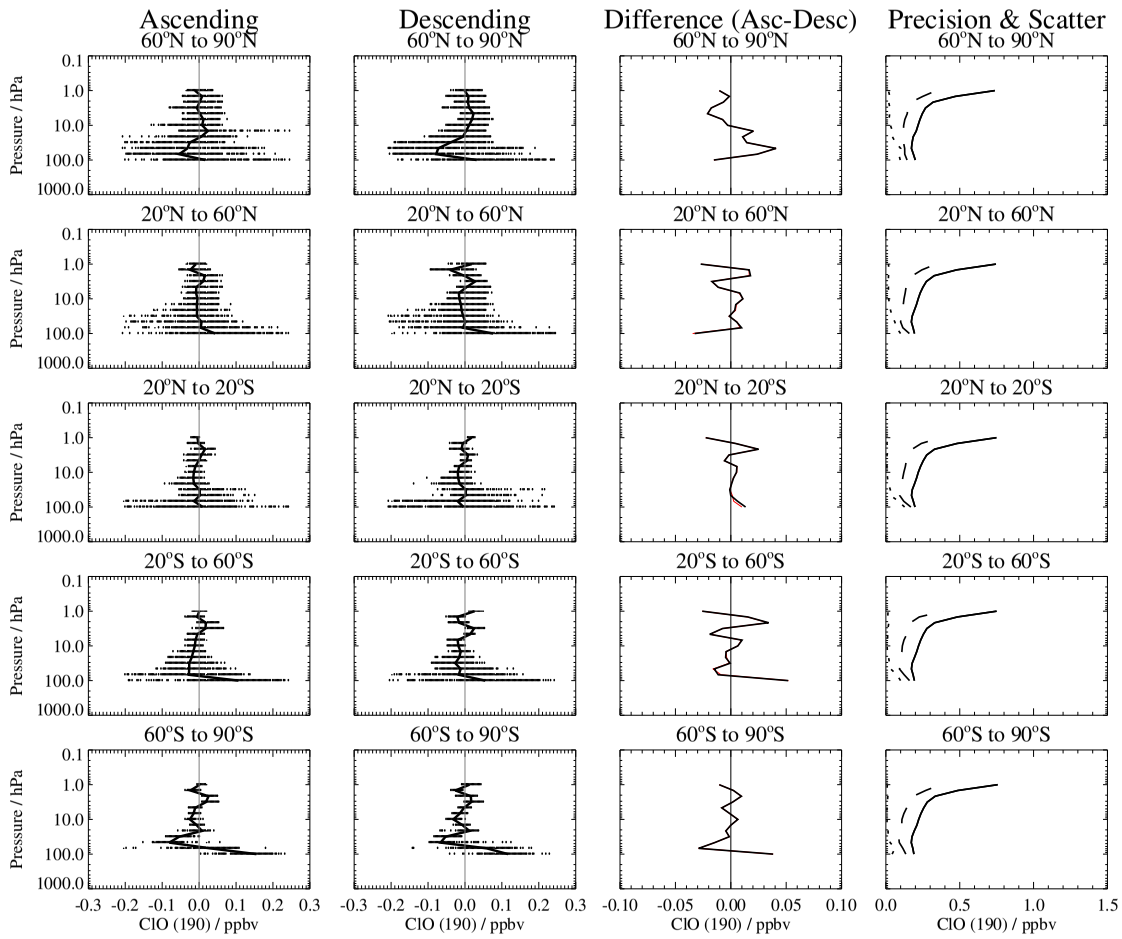

Figure A.4: A summary of the v1.5 data quality for 190 GHz ClO for the `1996d051` test data set. Each row of panels represents a broad latitude bin. The first two columns columns show, for the noise free case, the differences between the retrieved 190 GHz ClO and the true ClO as a function of pressure for the ascending and descending phases of the Aura orbit (corresponding to day and night observations respectively). Also shown is a solid line which indicates the median bias. The median bias of the `Status=0` profiles (i.e., those not significantly affected by clouds) is shown in red. The third column shows the difference in the median biases (solid lines in previous columns) between the ascending and descending side. The fourth column shows the mean estimated precision of 190 GHz ClO (solid line), and the rms scatter about the mean bias in the noisy (broken line) and noise free (dotted line) cases.

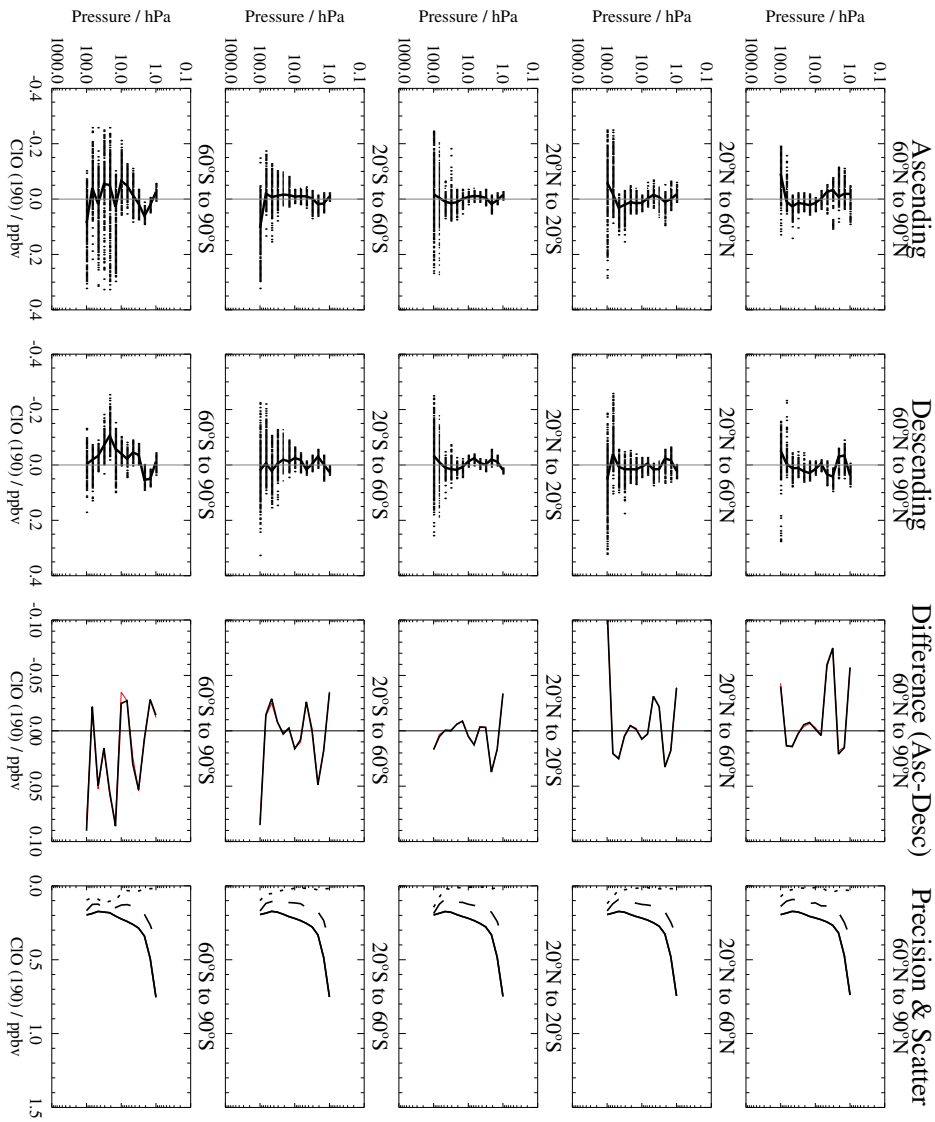

Figure A.5: A summary of the v1.5 data quality for 190 GHz ClO, as for figure A.4 but for the `2000d276` test data set.

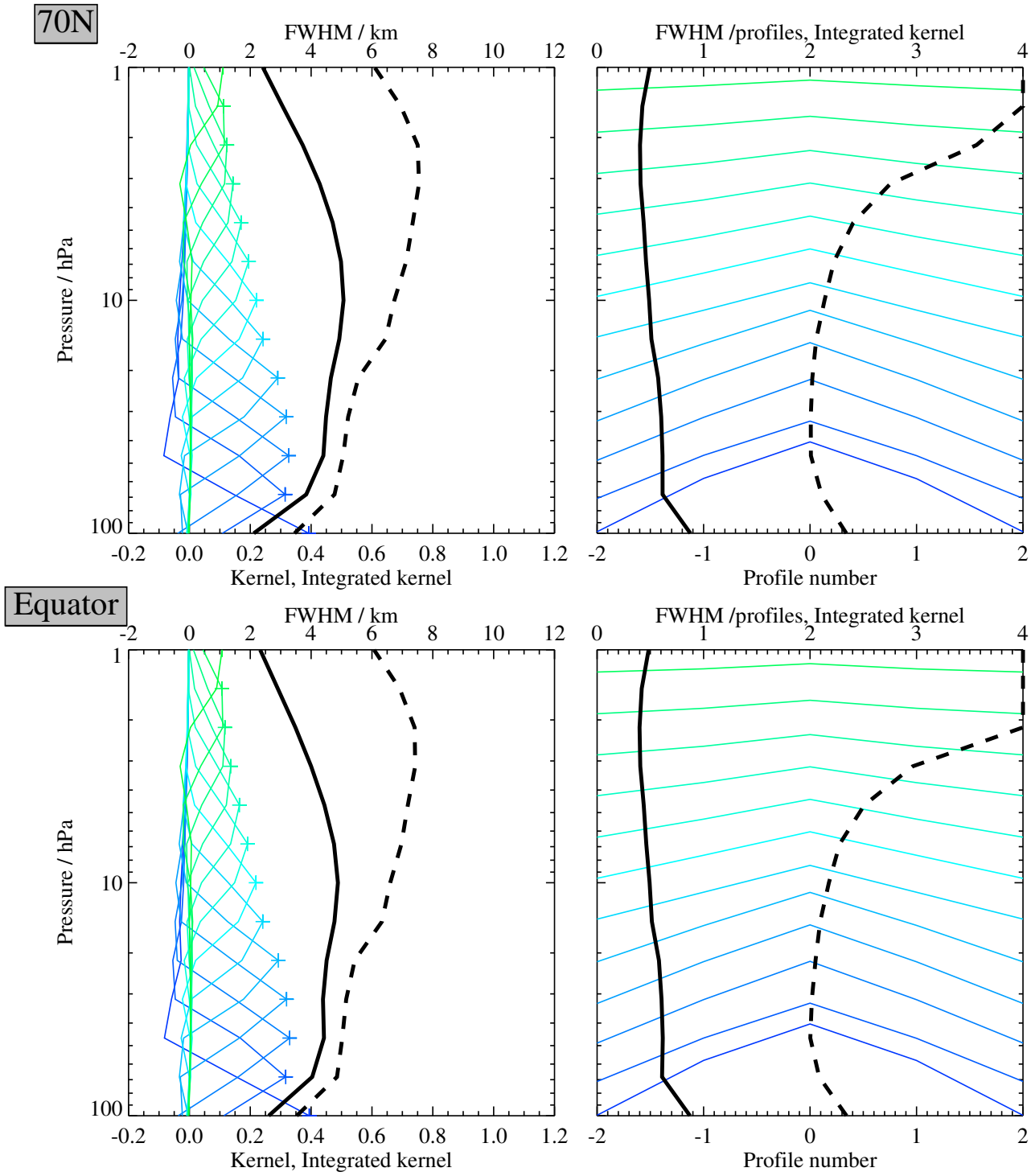

Figure A.6: The left hand plots show the vertical averaging kernel for 190 GHz ClO for the `1996d051` test data set. The colored lines denote the averaging kernels for individual retrieved surfaces (denoted with the matching color + symbols). The thick solid black line shows the integrated area under each colored line. The thick dashed black line denotes the vertical resolution (full width at half maximum) approximately scaled into kilometers. The right hand plots show the horizontal averaging kernels in a similar manner, where the profiles are spaced at 1.5° great circle angle (approximately 165 km).

A.4 190 GHz nitric acid

Swath name: `HNO3-190`

Useful range: 10 – 3.2 hPa

Vertical resolution: 4.0 to 4.5 km

Contact: Michelle Santee, **Email:** `<mls@mls.jpl.nasa.gov>`

The standard product for version 1.5 HNO_3 is taken from the Core+R2 (190 GHz) retrieval at and above 6.8 hPa; the `HNO3-190` retrievals are not recommended for use below 10 hPa because of their strongly oscillatory nature in the lower stratosphere.

Simulations

Simulations (see Figures A.7 and A.8) indicate that the `HNO3-190` retrievals exhibit strong vertical oscillations in the lower stratosphere in some latitude bands. Above 10 hPa, oscillations are much less pronounced and average biases are small (typically <0.2 ppbv).

Vertical resolution

Based on Figure A.9, the `HNO3-190` vertical resolution is ∼4 – 4.5 km from 10 – 3.2 hPa.

Early results and validation

The estimated single-profile precision reported by the Level 2 software is ∼1.5 ppbv over the range 10 – 3.2 hPa. The observed scatter in the data, evaluated in a 20°-wide latitude band centered around the equator where natural variability is expected to be small in the lower stratosphere, suggests a measurement precision of ∼1.0 ppbv over this range.

Artifacts

Oscillations: The `HNO3-190` profiles are strongly oscillatory below ∼10 hPa.

Priorities for future data version(s)

- Reduce oscillations in the `HNO3-190` profiles.

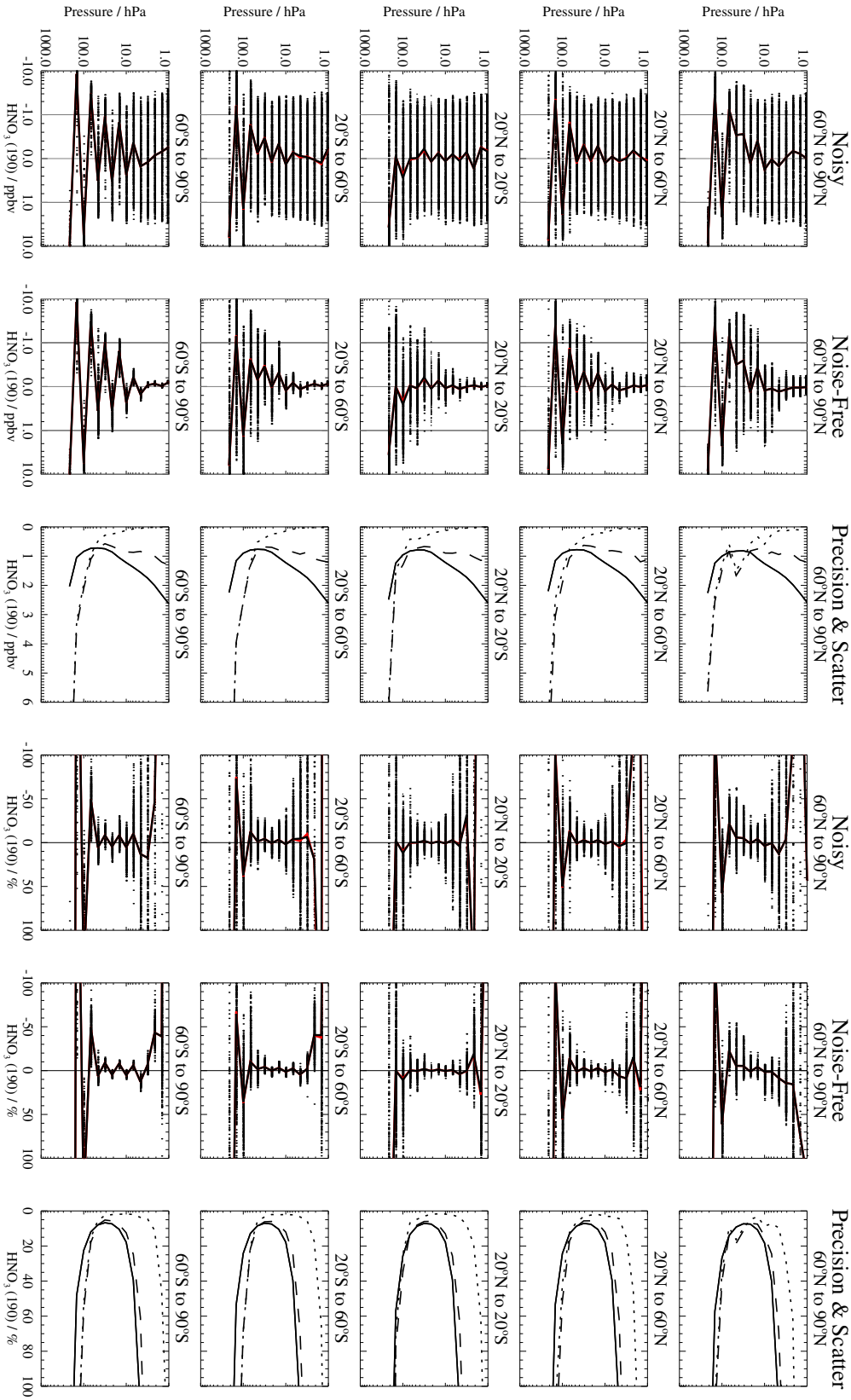

Figure A.7: A summary of the v1.5 data quality for 190 GHz HNO_3 for the `1996d051` test data set. Each row of panels represents a broad latitude bin. The first two columns columns show the differences between the retrieved 190 GHz HNO_3 and the true HNO_3 as a function of pressure, for the noisy and noise free case, along with a solid line which shows the median bias. The median bias of the `Status=0` profiles (i.e., those not significantly affected by clouds) is shown in red. The third column shows the mean estimated precision of 190 GHz HNO_3 (solid line), and the rms scatter about the mean bias in the noisy (broken line) and noise free (dotted line) cases. The remaining three columns show the same information as in the first three columns in the form of a percentage of the true values.

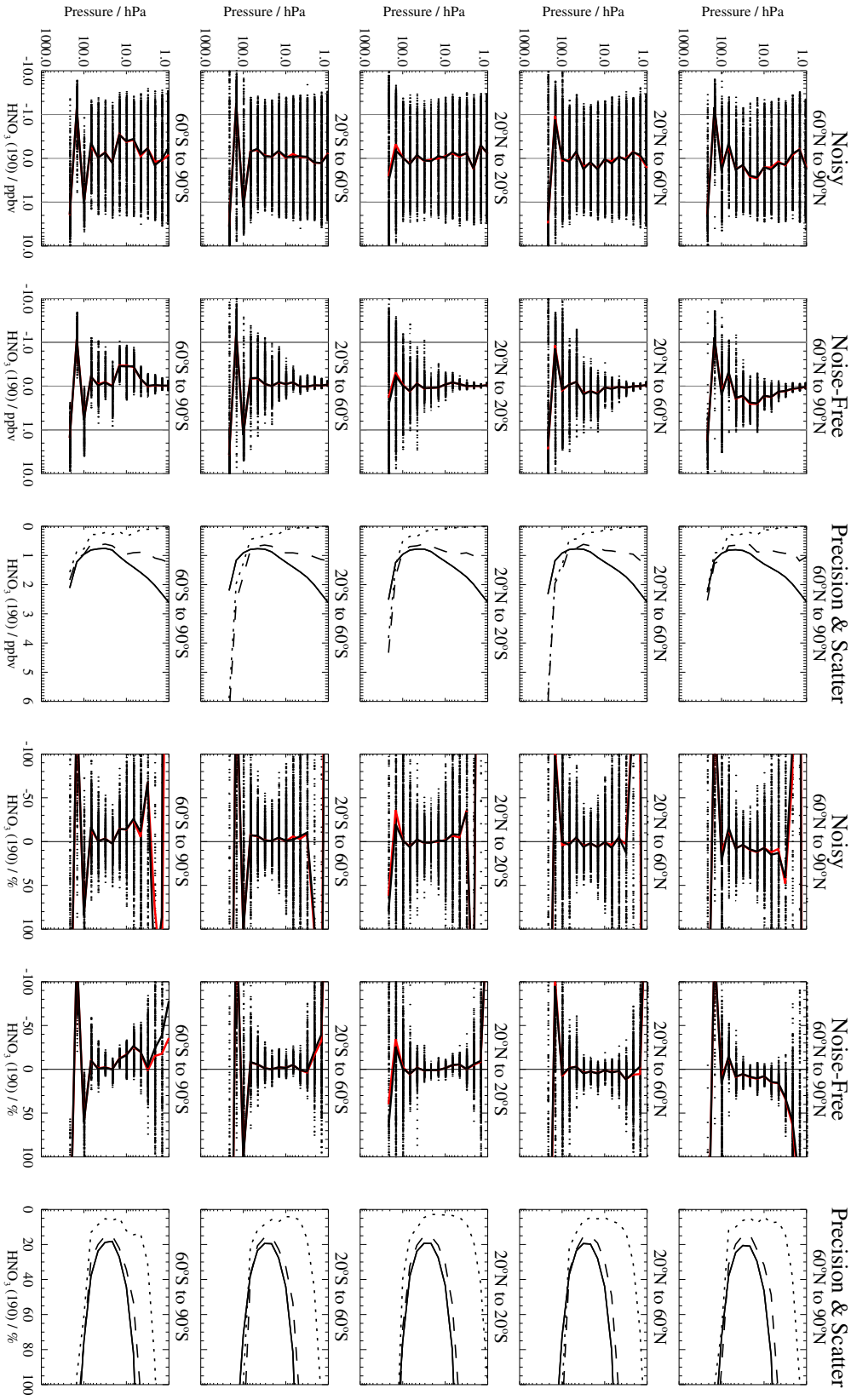

Figure A.8: A summary of the v1.5 data quality for 190 GHz HNO_3, as for figure A.7 but for the `2000d276` test data set.

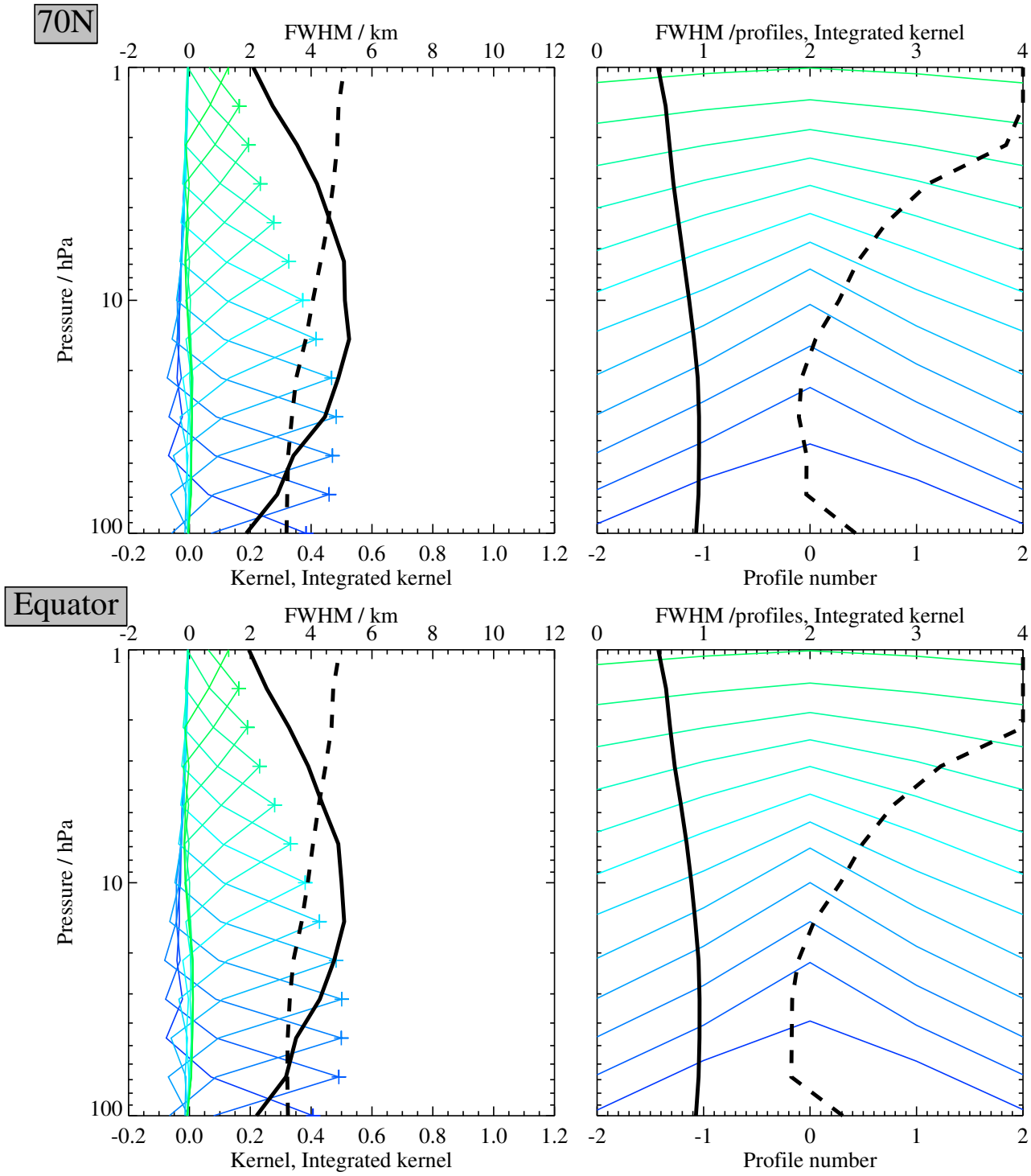

Figure A.9: The left hand plots show the vertical averaging kernel for 190 GHz HNO_3 for the `1996d051` test data set. The colored lines denote the averaging kernels for individual retrieved surfaces (denoted with the matching color + symbols). The thick solid black line shows the integrated area under each colored line. The thick dashed black line denotes the vertical resolution (full width at half maximum) approximately scaled into kilometers. The right hand plots show the horizontal averaging kernels in a similar manner, where the profiles are spaced at 1.5° great circle angle (approximately 165 km).

A.5 240 GHz nitric acid

Swath name: `HNO3-240`

Useful range: 147 – 10 hPa

Vertical resolution: 3.5 to 4.0 km

Contact: Michelle Santee, **Email:** `<mls@mls.jpl.nasa.gov>`

The standard product for version 1.5 HNO_3 is taken from the Core+R3 (240 GHz) retrieval at and below 10 hPa; the `HNO3-240` retrievals are not recommended for use above 10 hPa, where they exhibit significant negative biases.

Simulations

Simulations (see Figures A.10 and A.11) indicate that the `HNO3-240` retrievals are slightly oscillatory (though much less so than the `HNO3-190` retrievals); as a result, negative mixing ratios are not uncommon in the lower stratosphere, especially in regions in which HNO_3 is highly depleted, such as the Antarctic winter polar vortex. Above 10 hPa, large (up to 0.6 ppbv) negative average biases are present at all latitudes.

Vertical resolution

Based on Figure A.12, the `HNO3-240` vertical resolution is ∼3.5 – 4.0 km from 147 – 10 hPa.

Early results and validation

The estimated single-profile precision reported by the Level 2 software agrees well with the observed scatter in the data (evaluated in a 20°-wide latitude band centered around the equator where natural variability is expected to be small in the lower stratosphere): both suggest a measurement precision of 1.0 ppbv or better over the range 147 – 10 hPa.

Artifacts

Oscillations: The `HNO3-240` profiles are slightly oscillatory below ∼10 hPa.

Negative biases: Above 10 hPa, large (up to 0.6 ppbv) negative average biases are present at all latitudes.

Priorities for future data version(s)

- Reduce oscillations in the `HNO3-240` profiles.

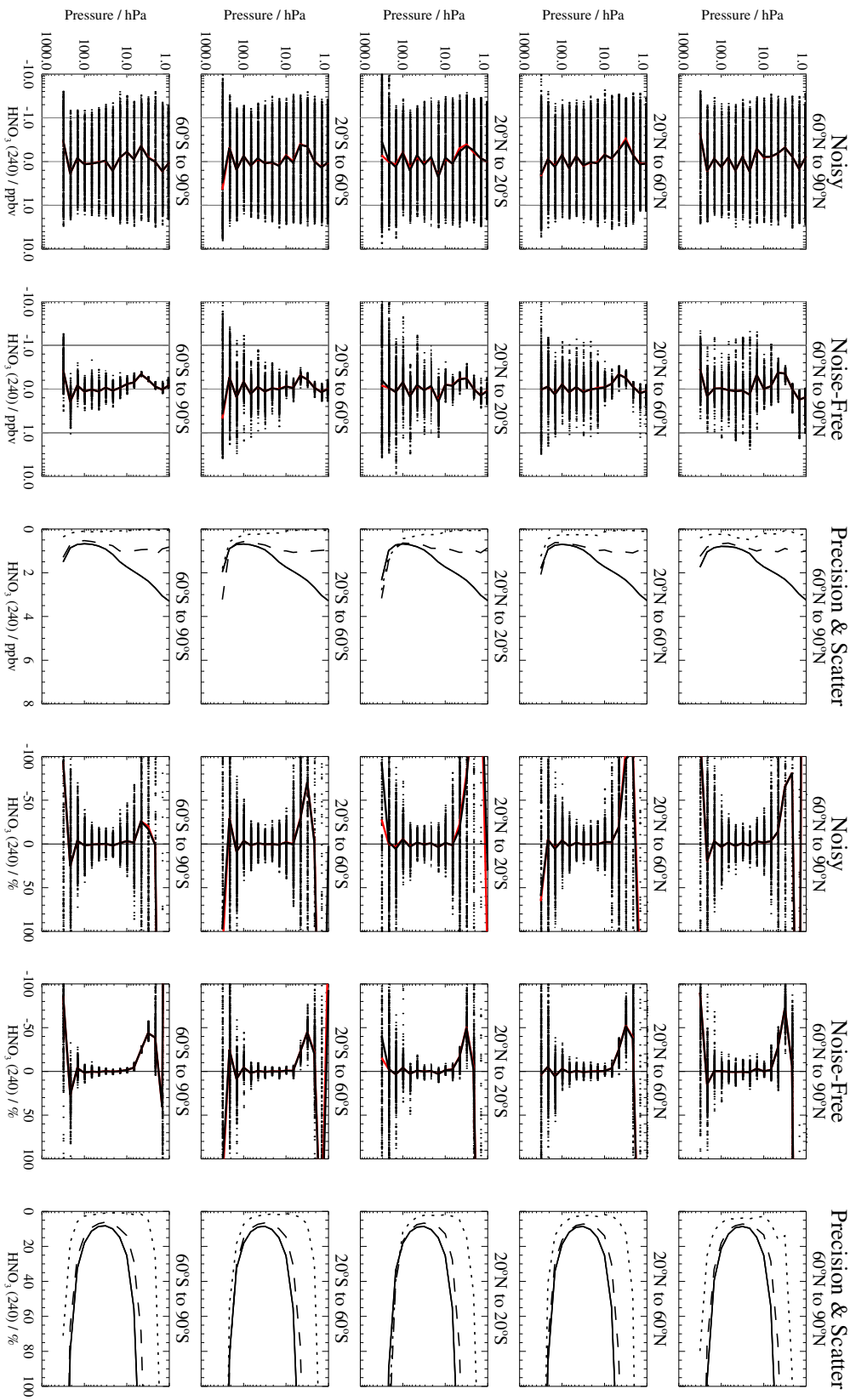

Figure A.10: A summary of the v1.5 data quality for 240 GHz HNO_3 for the `1996d051` test data set. Each row of panels represents a broad latitude bin. The first two columns columns show the differences between the retrieved 240 GHz HNO_3 and the true HNO_3 as a function of pressure, for the noisy and noise free case, along with a solid line which shows the median bias. The median bias of the `Status=0` profiles (i.e., those not significantly affected by clouds) is shown in red. The third column shows the mean estimated precision of 240 GHz HNO_3 (solid line), and the rms scatter about the mean bias in the noisy (broken line) and noise free (dotted line) cases. The remaining three columns show the same information as in the first three columns in the form of a percentage of the true values.

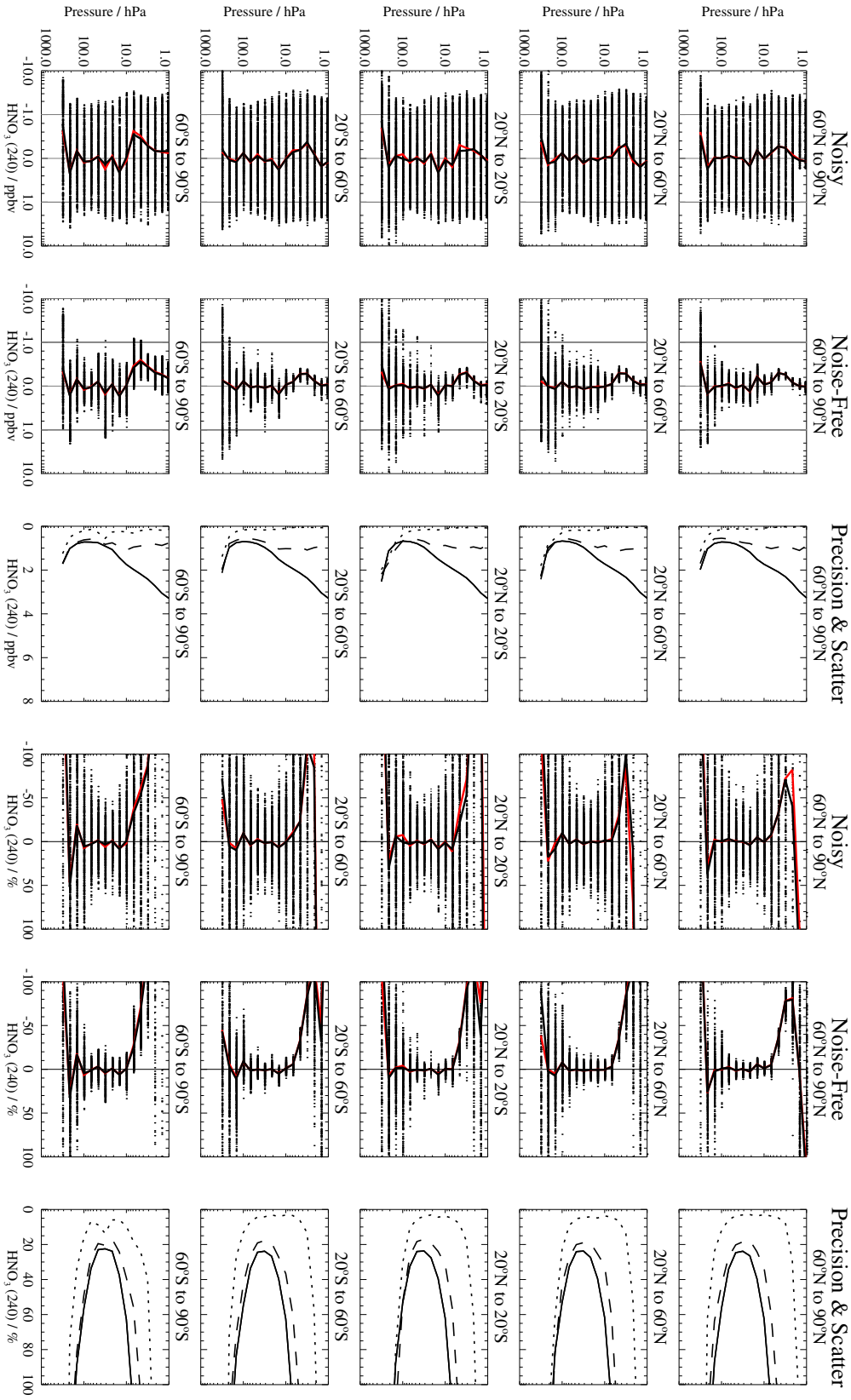

Figure A.11: A summary of the v1.5 data quality for 240 GHz HNO_3, as for figure A.10 but for the `2000d276` test data set.

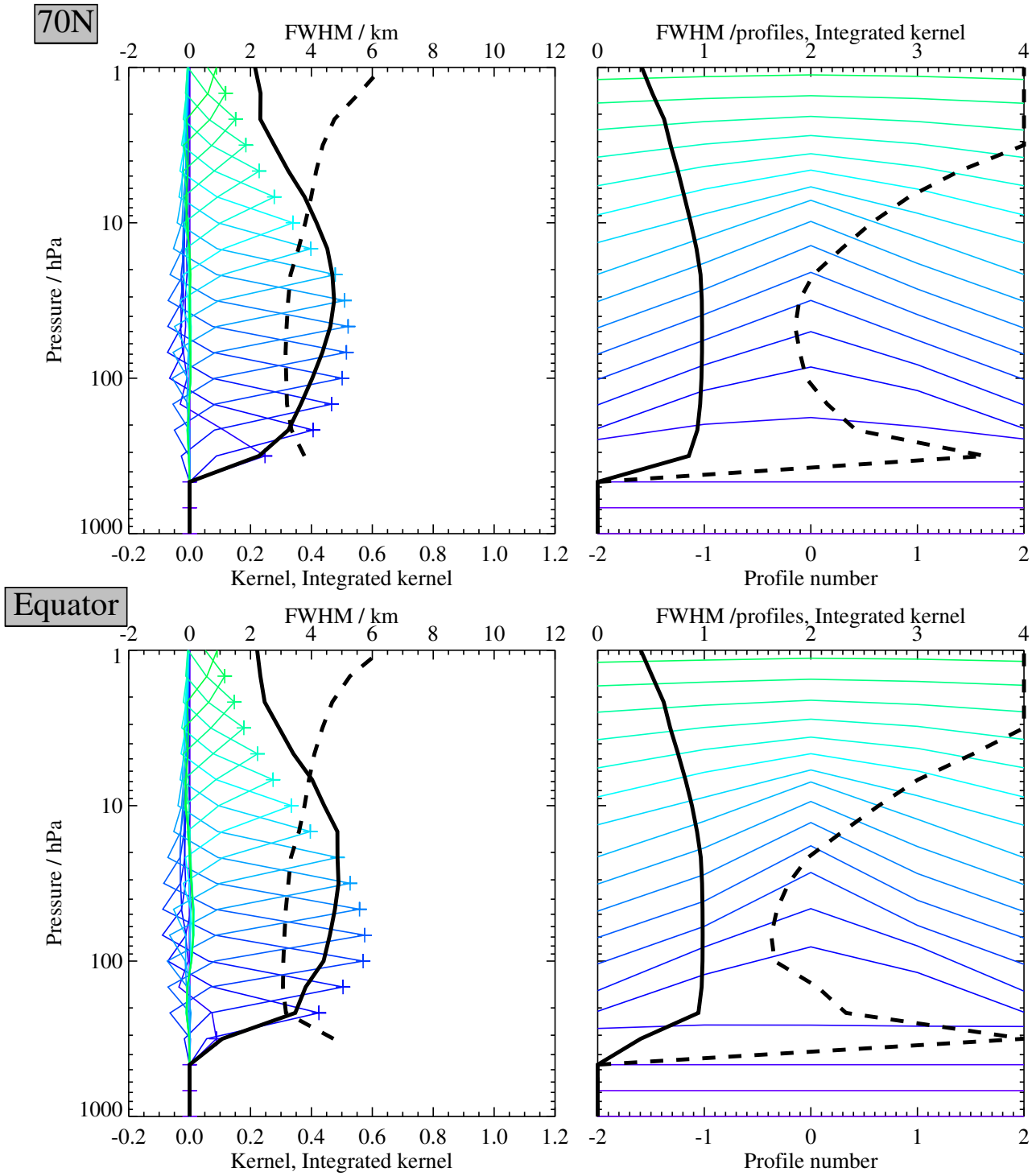

Figure A.12: The left hand plots show the vertical averaging kernel for 240 GHz HNO_3 for the `1996d051` test data set. The colored lines denote the averaging kernels for individual retrieved surfaces (denoted with the matching color + symbols). The thick solid black line shows the integrated area under each colored line. The thick dashed black line denotes the vertical resolution (full width at half maximum) approximately scaled into kilometers. The right hand plots show the horizontal averaging kernels in a similar manner, where the profiles are spaced at 1.5° great circle angle (approximately 165 km).

A.6 640 GHz nitric acid

Swath name: `HNO3-640`

Useful range: None

Vertical resolution: 3.5 to 5.0 km

Contact: Michelle Santee, **Email:** `<mls@mls.jpl.nasa.gov>`

The version 1.5 `HNO3-640` retrievals are characterized by slightly worse vertical resolution and considerably worse precision than the other HNO_3 data products and also by extremely large average biases throughout the vertical profile (but particularly in the lower stratosphere); as a result, the `HNO3-640` data are not recommended for use in any scientific studies.

Simulations

Simulations (see Figures A.13 and A.14) indicate that the `HNO3-640` retrievals exhibit large differences from truth throughout the vertical profile, with differences as large as 80–90% in some latitude bands in the lower stratosphere.

Vertical resolution

Based on Figure A.15, the `HNO3-640` vertical resolution ranges from ∼3.5–5.0 km.

Early results and validation

The estimated single-profile precision reported by the Level 2 software is ∼2–3 ppbv throughout the vertical profile. The observed scatter in the data, evaluated in a 20°-wide latitude band centered around the equator where natural variability is expected to be small in the lower stratosphere, suggests a measurement precision of ∼1.5 ppbv from the top of the profile down to about 32 hPa, degrading to almost 3 ppbv at 100 hPa. Comparisons with the standard HNO_3 product show that, at least at some altitudes, the morphology of the `HNO3-640` field generally follows expectation, although large excursions (positive and negative) from "reasonableness" are not uncommon. The `HNO3-640` retrievals also seem to typically underestimate the degree of HNO_3 depletion in regions where PSC activity can be inferred.

Data screening

Do not use: The v1.5 640 GHz HNO_3 data should not be used in scientific studies.

Artifacts

Biases: Large average biases are present throughout the profile in most latitude bands.

Priorities for future data version(s)

None in particular.

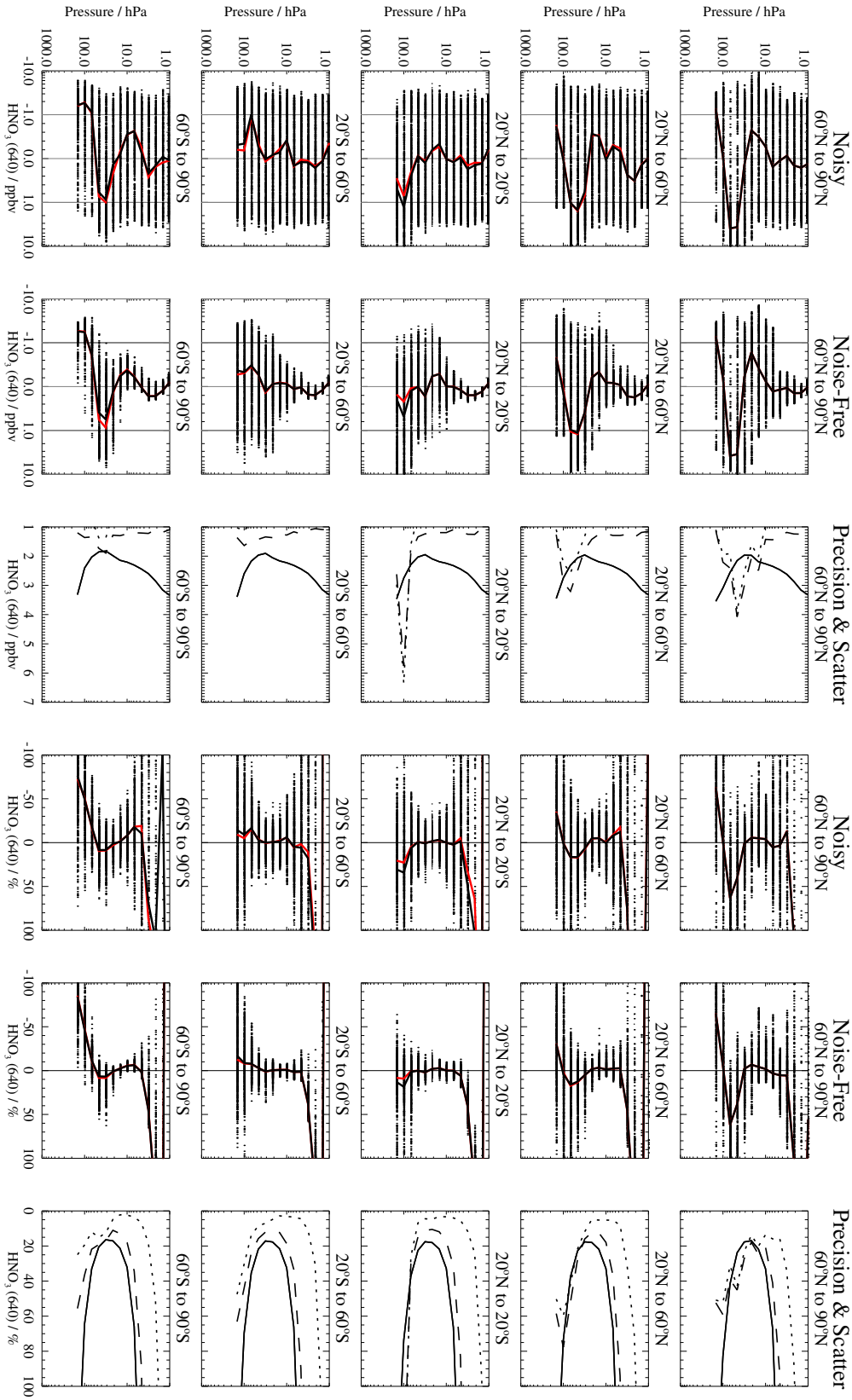

Figure A.13: A summary of the v1.5 data quality for 640 GHz HNO_3 for the `1996d051` test data set. Each row of panels represents a broad latitude bin. The first two columns columns show the differences between the retrieved 640 GHz HNO_3 and the true HNO_3 as a function of pressure, for the noisy and noise free case, along with a solid line which shows the median bias. The median bias of the `Status=0` profiles (i.e., those not significantly affected by clouds) is shown in red. The third column shows the mean estimated precision of 640 GHz HNO_3 (solid line), and the rms scatter about the mean bias in the noisy (broken line) and noise free (dotted line) cases. The remaining three columns show the same information as in the first three columns in the form of a percentage of the true values.

HNO_3

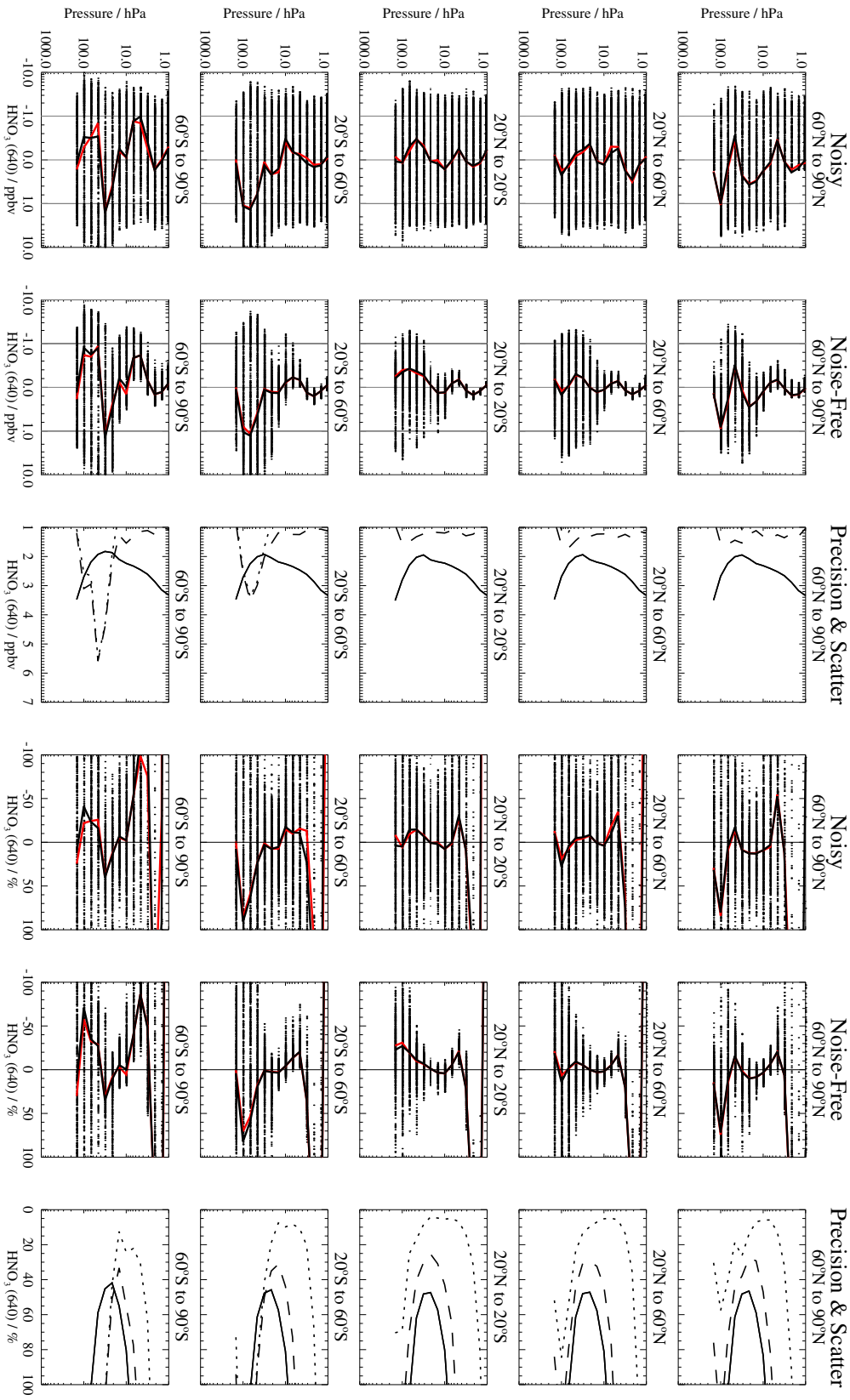

Figure A.14: A summary of the v1.5 data quality for 640 GHz HNO_3, as for figure A.13 but for the `2000d276` test data set.

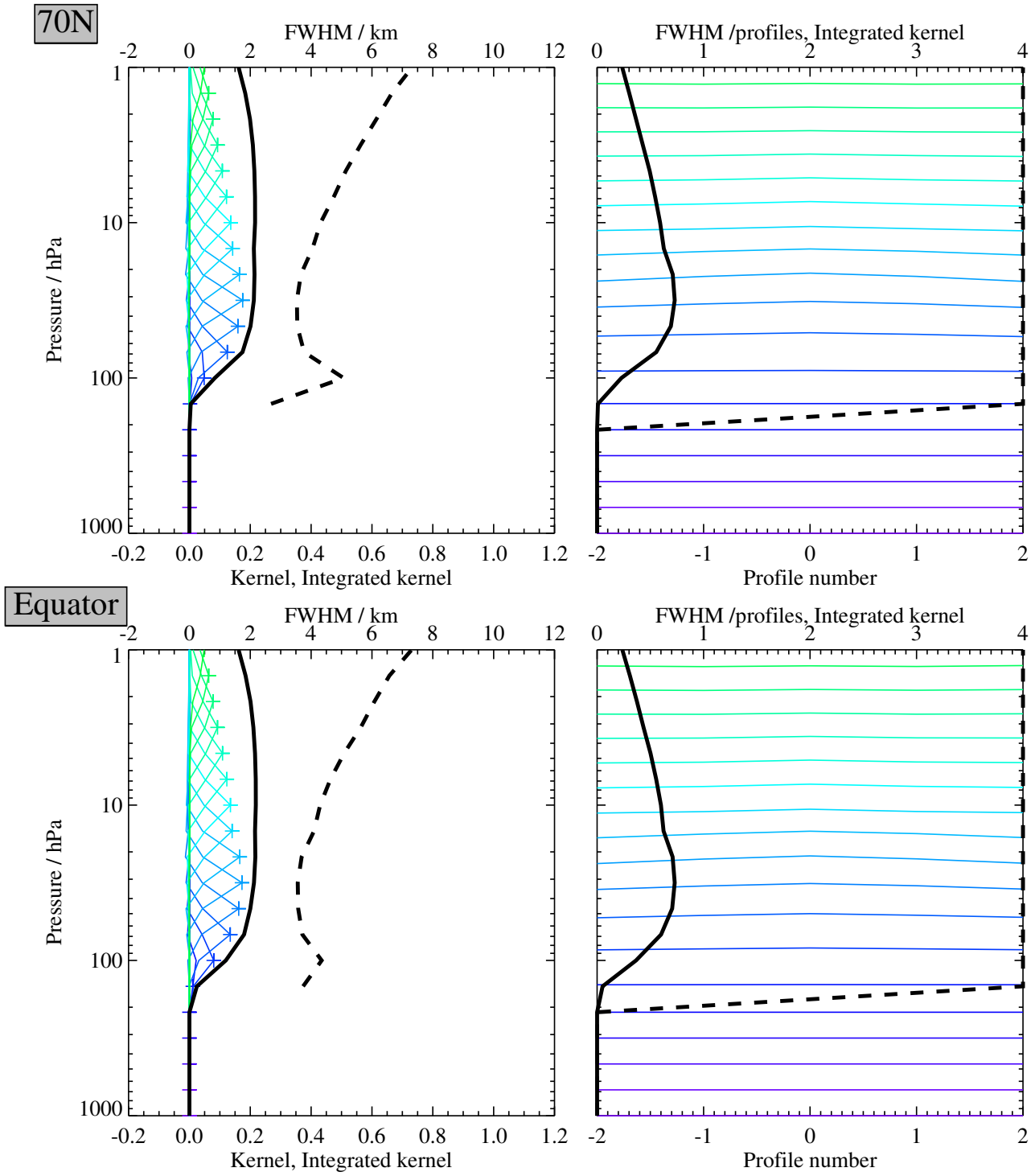

Figure A.15: The left hand plots show the vertical averaging kernel for 640 GHz HNO_3 for the `1996d051` test data set. The colored lines denote the averaging kernels for individual retrieved surfaces (denoted with the matching color + symbols). The thick solid black line shows the integrated area under each colored line. The thick dashed black line denotes the vertical resolution (full width at half maximum) approximately scaled into kilometers. The right hand plots show the horizontal averaging kernels in a similar manner, where the profiles are spaced at 1.5° great circle angle (approximately 165 km).

A.7 Diagnostic cloud products

Swath name: Various names, see text

Useful range: 1000 – 68 hPa

Contact: Dong Wu, **Email:** <dwu@mls.jpl.nasa.gov>
Jonathan Jiang, **Email:** <jonathan@mls.jpl.nasa.gov>

The cloud diagnostic products in v1.5 include a number of cloud-induced radiances (T_{cir}) and baseline radiances calculated at the end of each retrieval phase. These report the contributions to the MLS radiance observations thought to be due to cloud emission and scattering. These 'Minor frame based' quantities are stored in MLS `L2AUX-Cloud` files in a manner very different from the other `L2GP` quantities. Scientists wishing to use these data are advised to contact the science team for information on format and supporting geolocation information. Selected quantities are discussed here.

Description of cloud diagnostic products

Many different cloud diagnostics are produced at different stages in the retrieval process. The T_{cir} quantities are detailed below. They are named according to the designation of the EOS MLS channel whose radiances are being used to characterize cloud, the letters '`DT`' (delta-temperature) and the stage within the retrieval (preliminary, revised, core).

'`R1A:118.B32W:PT.S0.WF4-1.C1 DTprelim`' and
'`R2:190.B5F:CLO.S0.FB25-5.C1 DTprelim`'

are R1 and R2 cloud flags produced after InitPtan phase to give preliminary cloud screening for radiance used in the retrieval.

'`R1A:118.B32W:PT.S0.WF4-1.C1 DTrevised`' and
'`R2:190.B5F:CLO.S0.FB25-5.C1 DTrevised`'

are cloud flags generated after the UpdatePtan phase where better temperature and pressure information is established. The

'`R1A:118.B32W:PT.S0.WF4-1.C1 DTcore`' and
'`R2:190.B5F:CLO.S0.FB25-5.C1 DTcore`'

cloud flags are generated after InitUTH phase where realistic water vapor profiles are retrieved.

The final set of cloud flags

'`R1A:118.B32W:PT.S0.WF4-1.C1 DT`',
'`R1B:118.B34W:PT.S0.WF4-3 DT`',
'`R2:190.B5F:CLO.S0.FB25-5.C1 DT`',
'`R3:240.B33W:O3.S0.WF4-2.C3 DT`',
'`R4:640.B10F:CLO.S0.FB25-10.C3 DT`' and
'`R5H:2T5.B15F:OH.S5.FB25-15.C25 DT`'

is generated after Core+R2 phase where realistic pressure, Temperature, H_2O, O_3, HNO_3, and N_2O profiles are obtained.

The baseline quantities

'`BaselineMIFR2-Tcir`',
'`BaselineMIFR3-Tcir`' and
'`BaselineMIFR4-Tcir`'

are calculated for fine tuning of R2, R3 and R4 T_{cir}. Among these, '`BaselineMIFR3-Tcir`' is used to produce the standard IWC product. The '`BaselineMIFR3-Tcir`' quantity is generally very similar to the quantity '`R3:240.B33W:O3.S0.WF4-2.C3 DT`' at tangent pressures <300 hPa. The latter has meaningful values continuing to lower tangent heights while the former is cutoff at 300 hPa.

Because the window channels of MLS radiometers have different optical depths, the definition of high, mid, and low tangent heights will vary among these radiometers. Table A.1 gives the tangent pressure ranges of each radiometer's window channels for optically thin, thick and intermediate situations.

Table A.1: Ranges of tangent pressure / hPa for various radiometers and regimes

Optical depth	R1	R2	R3	R4	R5
$\ll 1$	< 60	< 150	< 200	< 80	< 40
~ 1	60 – 200	150 – 400	200 – 500	80 – 250	40 – 100
$\gg 1$	> 200	> 400	> 500	> 250	> 100

IWC

Artifacts

Figure A.16 gives a set of sample plots of various diagnostic cloud plots. Poor convergence in retrievals can lead to 'fliers' in the T_{cir} values from the various radiometers in some chunks (groups of ∼10 profiles that are retrieved together). Other issues with individual T_{cir} observations for each radiometer are detailed below.

R1: There is a 3.5% gain difference between R1A and R1B (for small radiances) plus a slight modulation along the orbital track, whose origin remains unknown. This systematic error has been identified by comparing pairs of channels (after the pointing offsets are corrected) in bands 32 and 34 for several days of observations.

R2: The morphology of T_{cir} is generally reasonable at tangent pressures less than 121 hPa and compares well with R3 T_{cir}. However, R2 clear-sky T_{cir} values show significant latitudinal variation, following the H_2O distribution in the tropics and subtropics. This bias becomes worse at 300 – 121 hPa, suggesting contamination from errors in the H_2O retrieval.

R3: The 240 GHz radiometer gives the best T_{cir} observations at pressures less than 215 hPa. At 200 – 300 hPa the morphology of R3 T_{cir} still compares well with climatology (e.g., OLR) but negative values begin to show up near deep convective cores. Large spikes are sometimes seen at winter high latitudes. Because the R3 window channels penetrate deep into the atmosphere, the T_{cir} at low tangent heights can be contaminated by the surface ice/snow (low emissivity) at polar latitudes.

R4: T_{cir} is normally valid only at pressures smaller than 100 hPa. Positive outliers (∼10 K) in the wintertime polar regions are probably due to HNO_3 retrieval errors. In the tropical upper troposphere, R4 T_{cir} is readily affected by H_2O retrieval errors. The biases in Figure A.16 (low at ∼ 20 km and high at ∼12 km), are probably caused by continuum errors.

Priorities for future data version(s)

Improving T_{cir} is crucial for MLS cloud ice measurements and depends largely on the quality of gas retrievals. Ideally T_{cir} should have clear-sky measurements clustered as closely as possible with little bias. Several areas can be improved on these diagnostic cloud products:

- Improve R2 T_{cir} calculations to reduce the biases in the tropics and subtropics.
- Improve the continuum models for R3 and R4 to reduce the height- dependent biases in T_{cir}.
- Retrieve cloud ice path from low-tangent-height T_{cir} for R1, R2, R3, R4 and R5.

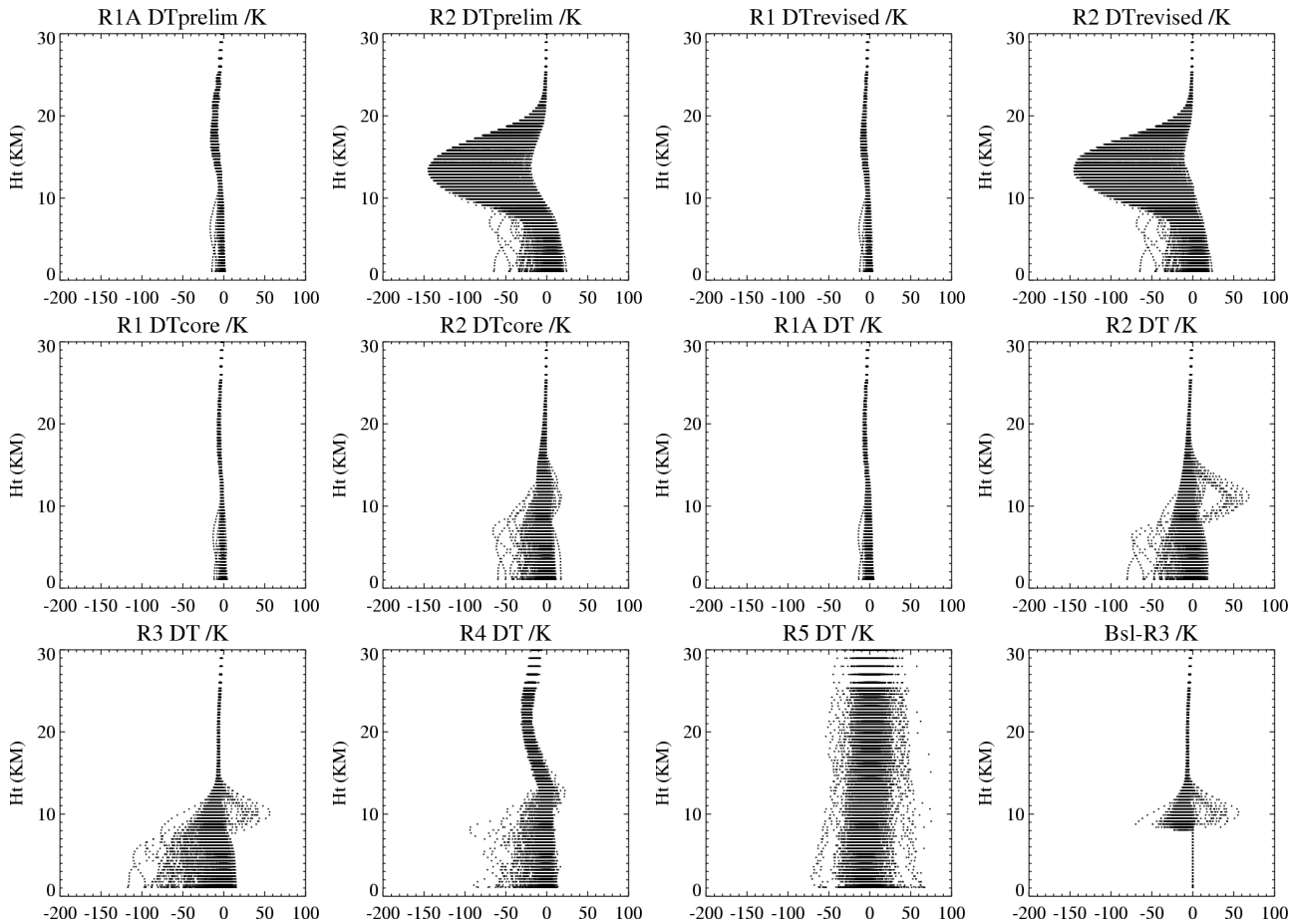

Figure A.16: Example of the MLS T_{cir} derived in different retrieval phases for `2005d123`. All the R*x* DT quantities denote the results calculated at the end of the Core+R2A phase. `Bsl-R3` is the refined baseline retrieval from R3 and R4 window radiances at the end of Core+R2 phase, which yields the standard IWC retrieval afterward.

IWC

IWC

A.8 190 GHz nitrous oxide

Swath name: `N2O-190`

Useful range: 33 – 0.1 hPa

Vertical resolution: 5.0 to 6.0 km

Contact: Nathaniel Livesey, **Email:** `<livesey@mls.jpl.nasa.gov>`

The 190 GHz N_2O product is retrieved in the Core+R2A phase whose main product is water vapor. The standard N_2O product (taken from the 640 GHz observations) should be used in preference to this product in scientific studies.

Simulations

The results of the simulation studies for the 190 GHz N_2O product are shown in Figures A.17 and A.18. These show average biases of 10% or better through most of the stratosphere.

Vertical resolution

The averaging kernel plots in Figure A.19 indicate that the vertical resolution of the 190 GHz N_2O product is around 5 – 6 km in the stratosphere.

Early results

In real MLS observations, the 190 GHz N_2O generally agrees well (10 – 20%) with the standard N_2O product (taken from the 640 GHz observations) in the middle and upper stratosphere. In the lower stratosphere (pressures of 46 hPa or greater), 190 GHz N_2O values are 50 – 70 ppbv higher on average than the standard product. This is clearly indicative of an unrealistic high bias in the 190 GHz N_2O product, as average values as high as ∼420 ppbv are seen at 100 hPa in the tropics (far larger than the accepted abundances, and than those seen in the standard product). The poor performance of the 190 GHz N_2O product in this region is consistent with known problems fitting the observed radiances in this spectral region, with residuals of 1 – 2 K remaining after the retrieval calculation. While the 190 GHz product is retrieved to lower altitudes than the standard product, the data quality at 147, and 220 hPa is very poor with unrealistic amounts of scatter.

Data screening

Do not use: There is no reason to use the 190 GHz N_2O product instead of the standard N_2O product.

Artifacts

The 190 GHz N_2O product displays positive biases of order 50 – 70 ppbv in the lower stratosphere.

Priorities for future versions

The 190 GHz radiances contain more useful information on N_2O in the lowermost stratosphere and upper troposphere than is found in the 640 GHz radiances currently used to retrieve the standard product. Future versions could use the 190 GHz information to extend the N_2O profile into these regions. A prerequisite to this approach is, however, a better fit to the radiances in this spectral region.

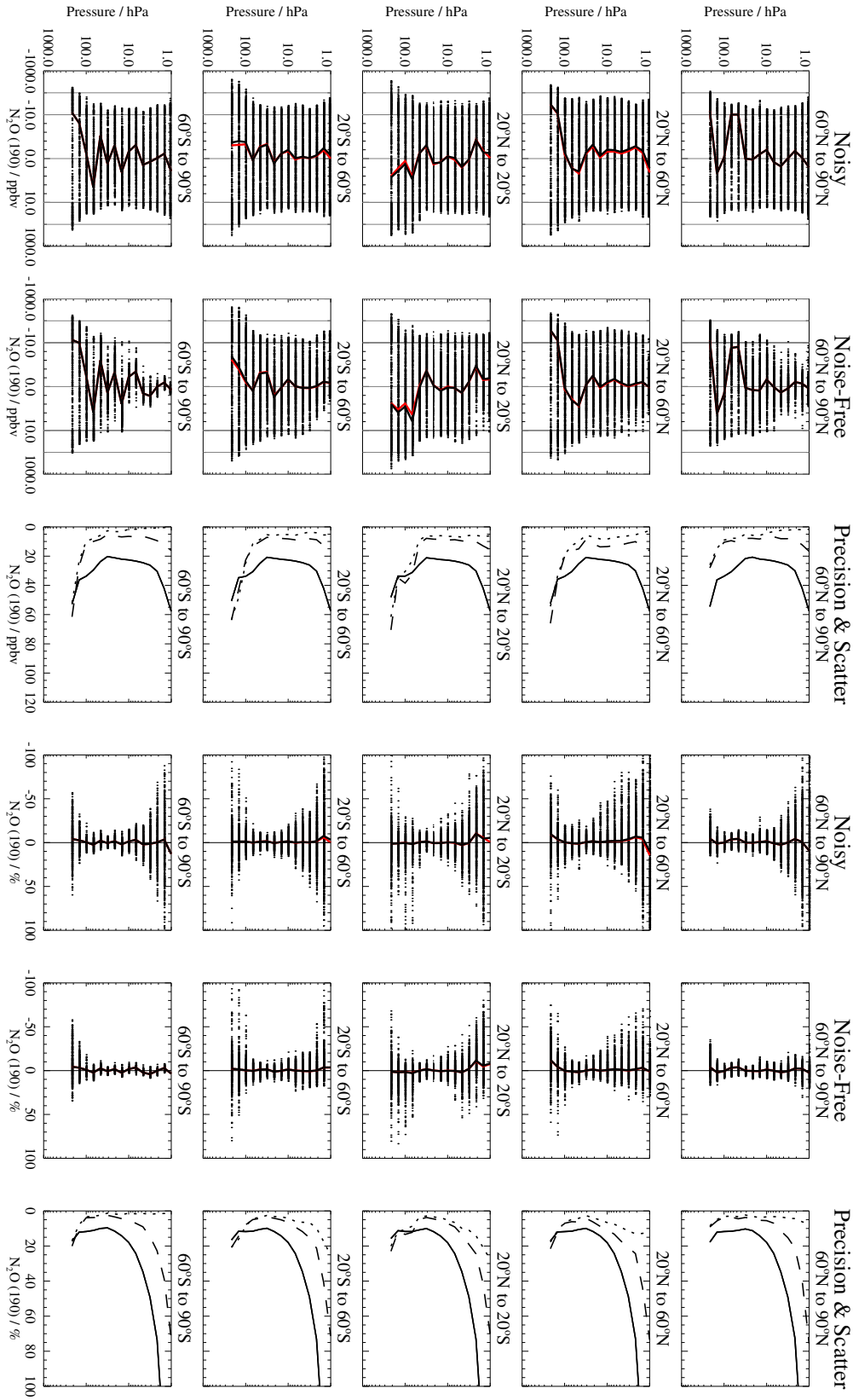

Figure A.17: A summary of the v1.5 data quality for 190 GHz N_2O for the `1996d051` test data set. Each row of panels represents a broad latitude bin. The first two columns columns show the differences between the retrieved 190 GHz N_2O and the true N_2O as a function of pressure, for the noisy and noise free case, along with a solid line which shows the median bias. The median bias of the `Status=0` profiles (i.e., those not significantly affected by clouds) is shown in red. The third column shows the mean estimated precision of 190 GHz N_2O (solid line), and the rms scatter about the mean bias in the noisy (broken line) and noise free (dotted line) cases. The remaining three columns show the same information as in the first three columns in the form of a percentage of the true values.

N_2O

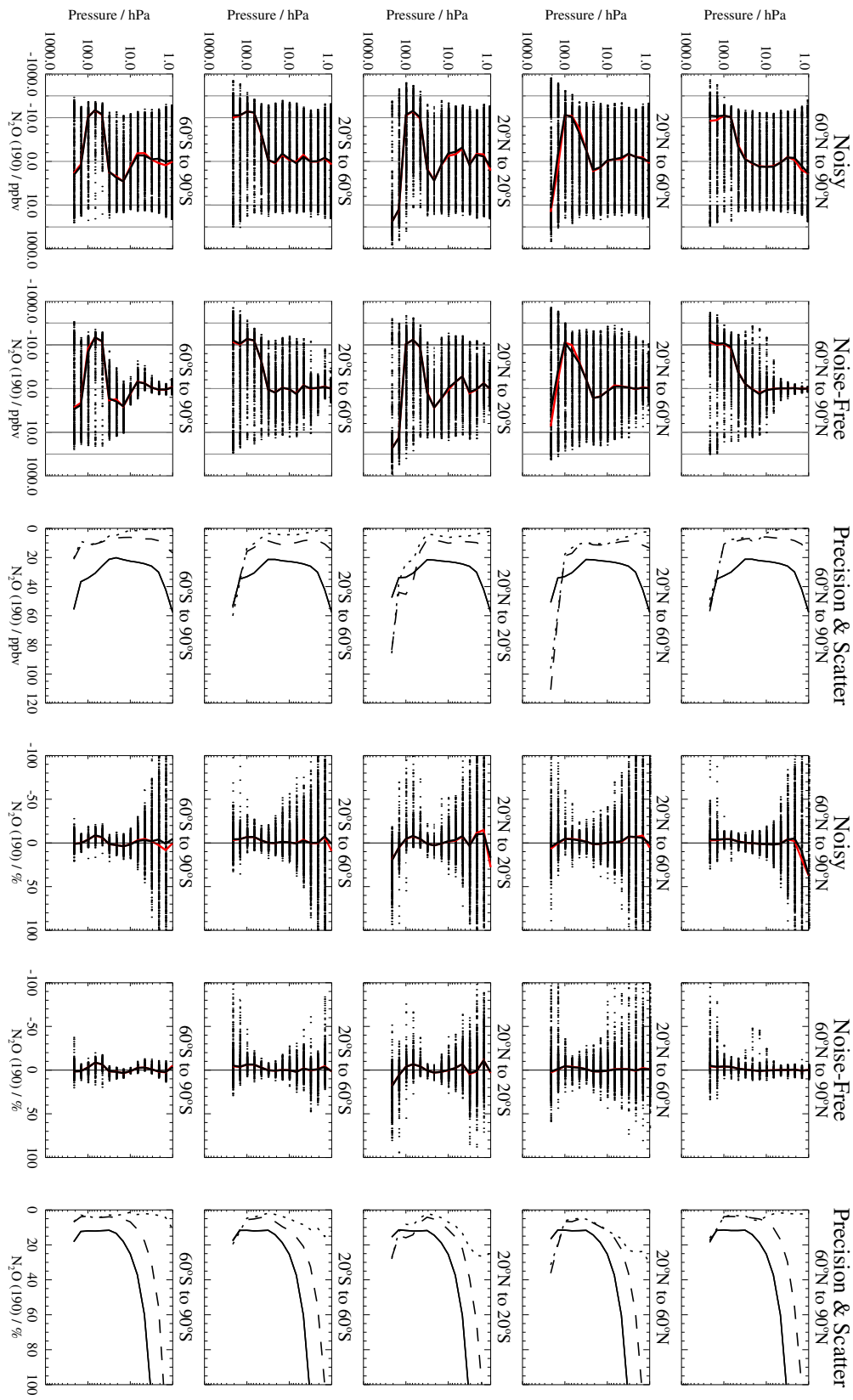

Figure A.18: A summary of the v1.5 data quality for 190 GHz N_2O, as for figure A.17 but for the `2000d276` test data set.

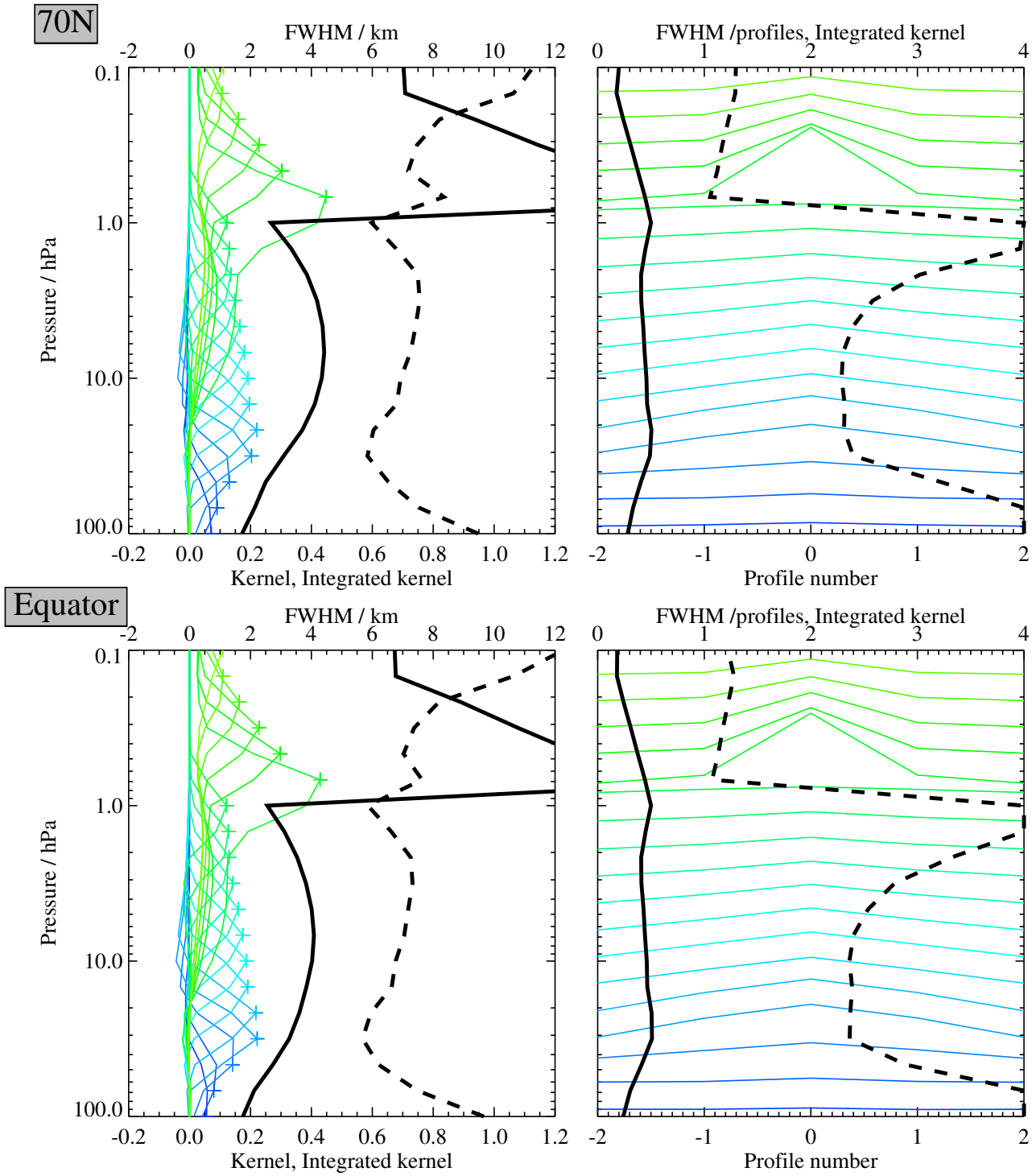

Figure A.19: The left hand plots show the vertical averaging kernel for 190 GHz N_2O for the `1996d051` test data set. The colored lines denote the averaging kernels for individual retrieved surfaces (denoted with the matching color + symbols). The thick solid black line shows the integrated area under each colored line. The thick dashed black line denotes the vertical resolution (full width at half maximum) approximately scaled into kilometers. The right hand plots show the horizontal averaging kernels in a similar manner, where the profiles are spaced at 1.5° great circle angle (approximately 165 km).

A.9 Ozone diagnostic products

Swath name: `O3-190, O3-640, O3-2T5`

Useful ranges: `O3-190`: 68 – 0.47 hPa, `O3-640`: 68 – 0.47 hPa, `O3-2T5`: 68 – 0.47 hPa

Vertical resolution: `O3-190`: 3 to 5 km, `O3-640`: 3 km, `O3-2T5`: 3 to 4 km

Contacts: Lucien Froidevaux, **Email:** `<lucien@mls.jpl.nasa.gov>`,
Yibo Jiang, **Email:** `<ybj@mls.jpl.nasa.gov>`

Introduction

The ozone diagnostic products for version 1.5 are taken from the 190 GHz ('Core+R2'), 640 GHz ('Core+R4') and 2.5 THz ('Core+R5') retrievals. These products (labeled with names `O3-190`, `O3-640`, and `O3-2T5`) are not trusted or retrieved down to heights as low as for the standard (240 GHz) ozone product. `O3-190` and `O3-640` retrievals go down to 147 hPa, whereas `O3-2T5` retrievals stop at 68 hPa. The poorer results and oscillations at the higher pressures arise largely because these retrievals use a linearized forward model rather than the fully non-linear method used for the `O3-240` retrievals. In fact, the recommended useful range starts at 68 hPa.

The standard product (from the 240 GHz Core+R3 retrievals) remains the MLS ozone product of choice for its recommended vertical range (215 – 0.47 hPa). There is some useful information in the mesosphere for all these products, but this region requires further investigation.

Simulations

190 GHz O_3: The `O3-190` is in excellent agreement with the 'true simulated profile' within 5% in the stratosphere and lower mesosphere, but the differences increase to around 20% in the lower stratosphere and upper troposphere. Systematic biases oscillate in the middle stratosphere but are within 0.1 ppmv. The scatter is comparable to the estimated precision in the altitude range below 10 hPa, but lower than the precision above 10 hPa.

640 GHz O_3: Simulations indicate excellent retrieval closure (to better than a few percent) in the stratosphere, with some exceptions in the lower stratosphere and upper troposphere where biases of about 10% are seen in the northern higher latitude bins. Systematic biases oscillate especially in the mesosphere, but are within 10% (0.1 ppmv). In high latitudes, the biases at 147 hPa can be higher than 0.1 ppmv, which amounts to more than 40%. In general, the scatter is slightly lower than the estimated precision in the whole retrieval range. The precision is lower (around 5%) in the middle stratosphere, and higher (50%) in both lower mesosphere and lower stratosphere.

2.5 THz O_3 The `O3-2T5` is generally in agreement with the simulations to within 30%, but shows larger differences ($\leq$40%) at high latitudes near 68 hPa and overall poorer fits than the other ozone bands, especially for `2004d051`. The scatter for `2005d051` shows a maximum near 10 hPa that is of order 10 – 20% and larger than the estimated precision.

Vertical Resolution

- Based on Figure A.26, the vertical resolution for `O3-190` is 3 km in the lower stratosphere, and degrades to about 5 km in the upper stratosphere.

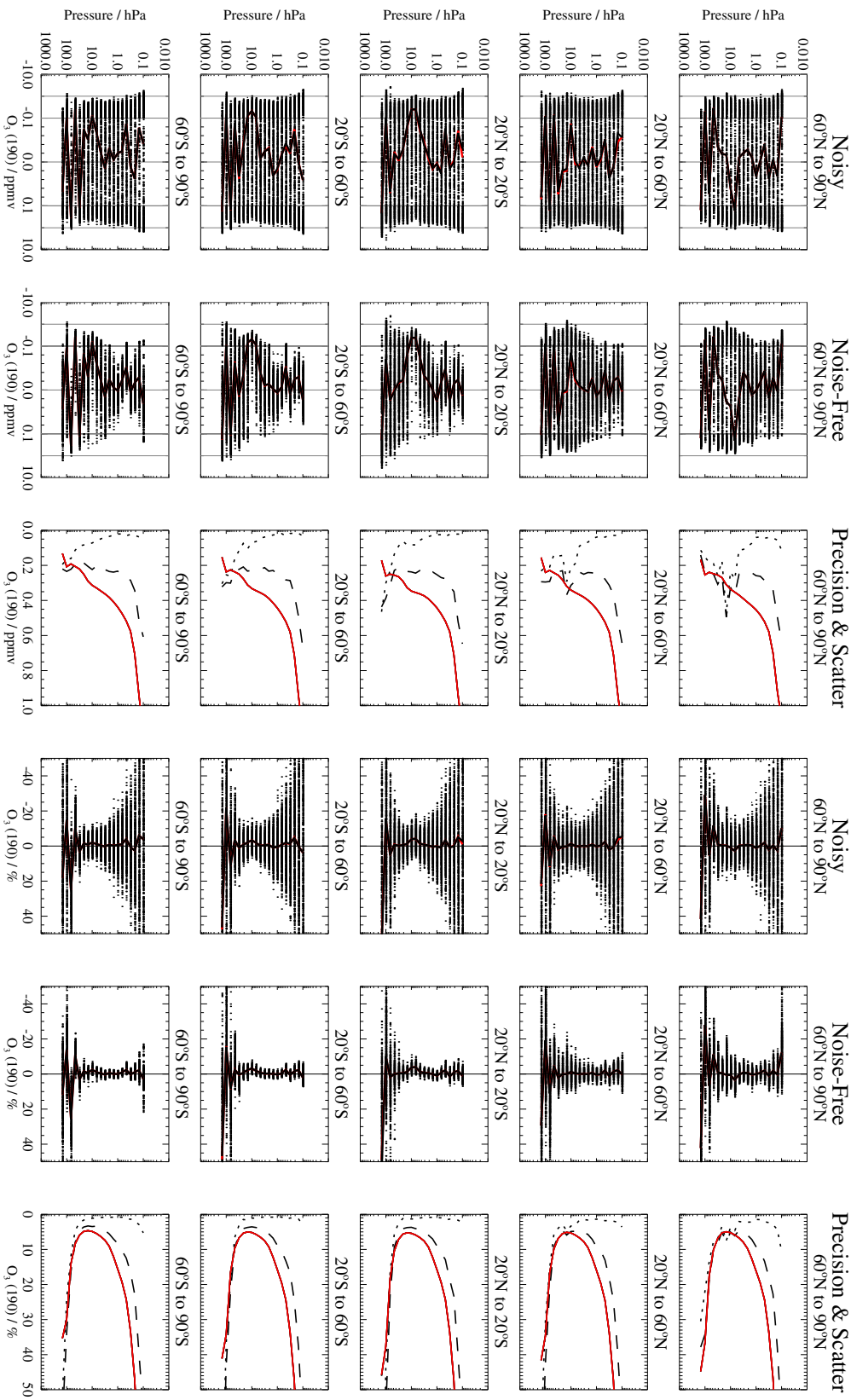

Figure A.20: A summary of the v1.5 data quality for 190 GHz O_3 for the `1996d051` test data set. Each row of panels represents a broad latitude bin. The first two columns columns show the differences between the retrieved 190 GHz O_3 and the true O_3 as a function of pressure, for the noisy and noise free case, along with a solid line which shows the median bias. The median bias of the `Status=0` profiles (i.e., those not significantly affected by clouds) is shown in red. The third column shows the mean estimated precision of 190 GHz O_3 (solid line), and the rms scatter about the mean bias in the noisy (broken line) and noise free (dotted line) cases. The remaining three columns show the same information as in the first three columns in the form of a percentage of the true values.

O_3

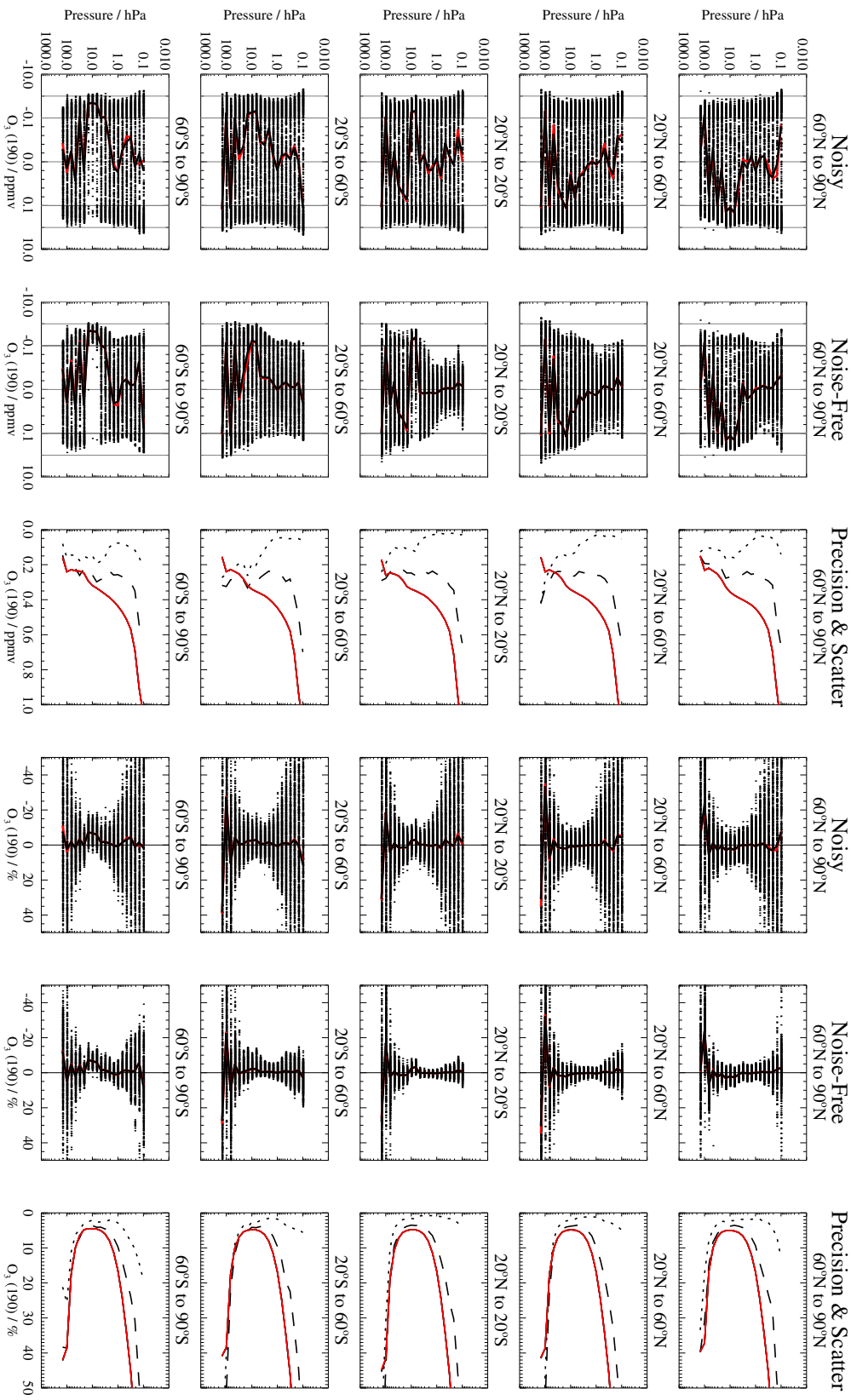

Figure A.21: A summary of the v1.5 data quality for 190 GHz O_3, as for figure A.20 but for the `2000d276` test data set.

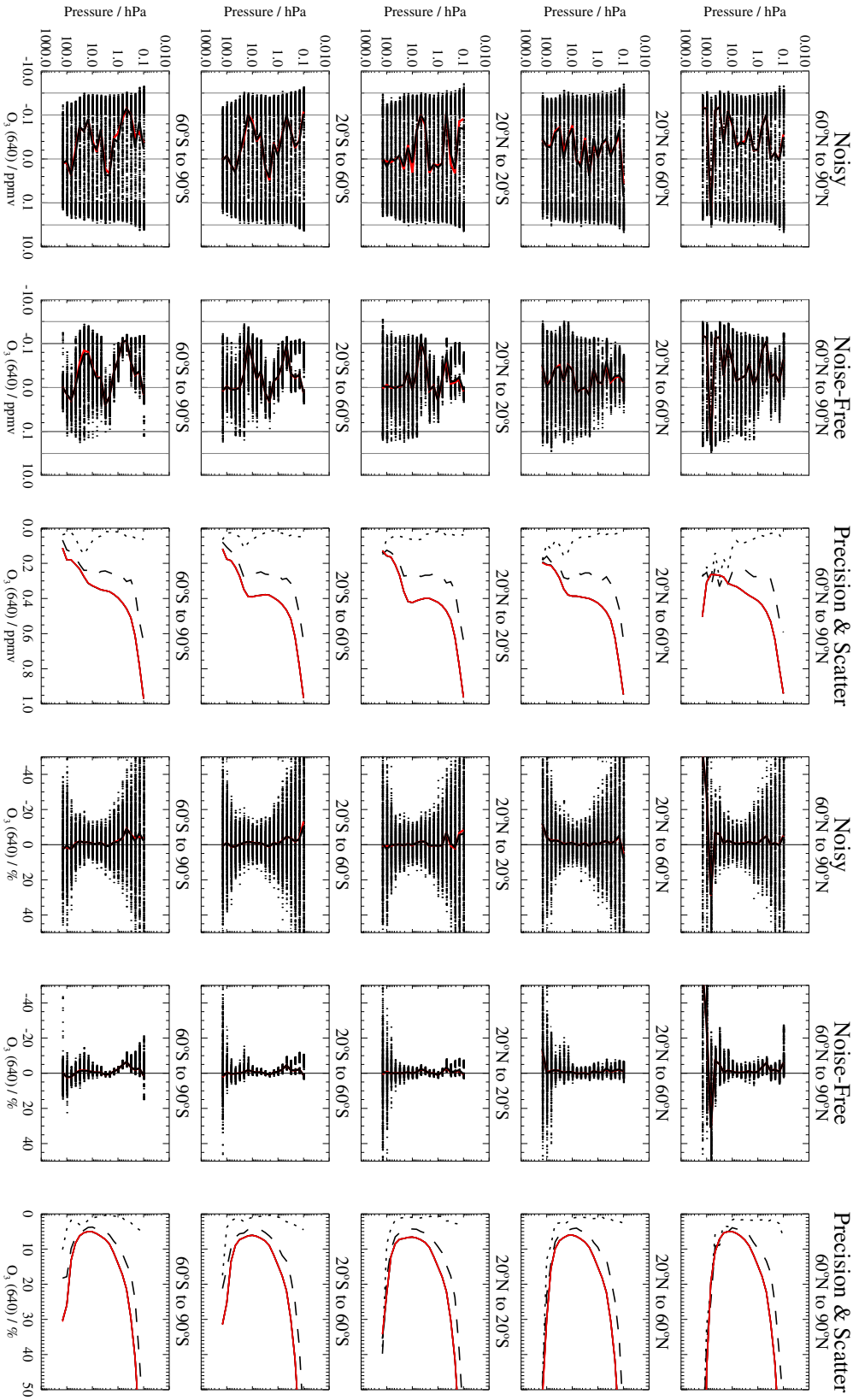

Figure A.22: A summary of the v1.5 data quality for 640 GHz O_3 for the `1996d051` test data set. Each row of panels represents a broad latitude bin. The first two columns columns show the differences between the retrieved 640 GHz O_3 and the true O_3 as a function of pressure, for the noisy and noise free case, along with a solid line which shows the median bias. The median bias of the `Status=0` profiles (i.e., those not significantly affected by clouds) is shown in red. The third column shows the mean estimated precision of 640 GHz O_3 (solid line), and the rms scatter about the mean bias in the noisy (broken line) and noise free (dotted line) cases. The remaining three columns show the same information as in the first three columns in the form of a percentage of the true values.

O_3

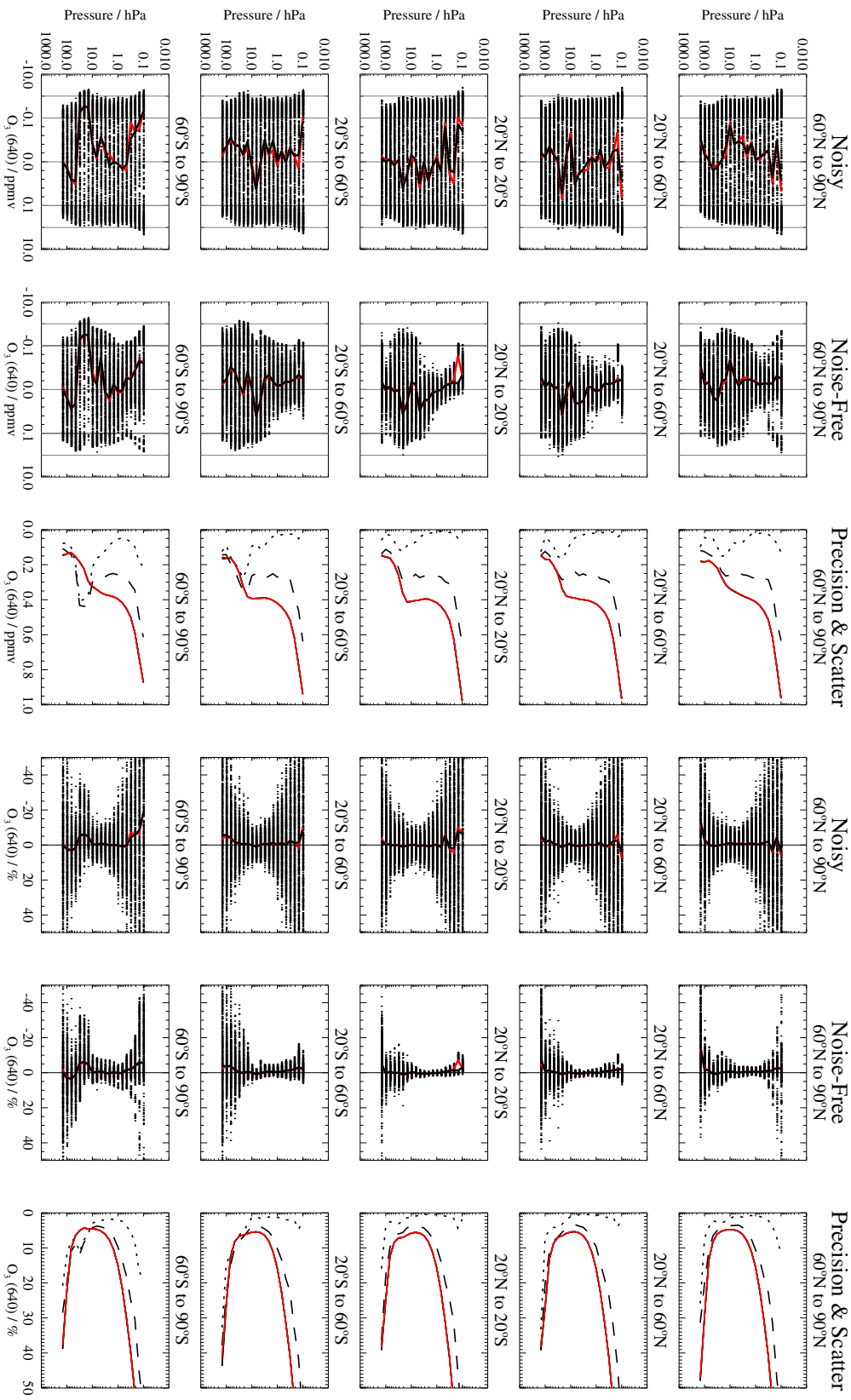

Figure A.23: A summary of the v1.5 data quality for 640 GHz O_3, as for figure A.22 but for the `2000d276` test data set.

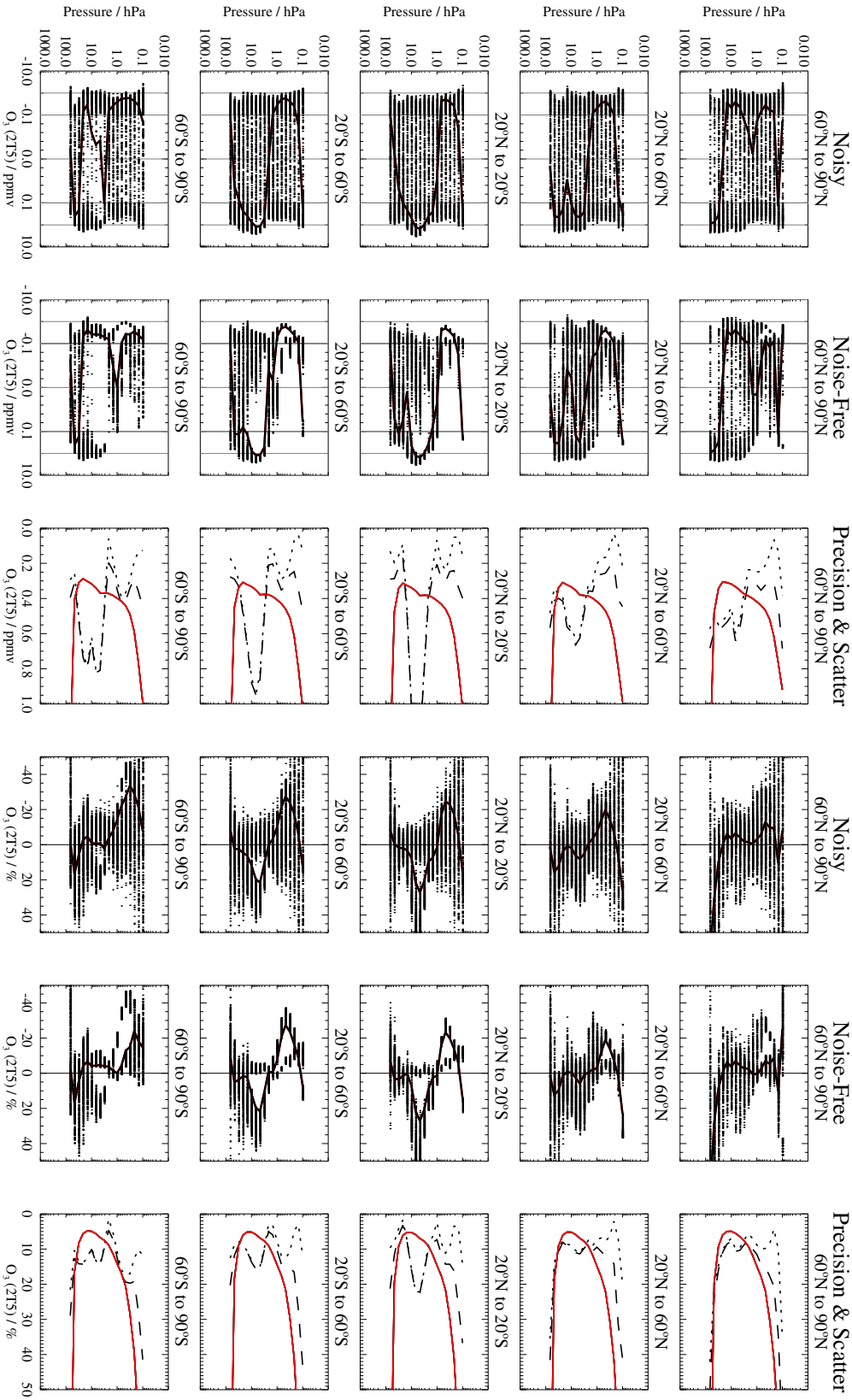

Figure A.24: A summary of the v1.5 data quality for 2.5 THz O_3 for the `1996d051` test data set. Each row of panels represents a broad latitude bin. The first two columns columns show the differences between the retrieved 2.5 THz O_3 and the true O_3 as a function of pressure, for the noisy and noise free case, along with a solid line which shows the median bias. The median bias of the `Status=0` profiles (i.e., those not significantly affected by clouds) is shown in red. The third column shows the mean estimated precision of 2.5 THz O_3 (solid line), and the rms scatter about the mean bias in the noisy (broken line) and noise free (dotted line) cases. The remaining three columns show the same information as in the first three columns in the form of a percentage of the true values.

O_3

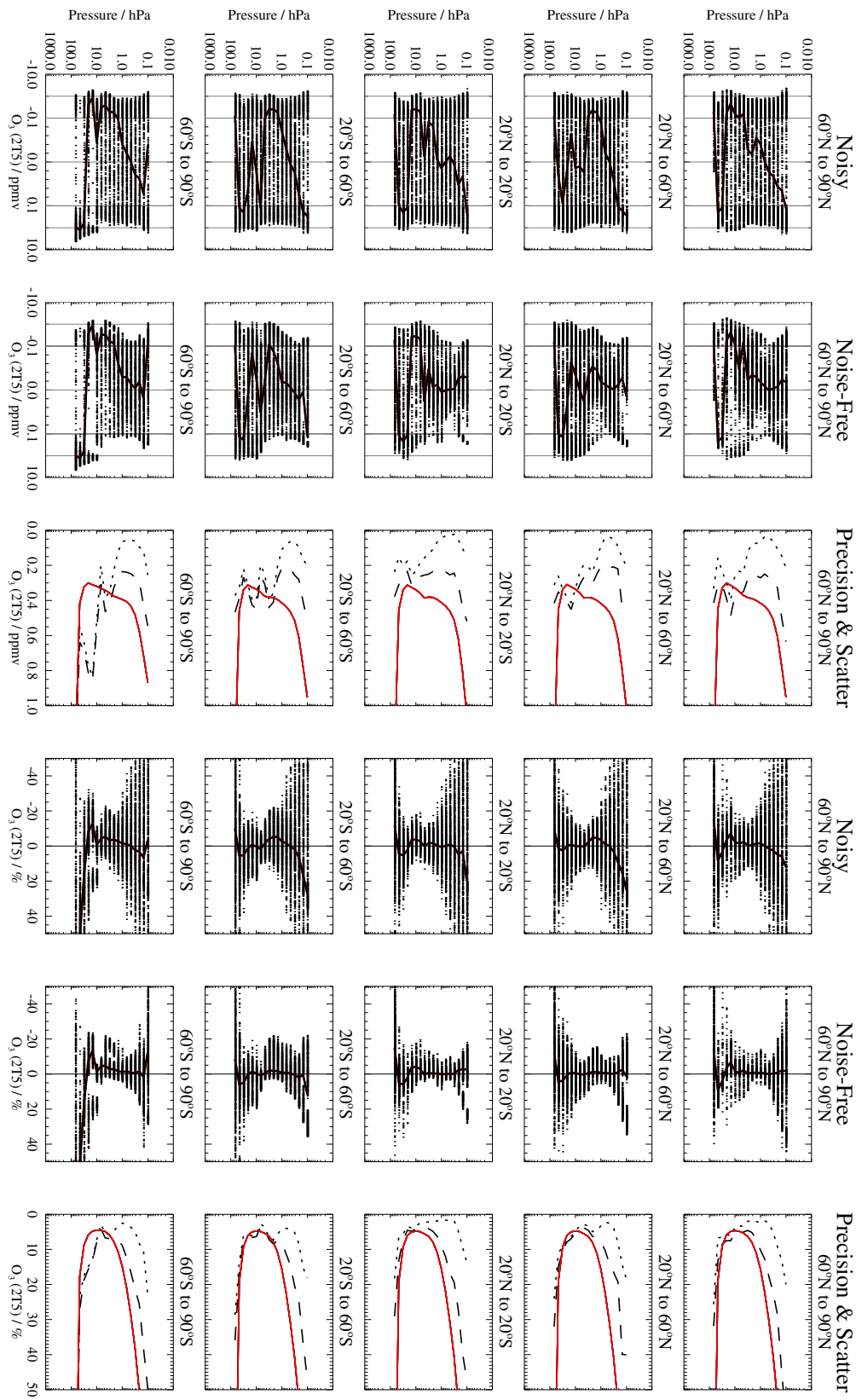

Figure A.25: A summary of the v1.5 data quality for 2.5 THz O_3, as for figure A.24 but for the `2000d276` test data set.

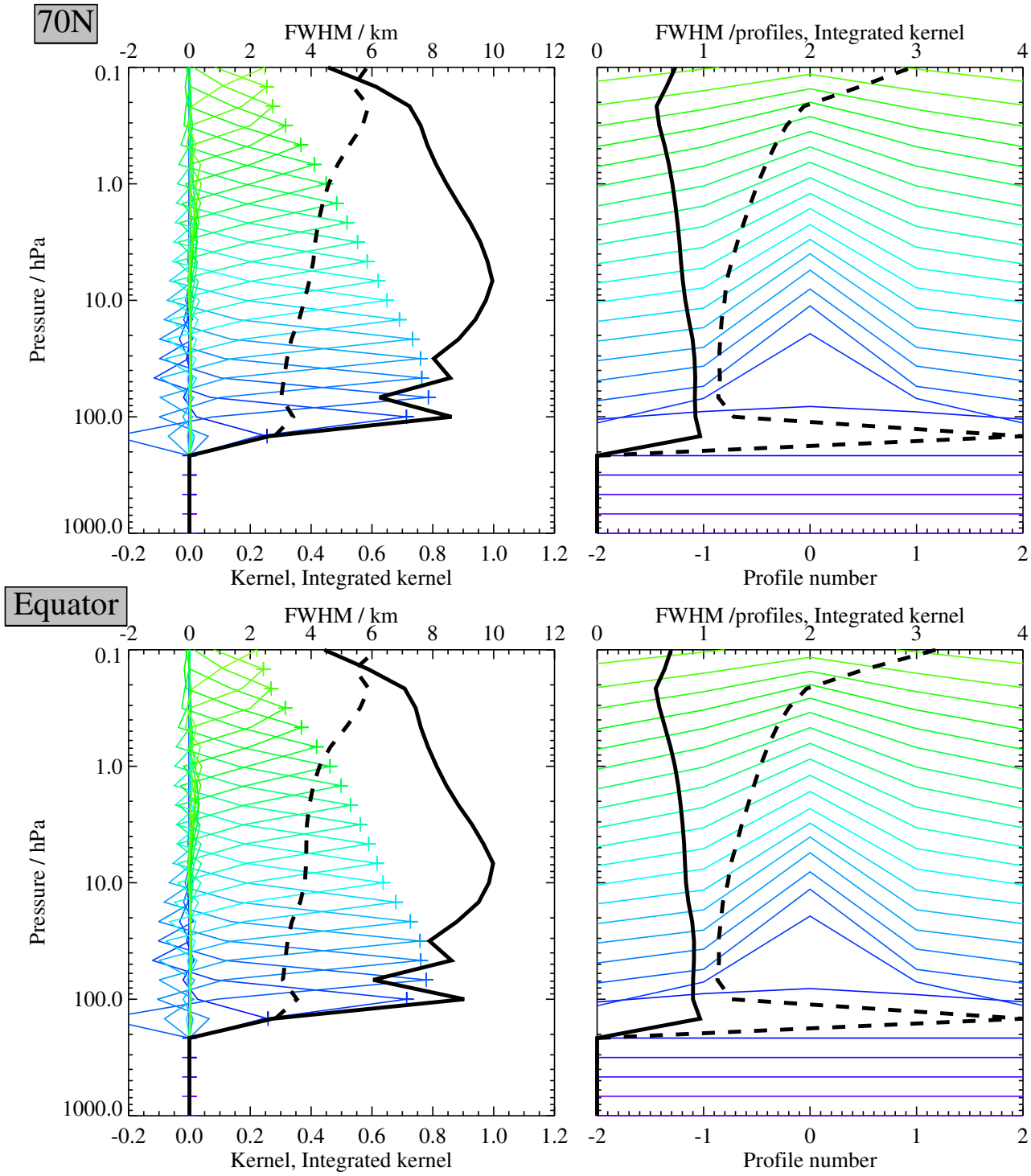

Figure A.26: The left hand plots show the vertical averaging kernel for 190 GHz O_3 for the `1996d051` test data set. The colored lines denote the averaging kernels for individual retrieved surfaces (denoted with the matching color + symbols). The thick solid black line shows the integrated area under each colored line. The thick dashed black line denotes the vertical resolution (full width at half maximum) approximately scaled into kilometers. The right hand plots show the horizontal averaging kernels in a similar manner, where the profiles are spaced at 1.5° great circle angle (approximately 165 km).

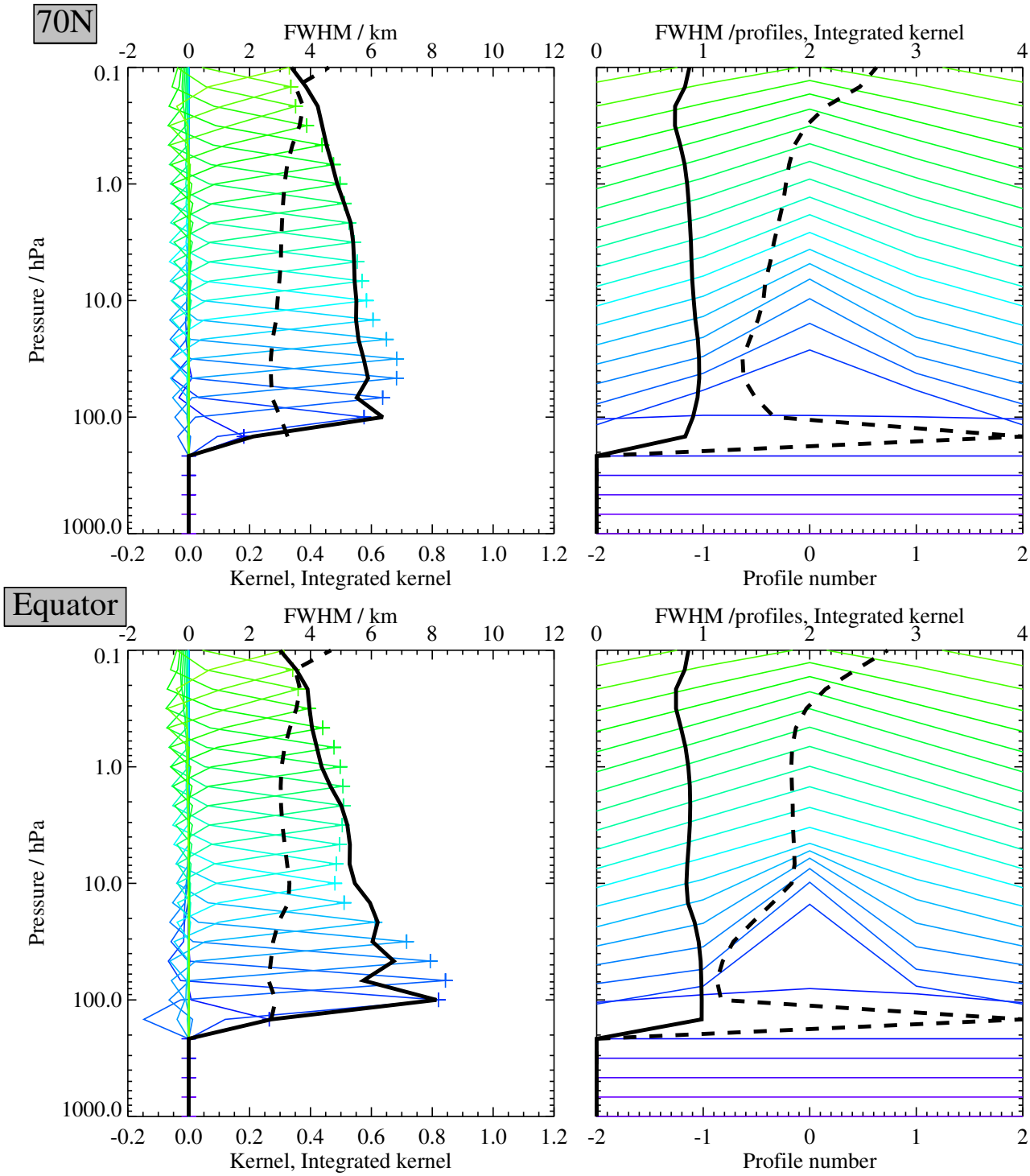

Figure A.27: The left hand plots show the vertical averaging kernel for 640 GHz O_3 for the `1996d051` test data set. The colored lines denote the averaging kernels for individual retrieved surfaces (denoted with the matching color + symbols). The thick solid black line shows the integrated area under each colored line. The thick dashed black line denotes the vertical resolution (full width at half maximum) approximately scaled into kilometers. The right hand plots show the horizontal averaging kernels in a similar manner, where the profiles are spaced at 1.5° great circle angle (approximately 165 km).

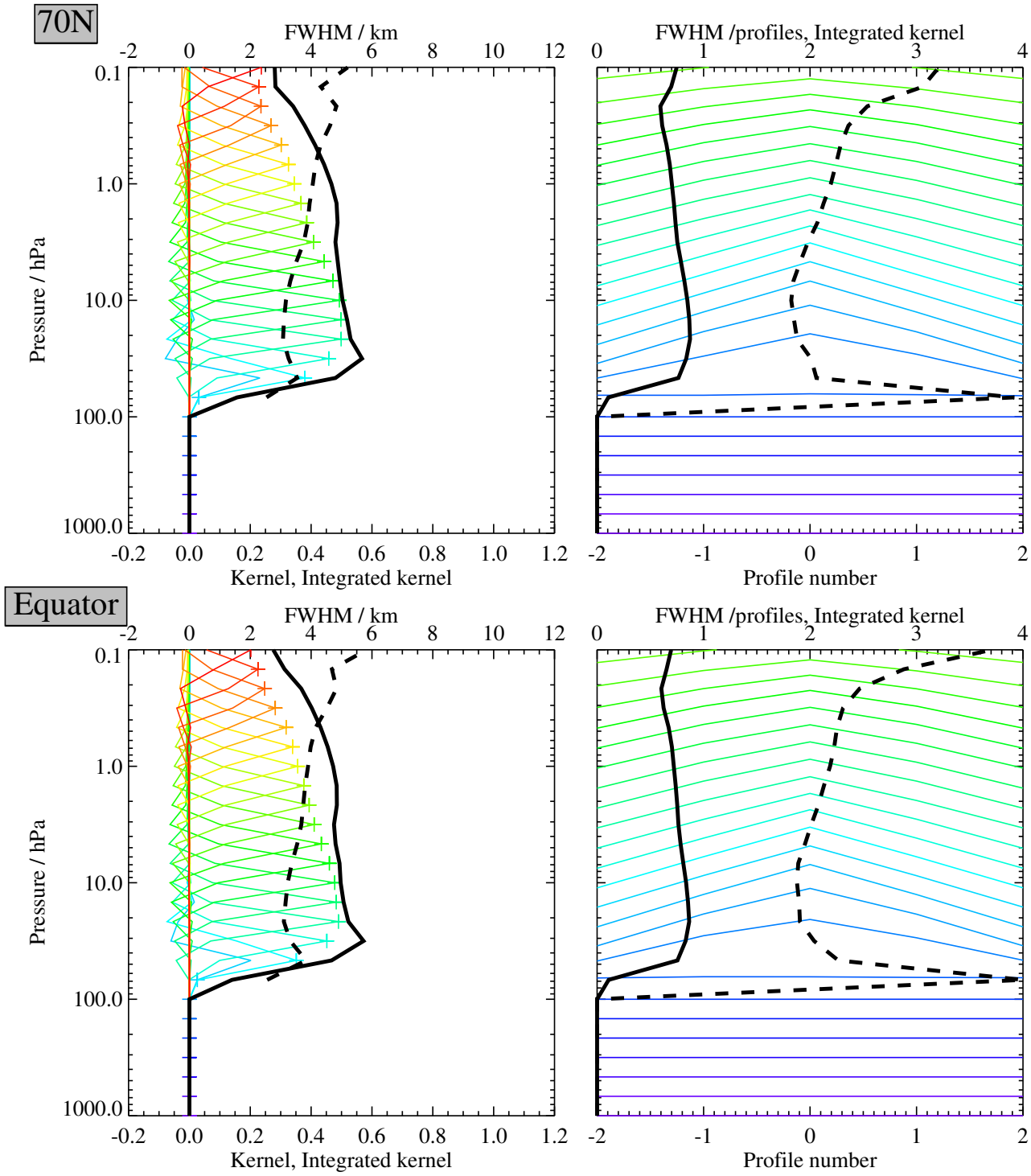

Figure A.28: The left hand plots show the vertical averaging kernel for 2.5 THz O_3 for the `1996d051` test data set. The colored lines denote the averaging kernels for individual retrieved surfaces (denoted with the matching color + symbols). The thick solid black line shows the integrated area under each colored line. The thick dashed black line denotes the vertical resolution (full width at half maximum) approximately scaled into kilometers. The right hand plots show the horizontal averaging kernels in a similar manner, where the profiles are spaced at 1.5° great circle angle (approximately 165 km).

- Based on Figure A.27, the vertical resolution for `O3-640` is 3 km in the lower stratosphere, and about 3 km in the recommended useful vertical range.
- Based on Figure A.28, the vertical resolution for `O3-2T5` is 3 km in the lower stratosphere, and increases to 4 km near 0.46 hPa.

Early Results and Validation

Since the ozone standard product (`O3-240`) is the main ozone product and is being validated in a variety of ways, we will mostly provide comparisons of the diagnostic products with the standard ozone product. We have observed that in the cases studied to date (see Figure A.29, as an example versus SAGE II data), the `O3-240` retrievals provide the best overall comparisons, although this may not be true in the lower mesosphere, where it tends to have somewhat of a high bias. There is a slightly low bias in the uppermost stratosphere for all O_3 products.

Figure A.30 shows an example of zonal mean diagnostic ozone products compared to the standard ozone product (`O3-240`) for June 15, 2005. The `O3-190` is on the low side but within 10%, except above the stratopause. `O3-640` is in general closer to the standard product values than is `O3-190` in the stratosphere but has some higher ozone values around the ozone peak. `O3-2T5` is comparable to `O3-640` in the stratosphere, but it goes in the opposite direction in the mesosphere (higher than the standard ozone values).

Real data retrievals (August 2004 – June 2005) indicate that zonal averaged differences (in 5°bins) between the `O3-190`, `O3-640`, `O3-2T5` products and the standard ozone product are within 10% in the lower mesosphere and stratosphere with some exceptions (Figure A.31, Figure A.32).

Figure A.33 shows the percent difference of diagnostic ozone against standard ozone on six typical pressure levels for all the retrievals as of the time of writing this document. Both Figure A.33 and Figure A.34 indicate that the retrievals are generally stable for all the diagnostic products. The largest differences occur at high latitudes and large pressures.

190 GHz O_3 `O3-190` has generally lower values than the standard ozone product, with differences reaching −0.9 ppmv in the equatorial region around the peak of the profile. In the 100 – 147 hPa range especially at low latitudes, `O3-190` shows larger percentage differences (>20%) and is not recommended there.

640 GHz O_3 shows a consistently higher bias (10% or as high as 1 ppmv) against the standard ozone product between 20 – 30 hPa just below the peak of the ozone profile in the equatorial and mid-latitude range. It oscillates between −5% and 5% of the standard product values in most of the stratosphere and lower mesosphere, but is generally higher than the standard ozone by about 5% in the stratosphere. Larger differences (of more than 10%) occur in the lower latitudes (≤60°) around 20 hPa. Both `O3-190` and `O3-640` are lower than the standard ozone by up to 30% in the lower mesosphere. `O3-640` matches the standard ozone values better than `O3-190` in this region. However, the standard product seems to be biased high there. We will continue to investigate this issue. In the lower stratosphere and upper troposphere, the differences depend on both latitude and season. Accordingly this diagnostic product is not recommended for use at altitudes below 68 hPa, especially latitudes equatorward of 55°. Larger differences occur in the Antarctic ozone hole period in the lower stratosphere in both the `O3-190` and `O3-640`, so one needs to use caution in this time and region; more validation is needed in this respect for all the ozone products, but the standard product is still the product of choice.

2.5 THz O_3 is in general significantly noisier and has higher values than the standard ozone product in the mesosphere and lower stratosphere, but it shows lower values in the upper stratosphere. It is lower than the standard ozone by about 10 – 15% in the upper stratosphere and higher by about 10 – 15% in the lower stratosphere. Figure A.31 and Figure A.32 show a strong seasonal dependence of `O3-2T5` differences

with respect to the standard ozone product. The maximum differences (∼25%) appear in the winter polar region. Localized anomalies of about 10% (Figure A.32) in the equatorial region above 10 hPa, shown in June 2005, need to be further investigated. The O_3 emission temperature sensitivity (which is large for the 2.5 THz lines) is somewhat uncertain and seems to be affecting the stability of this product.

Data Screening

Pressure range: Values outside the recommended ranges are not recommended for use. The standard ozone product is preferred for all heights.

Estimated Precision: Values at altitudes where the estimated precision is flagged negative should not be used, to avoid too strong an *a priori* influence (see section 1.3).

Status flag: Any profile for which status is an odd number should not be used (see section 1.4).

Clouds: Given that we are not recommending these non-standard ozone products for pressure $\geq$ 68 hPa, there is currently no apparent need to discard profiles or profile portions where status values indicate the existence/influence of clouds (see section 1.4).

Artifacts

- Significant oscillations are observed in the tropical lower stratosphere and upper troposphere, where these products are losing sensitivity and are not recommended for use.
- The THz product (`O3-2T5`) seems to have a temperature/seasonal dependence.

Priorities for future data version(s)

We will continue investigations of the larger differences between the various bands, but many of the results are not outside our expectations, given the 5% or larger (especially for the THz data) uncertainties that are expected from potential errors in spectroscopy and its temperature dependence. Priority will be given to improving the 240 GHz standard ozone product.

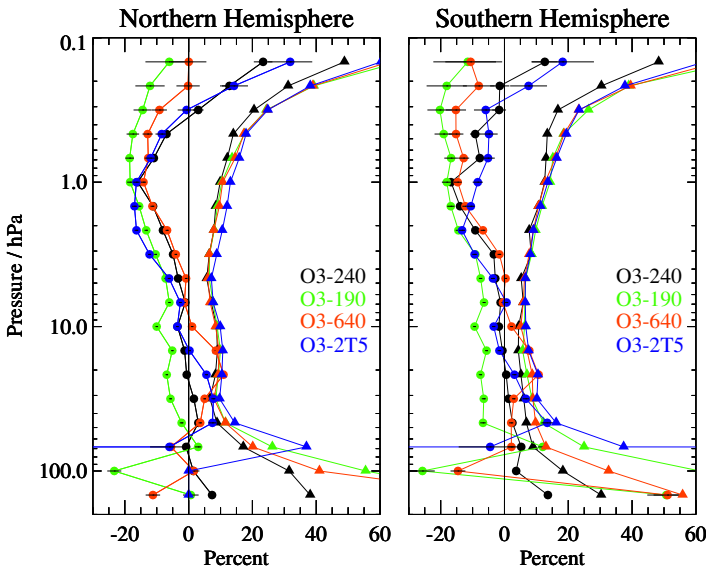

Figure A.29: MLS and SAGE II O3 comparisons: Average differences (circles) for northern hemisphere (left panel) and southern hemisphere (right panel) are given for MLS minus SAGE II abundances, expressed as a percent difference from the corresponding averaged SAGE II profiles, with error bars representing twice the estimated error in the means; if no error bar is apparent, it is small and hidden by the symbol itself. Also shown are the standard deviations of the differences (triangles).

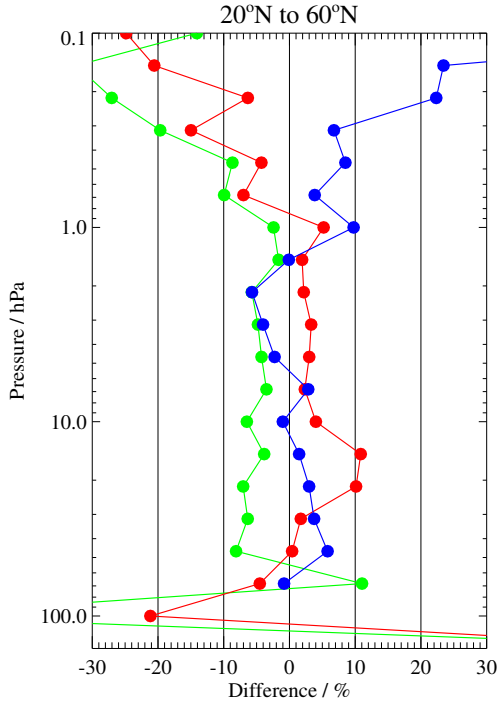

Figure A.30: Example of diagnostic ozone vertical profile zonal mean comparisons (percent differences from the standard product) on June 15, 2005. Red line is `O3-640`, green line is `O3-190`, and blue line is `O3-2T5`.

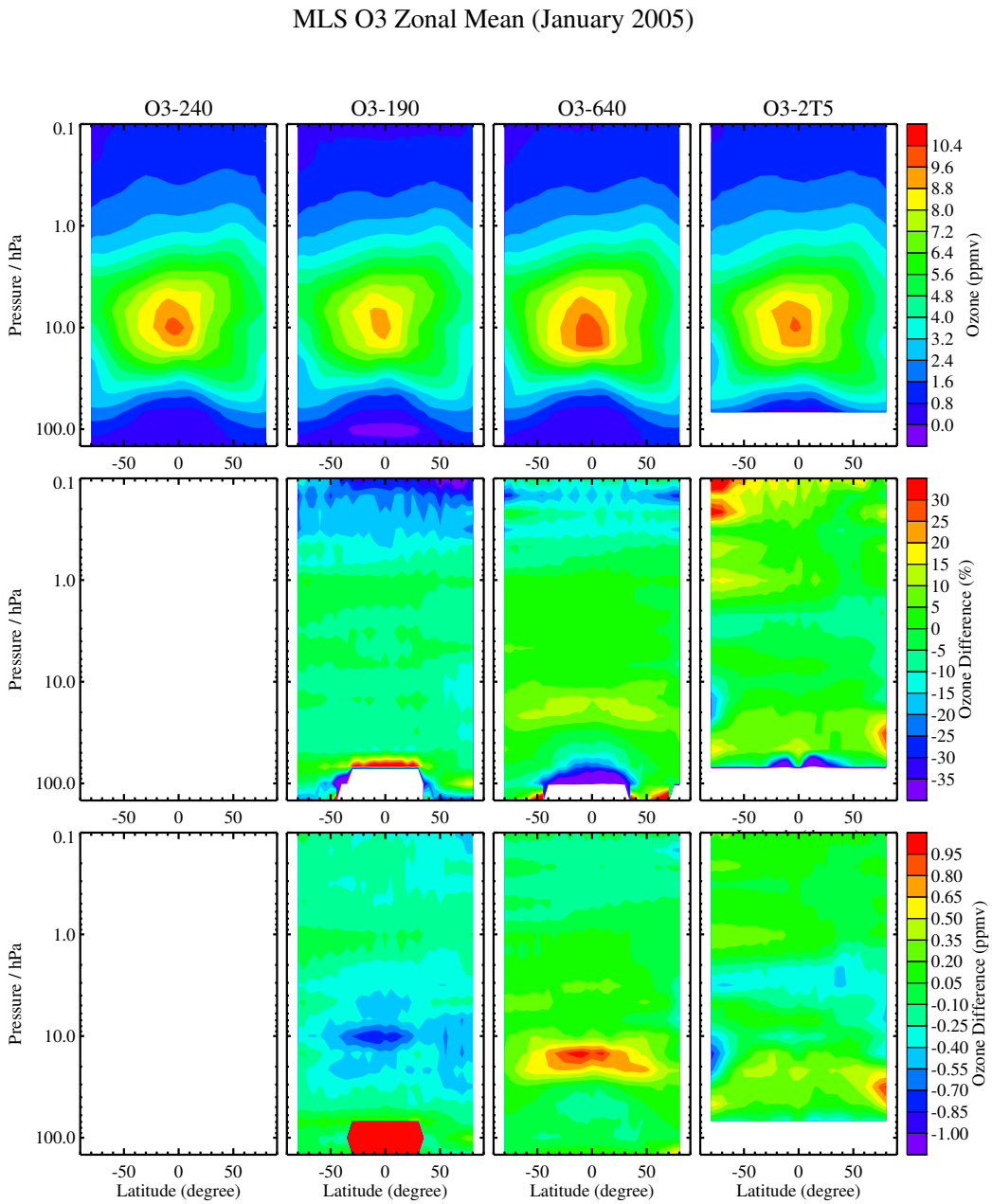

Figure A.31: Example of the diagnostic and standard ozone products for January 2005. The top panel shows the ozone abundances; the middle panel gives the percentage differences between the diagnostic ozone and standard ozone; the bottom panel shows the absolute differences in ppmv.

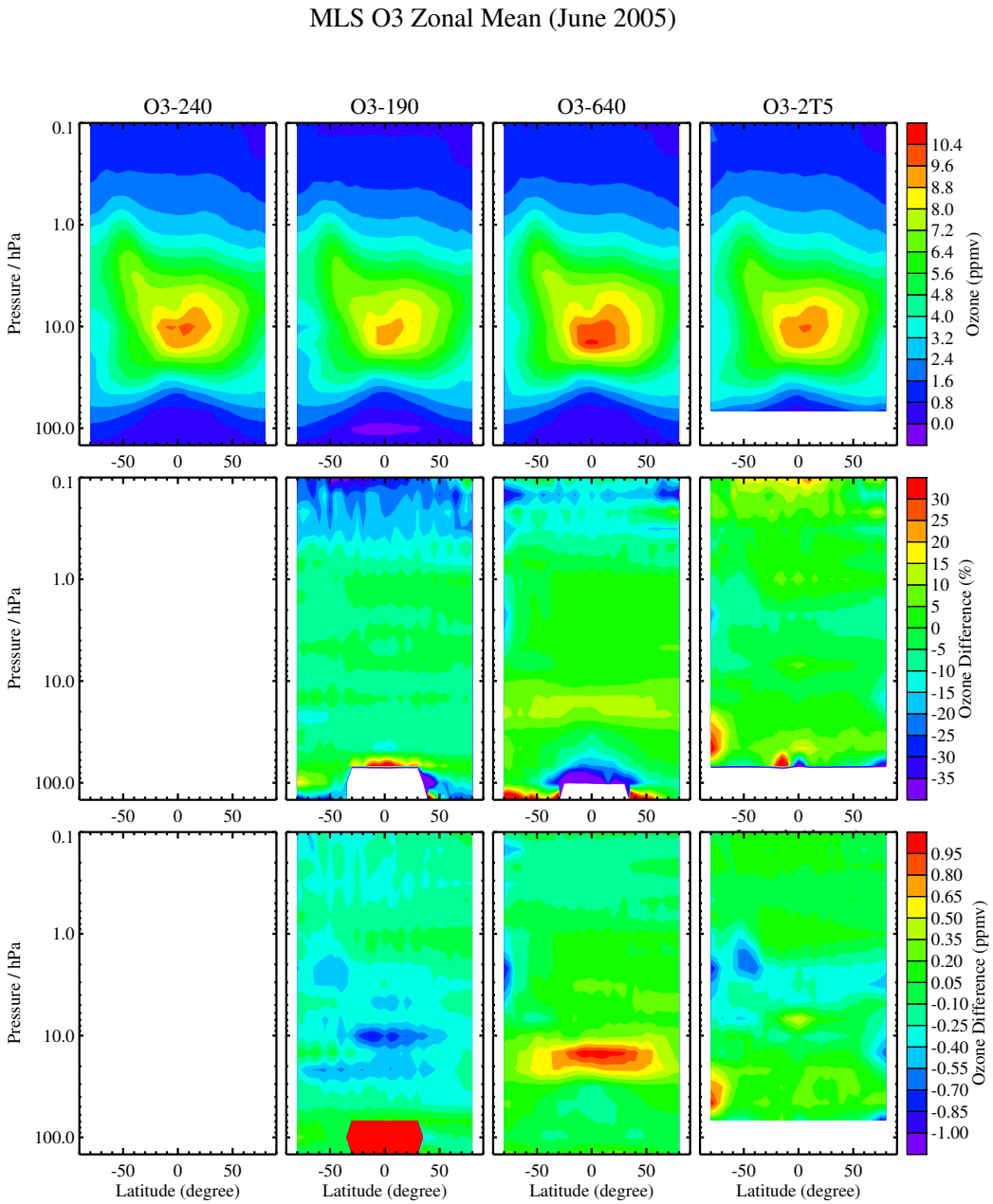

Figure A.32: Same as last figure, except for June 2005.

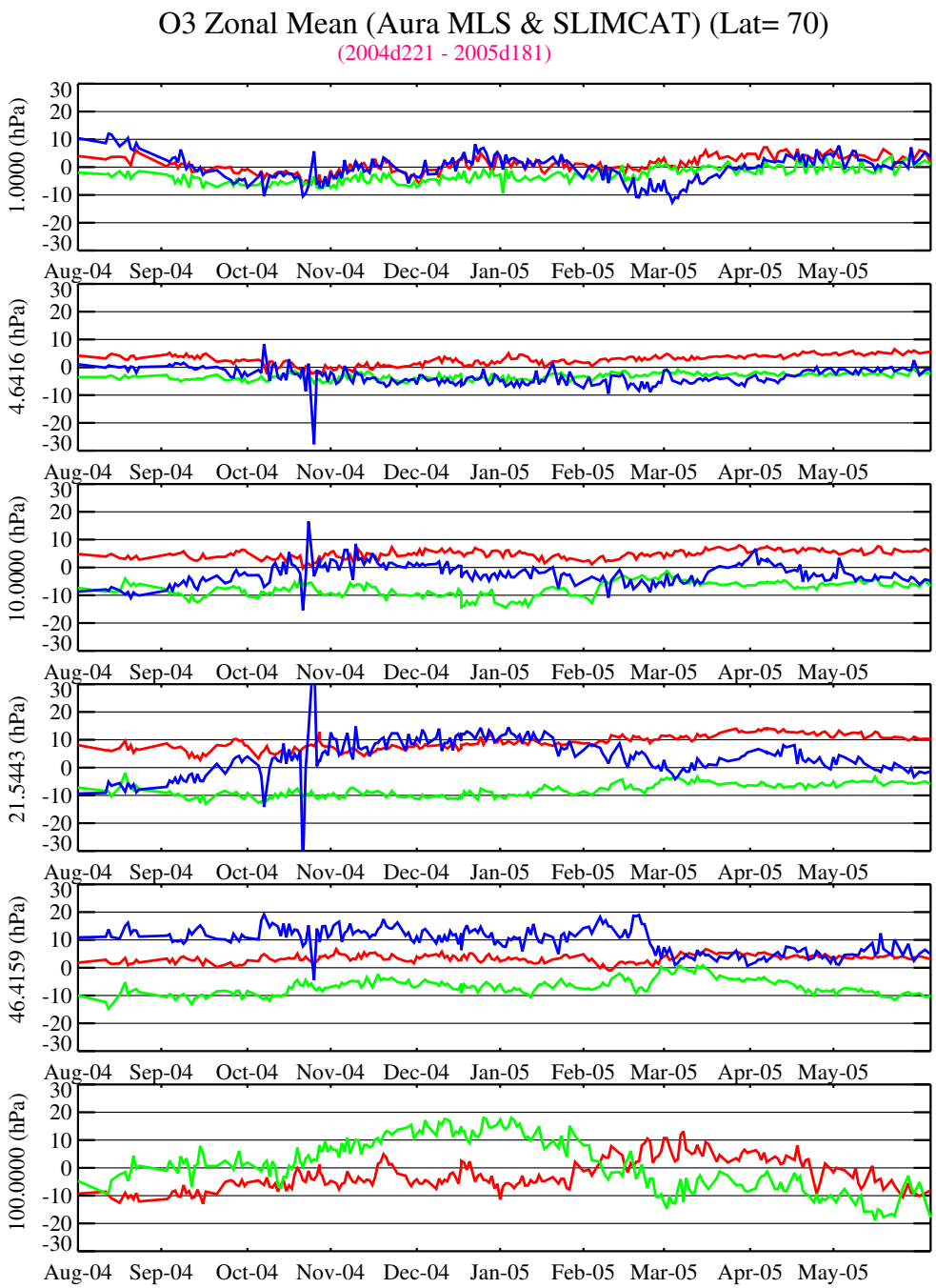

Figure A.33: Percent differences at 70°N on six pressure levels between the various MLS retrievals of O_3 and the standard (240 GHz) MLS O_3 retrieval from January to June 2005. Red line is `O3-640`, green line is `O3-190`, and blue line is `O3-2T5`.

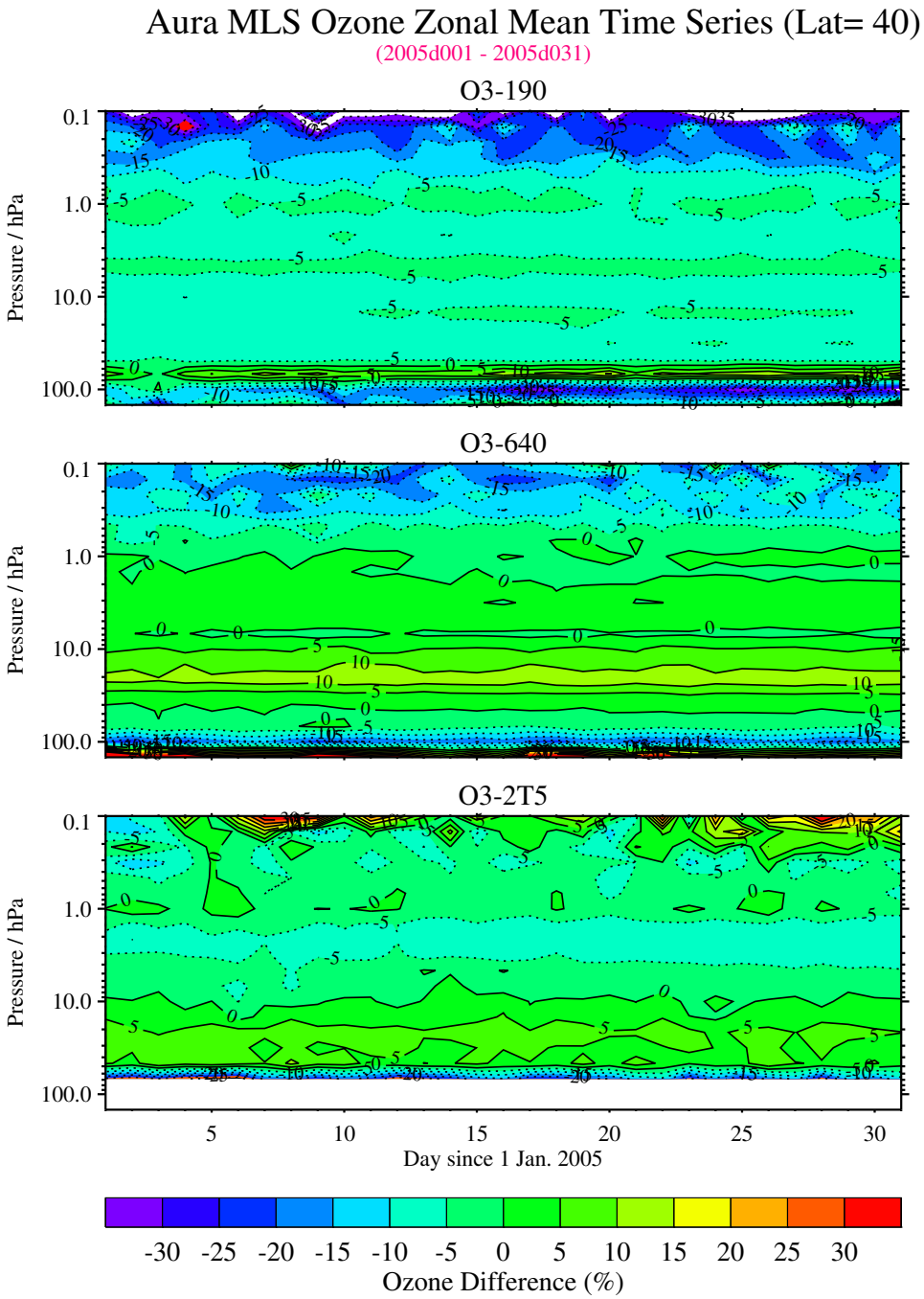

Figure A.34: Percent differences at 40°N between the various MLS retrievals of O3 (top panel for `O3-190`, middle panel for `O3-640` and bottom panel for `O3-2T5`) and the standard (240 GHz) MLS O_3 retrieval during January 2005. A positive difference means that the diagnostic ozone products give a larger value than the standard product.

A.10 Temperature from various retrieval phases

Swath name: `Temperature-phase`

Contact: Michael Schwartz, **Email:** `<michael@mls.jpl.nasa.gov>`

Each phase of the MLS v1.5 software produces it's own temperature retrieval, consistent with the set of radiances and uncertainties used in that phase. Some radiances (e.g., band 1) are used in all phases while others (e.g., band 8 in Core+R3) are only used in a single phase.

The standard product for temperature is taken from the Core retrieval from 316 – 1.41 hPa and from Core+R2A from 1 – 0.001 hPa. Temperature from other phases are stored as diagnostic products. Temperatures from Core+R2A and Core+R3 have superior vertical resolution to those of Core in the upper troposphere and lower stratosphere (UTLS)

but preliminary validation shows them to have larger biases than Core (see Figure A.56) and have instability to vertical oscillations at the lowest retrieval levels (316 – 100 hPa.) Core+R2A includes a full-forward-model calculation in the opaque 183-GHz H_2O line center; its temperature has slightly better vertical resolution in the troposphere and is expected to be more accurate than that of the linearized Core+R2B.

Simulations

Simulated retrievals (see Figures A.35 – A.48) have similar biases and estimated precisions for all phases, with larger systematic differences between the two test days than among the phases. Biases in simulations are generally less than 1 K in the upper troposphere and stratosphere, except as noted below. The lowest retrieved level often shows larger biases (for example in Figure A.36 in the northernmost bin.) Retrieval biases for `1996d051` have a vertical oscillation in the upper stratosphere and lower mesosphere (near 1 hPa) of $\pm 1 - 2$ K magnitude and the `2000d276` simulations are poorly-behaved in the upper mesosphere and lower thermosphere (above 0.1 hPa.) The Core+R4A and Core+R4B retrieval range is 141 – 0.001 hPa and the Core+R5 retrieval range is 100 – 0.001 hPa and the 2000d276 retrieval shows a 1-K vertical oscillation in the lowest retrieved levels.

Vertical resolution

Vertical resolutions of the temperatures from the different phases (shown in Figures A.49 – A.55) are generally similar to that of the standard product except in the UTLS. Here, the Core+R2A and Core+R3 products have superior vertical resolution to that of Core, particularly in the upper troposphere and lower stratosphere where they benefit from isotopic O_2 line in band 8 and the saturated water vapor line in band 2, respectively. Averaging kernel FWHM in the UTLS peak at 8 km for Core at 141 hPa, 5.5 km for Core+R2A at 215 hPa, 6 km for Core+R2B at 215 hPa, 4.5 km for Core+R3 at 215 hPa and at 6 km for Core+R4A,B at 100 hPa. Core+R2A's use of a full forward model on strong water vapor lines accounts for its superior vertical resolution to Core+R2B.

Early results and validation

Figure A.56 compares shows average differences between the various MLS temperature products and the temperature from the GEOS assimilation model. Core+R3, which has the best vertical resolution of the phases, displays vertical oscillation in its lowermost levels. Day averages are 8 – 9 K warmer than GEOS-4 at 316 hPa, cooler by 2 – 3 K at 100 hPa and have larger variances at these levels than can be attributed to narrower averaging kernels. It is hoped that the contribution of Core+R3's vertical resolution can be utilized in future versions, it is not recommended for use at this time.

Core+R2A Temperature is significantly better-behaved than Core+R3 Temperature in preliminary validation studies, although it does appear to be somewhat more prone to vertical oscillations than Core. Both Core+R2A and Core+R3 are significantly more stable than they were in previous versions of the software. Core is conservatively recommended as the standard temperature at retrieval levels below 1 hPa, but Core+R2A Temperature may be preferred for some work.

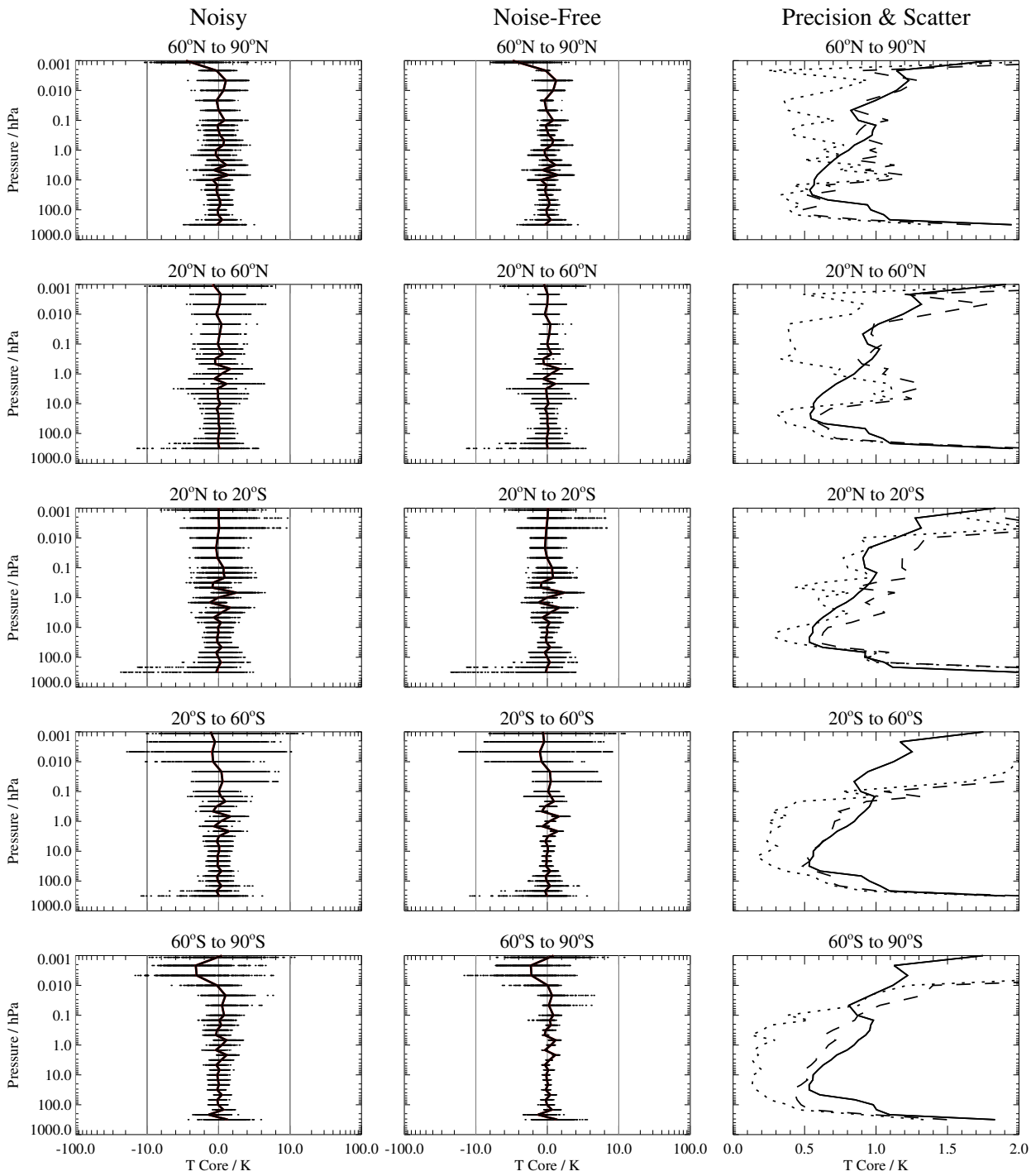

Figure A.35: A summary of the v1.5 data quality for Core Temperature for the `1996d051` test data set. Each row of panels represents a broad latitude bin. The first two columns show the differences between the retrieved Core Temperature and the true Temperature as a function of pressure, for the noisy and noise free case, along with a solid line which shows the median bias. The median bias of the `Status=0` profiles (i.e., those not significantly affected by clouds) is shown in red. The third column shows the mean estimated precision of Core Temperature (solid line), and the rms scatter about the mean bias in the noisy (broken line) and noise free (dotted line) cases.

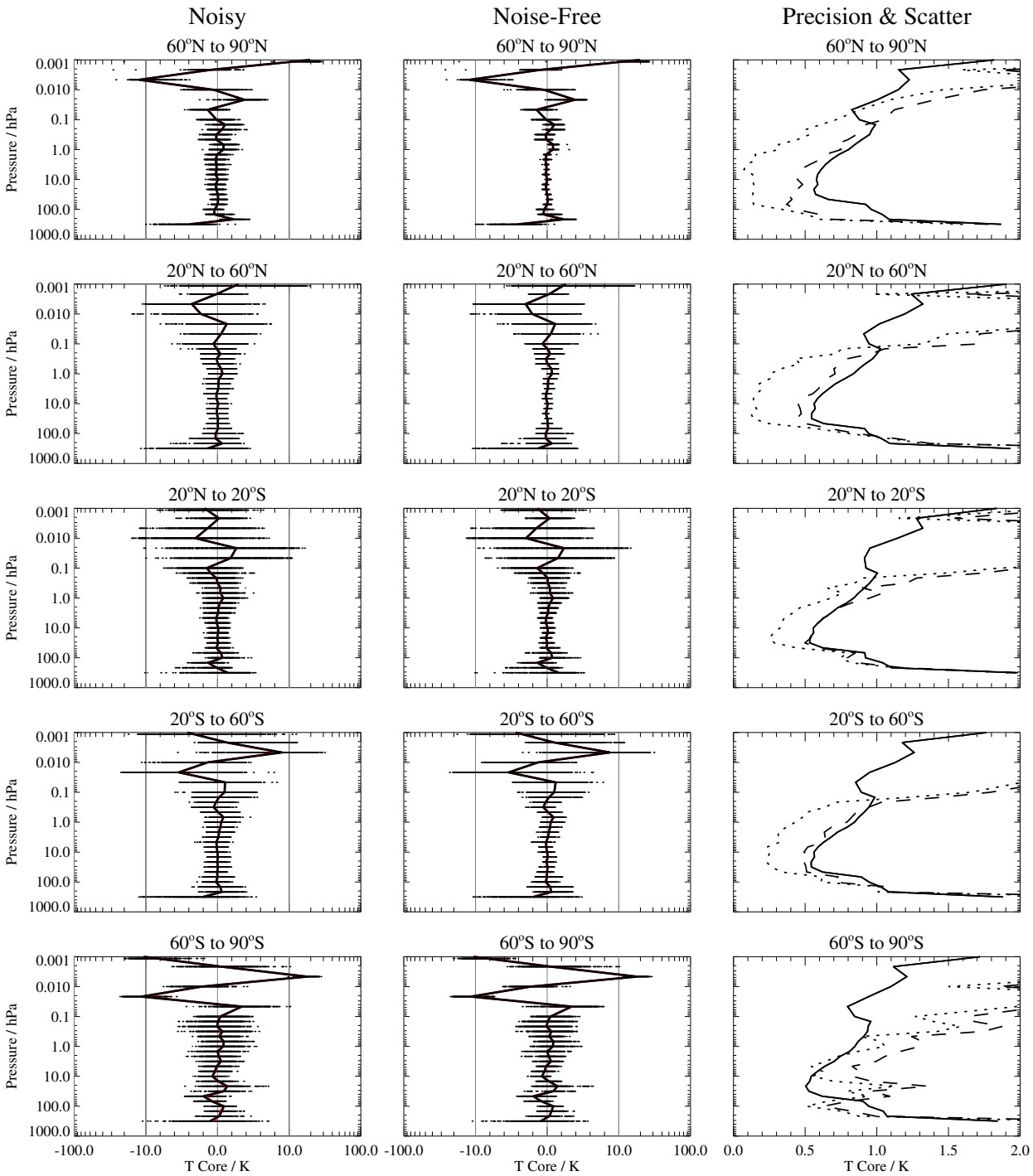

Figure A.36: A summary of the v1.3 data quality for Core Temperature, as for figure A.35 but for the `2000d276` test data set.

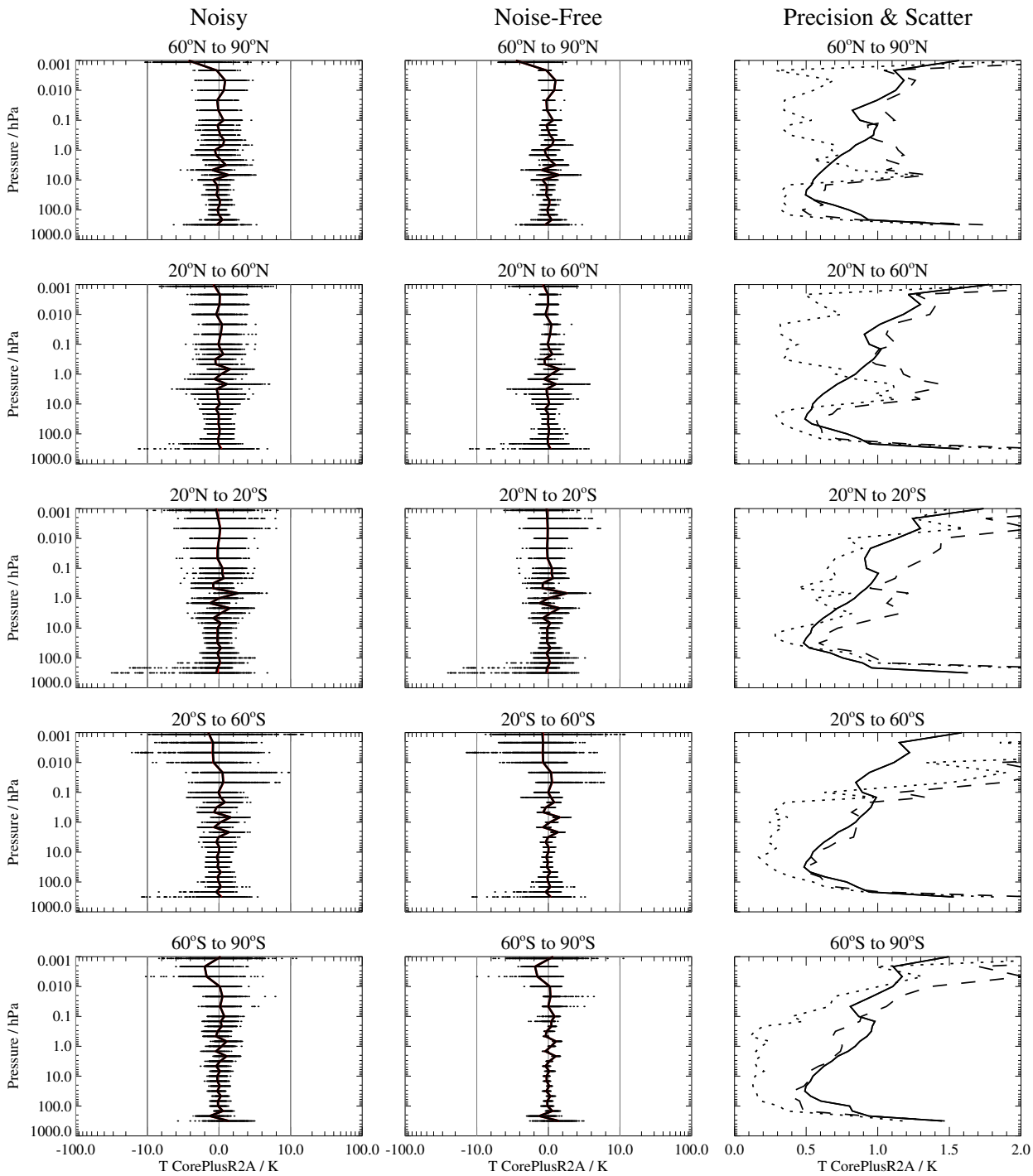

Figure A.37: A summary of the v1.5 data quality for Core+R2A Temperature for the `1996d051` test data set. Each row of panels represents a broad latitude bin. The first two columns show the differences between the retrieved Core+R2A Temperature and the true Temperature as a function of pressure, for the noisy and noise free case, along with a solid line which shows the median bias. The median bias of the `Status=0` profiles (i.e., those not significantly affected by clouds) is shown in red. The third column shows the mean estimated precision of Core+R2A Temperature (solid line), and the rms scatter about the mean bias in the noisy (broken line) and noise free (dotted line) cases.

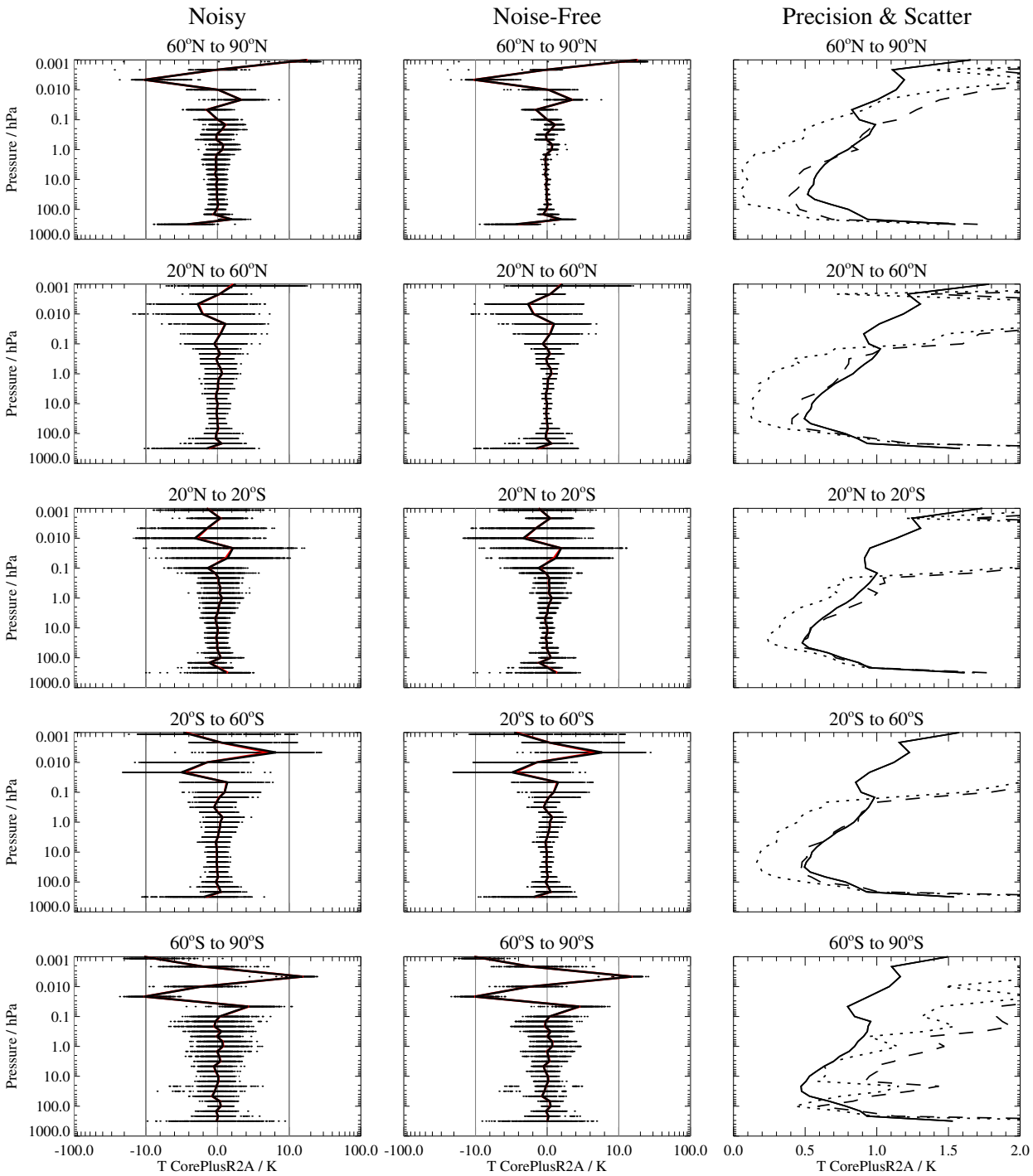

Figure A.38: A summary of the v1.3 data quality for Core+R2A Temperature, as for figure A.37 but for the `2000d276` test data set.

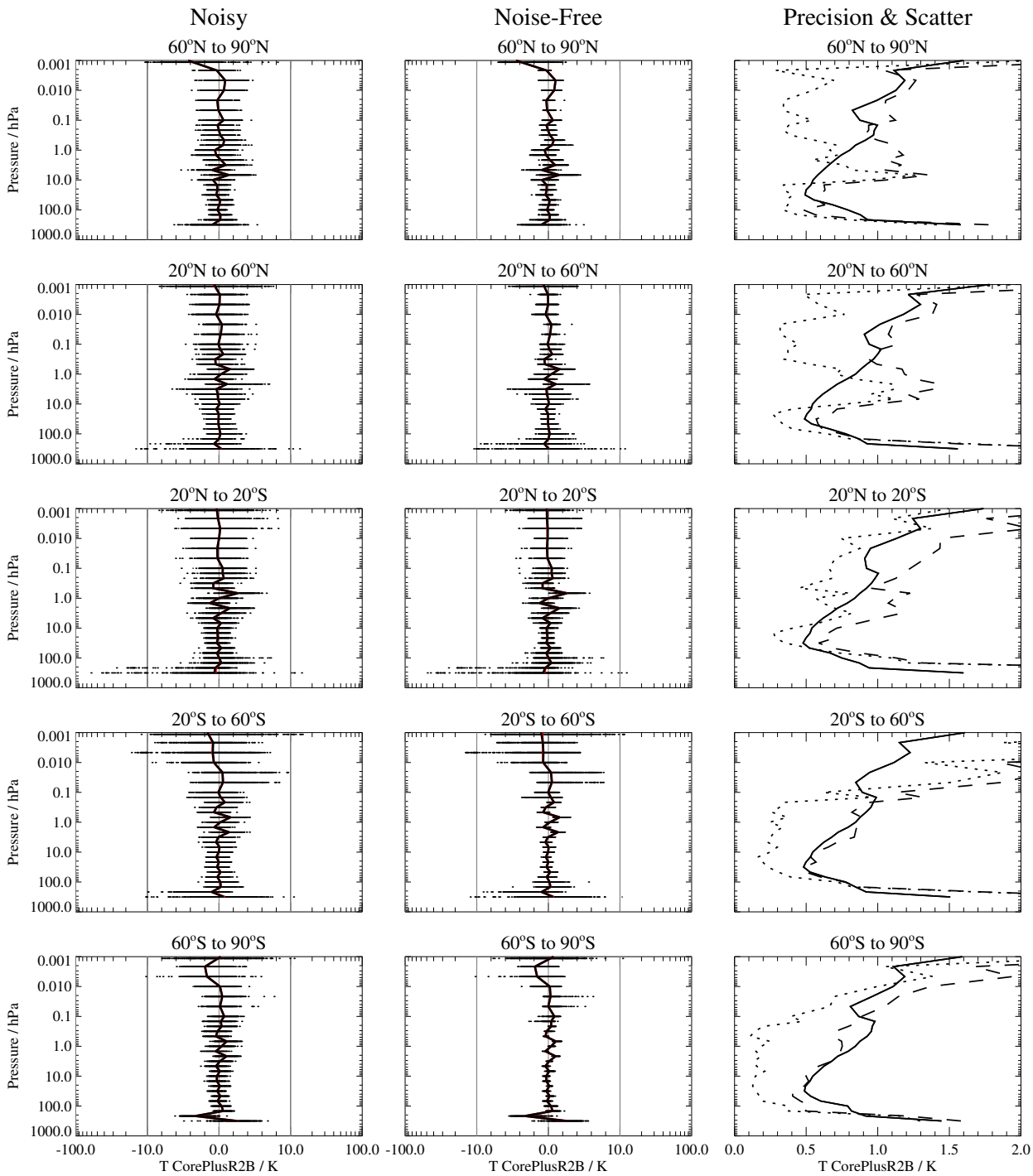

Figure A.39: A summary of the v1.5 data quality for Core+R2B Temperature for the `1996d051` test data set. Each row of panels represents a broad latitude bin. The first two columns show the differences between the retrieved Core+R2B Temperature and the true Temperature as a function of pressure, for the noisy and noise free case, along with a solid line which shows the median bias. The median bias of the `Status=0` profiles (i.e., those not significantly affected by clouds) is shown in red. The third column shows the mean estimated precision of Core+R2B Temperature (solid line), and the rms scatter about the mean bias in the noisy (broken line) and noise free (dotted line) cases.

T

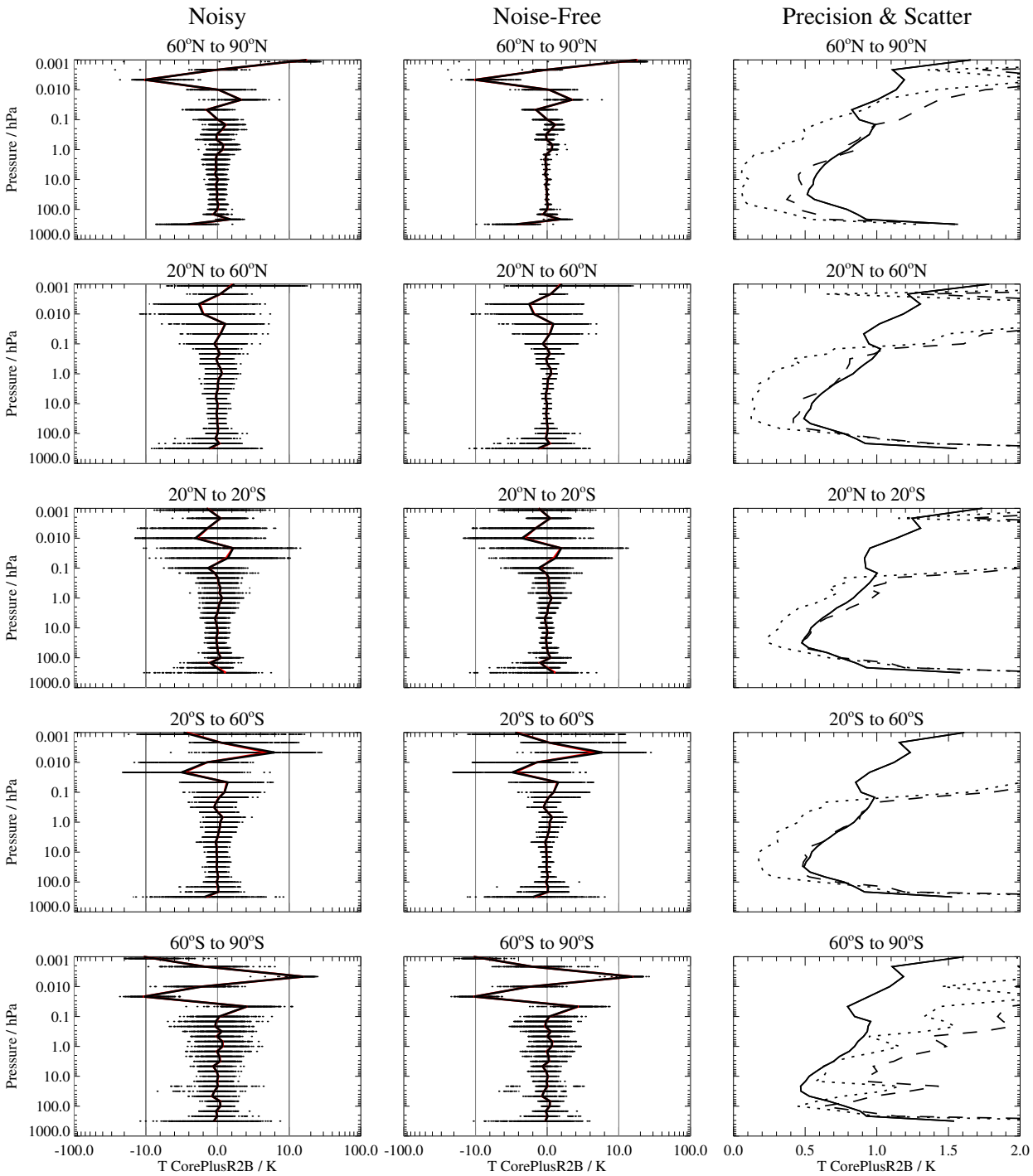

Figure A.40: A summary of the v1.3 data quality for Core+R2B Temperature, as for figure A.39 but for the `2000d276` test data set.

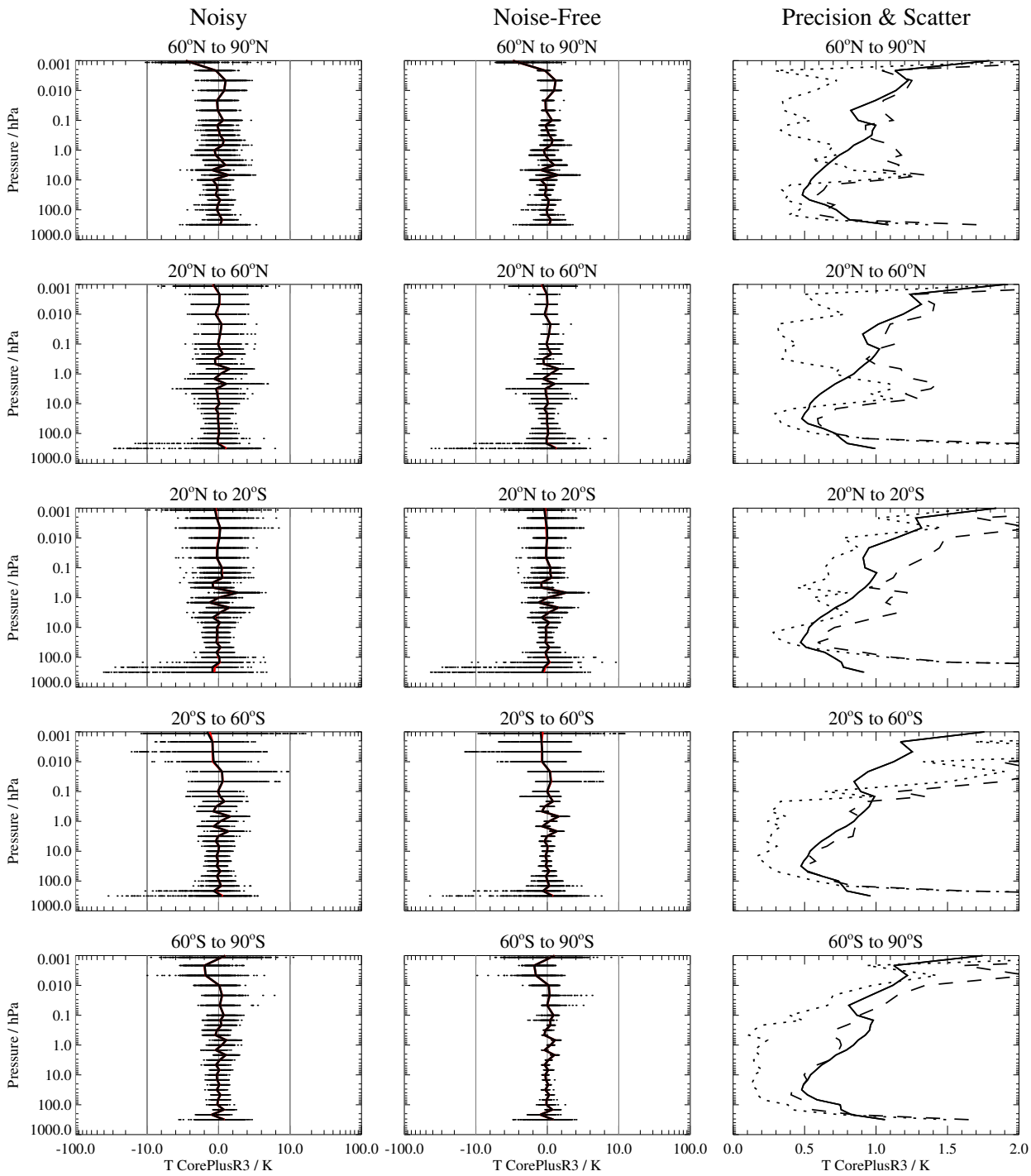

Figure A.41: A summary of the v1.5 data quality for Core+R3 Temperature for the `1996d051` test data set. Each row of panels represents a broad latitude bin. The first two columns show the differences between the retrieved Core+R3 Temperature and the true Temperature as a function of pressure, for the noisy and noise free case, along with a solid line which shows the median bias. The median bias of the `Status=0` profiles (i.e., those not significantly affected by clouds) is shown in red. The third column shows the mean estimated precision of Core+R3 Temperature (solid line), and the rms scatter about the mean bias in the noisy (broken line) and noise free (dotted line) cases.

T

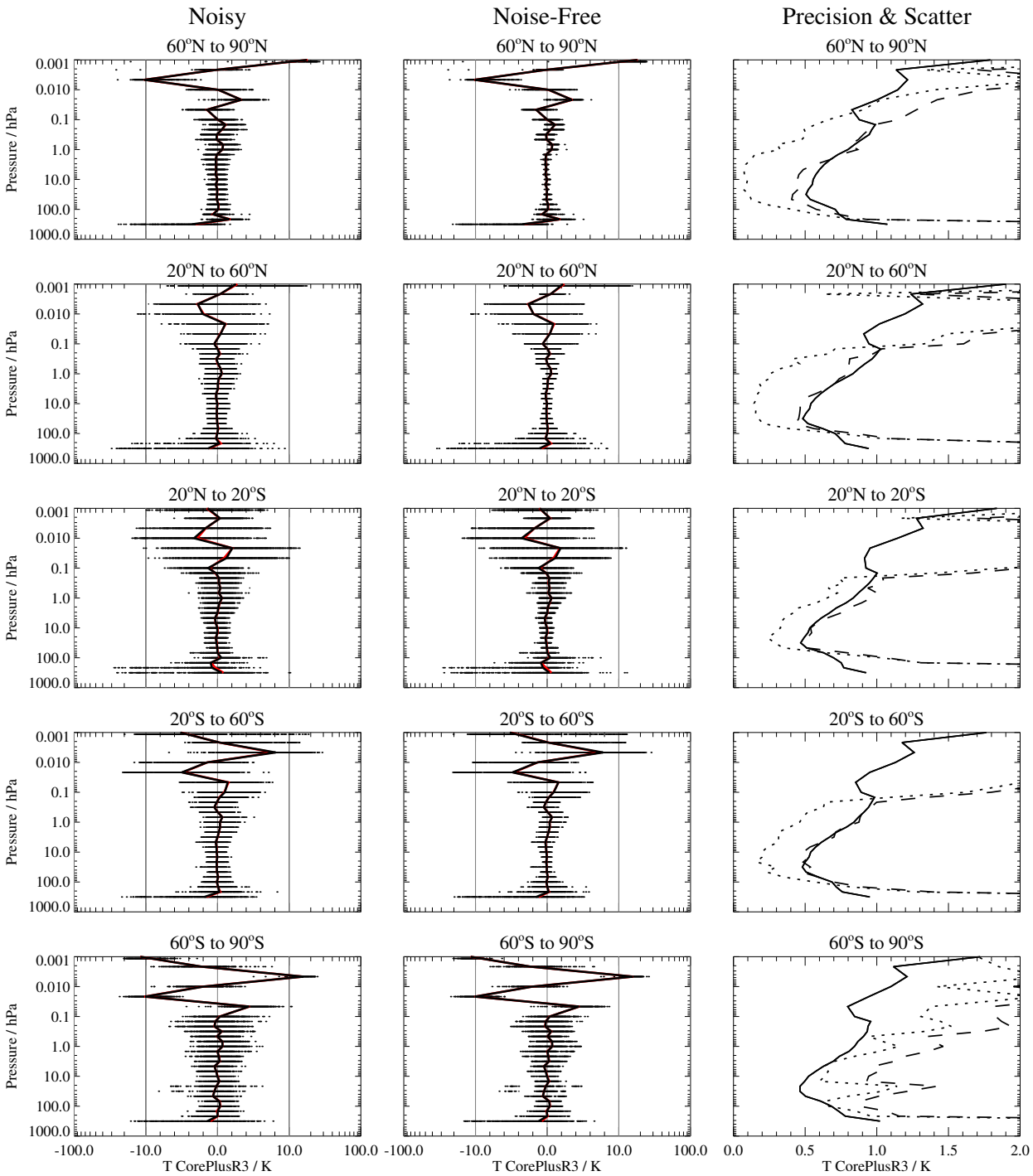

Figure A.42: A summary of the v1.3 data quality for Core+R3 Temperature, as for figure A.41 but for the `2000d276` test data set.

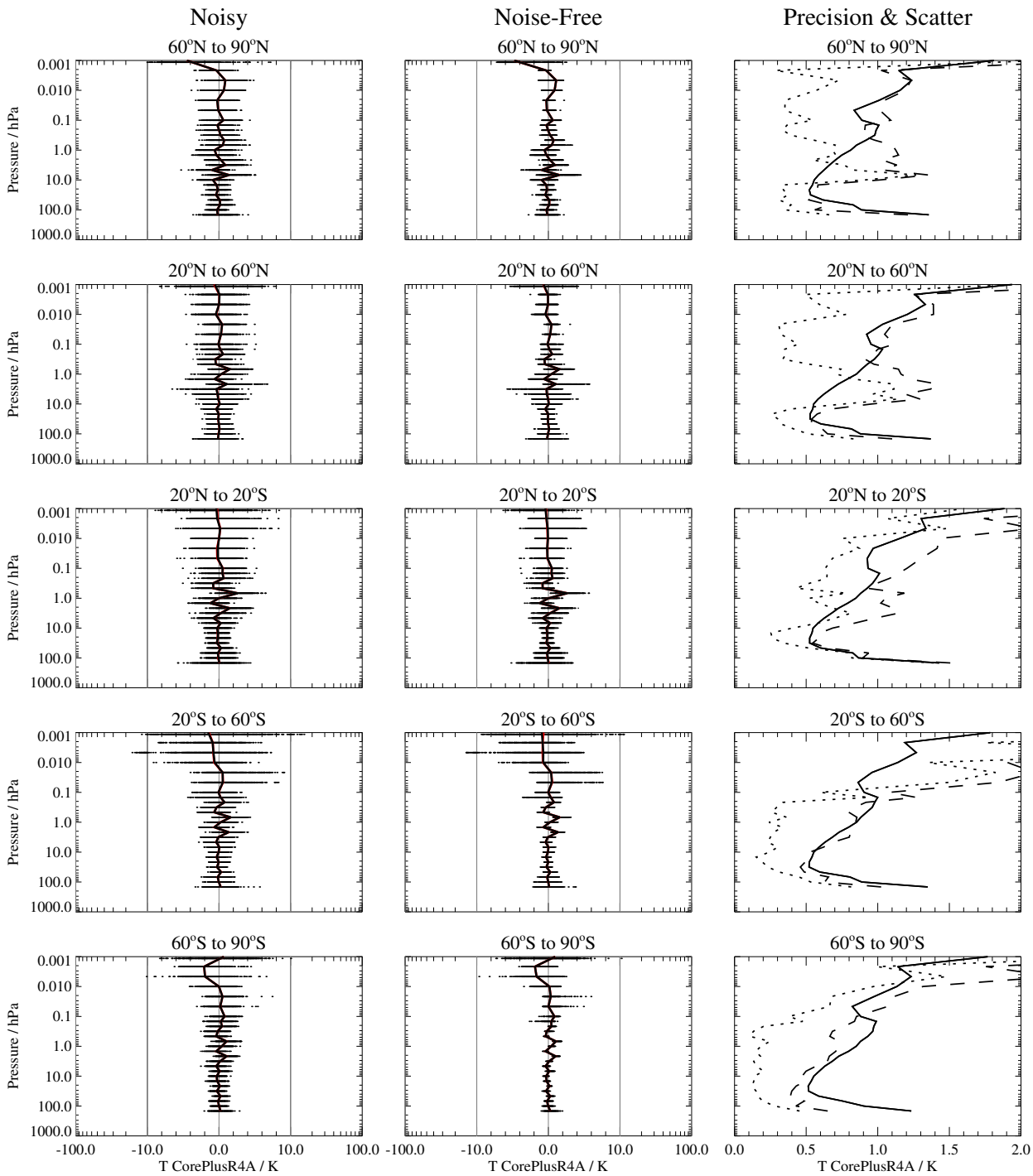

Figure A.43: A summary of the v1.5 data quality for Core+R4A Temperature for the `1996d051` test data set. Each row of panels represents a broad latitude bin. The first two columns show the differences between the retrieved Core+R4A Temperature and the true Temperature as a function of pressure, for the noisy and noise free case, along with a solid line which shows the median bias. The median bias of the `Status=0` profiles (i.e., those not significantly affected by clouds) is shown in red. The third column shows the mean estimated precision of Core+R4A Temperature (solid line), and the rms scatter about the mean bias in the noisy (broken line) and noise free (dotted line) cases.

T

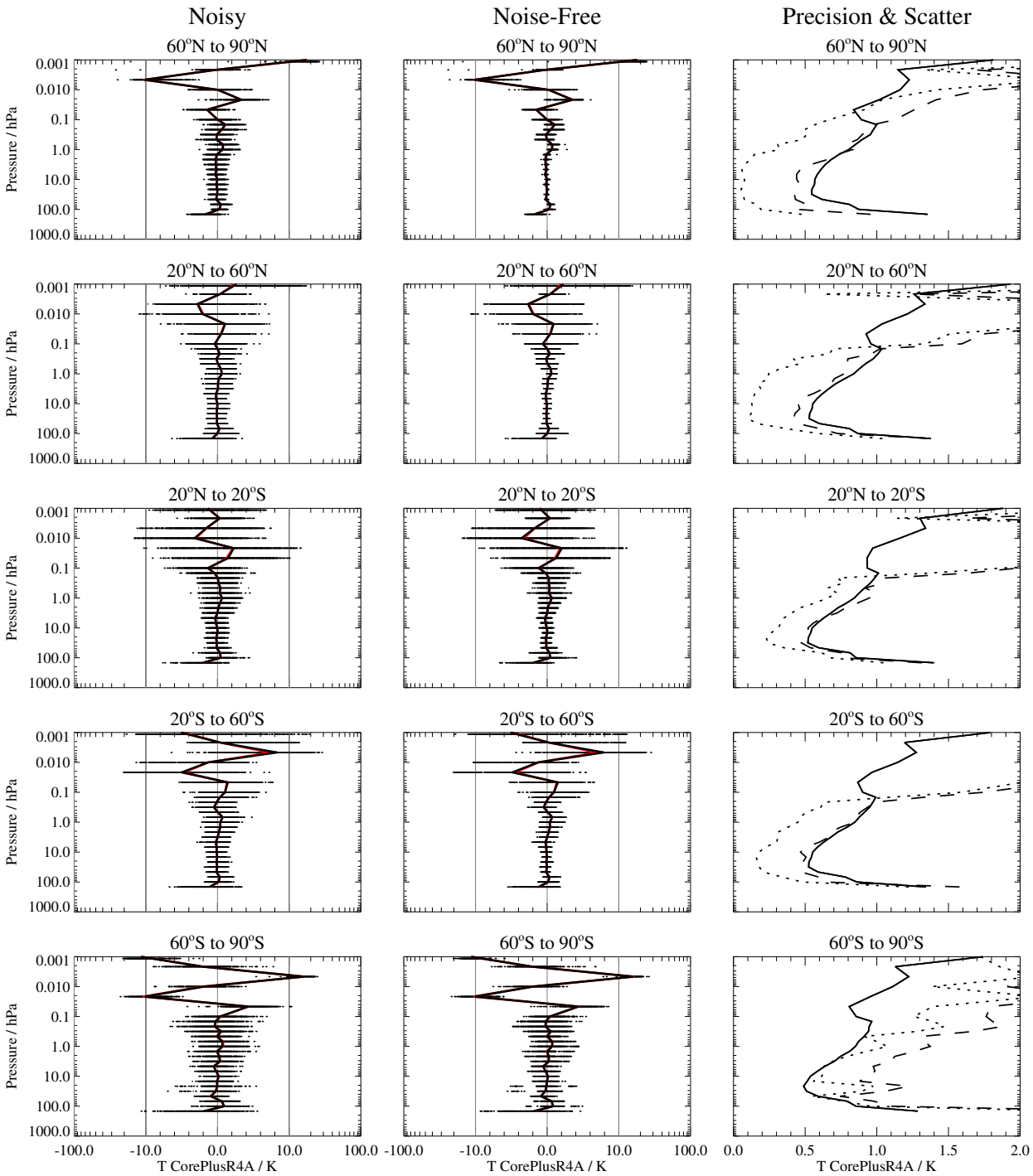

Figure A.44: A summary of the v1.3 data quality for Core+R4A Temperature, as for figure A.43 but for the `2000d276` test data set.

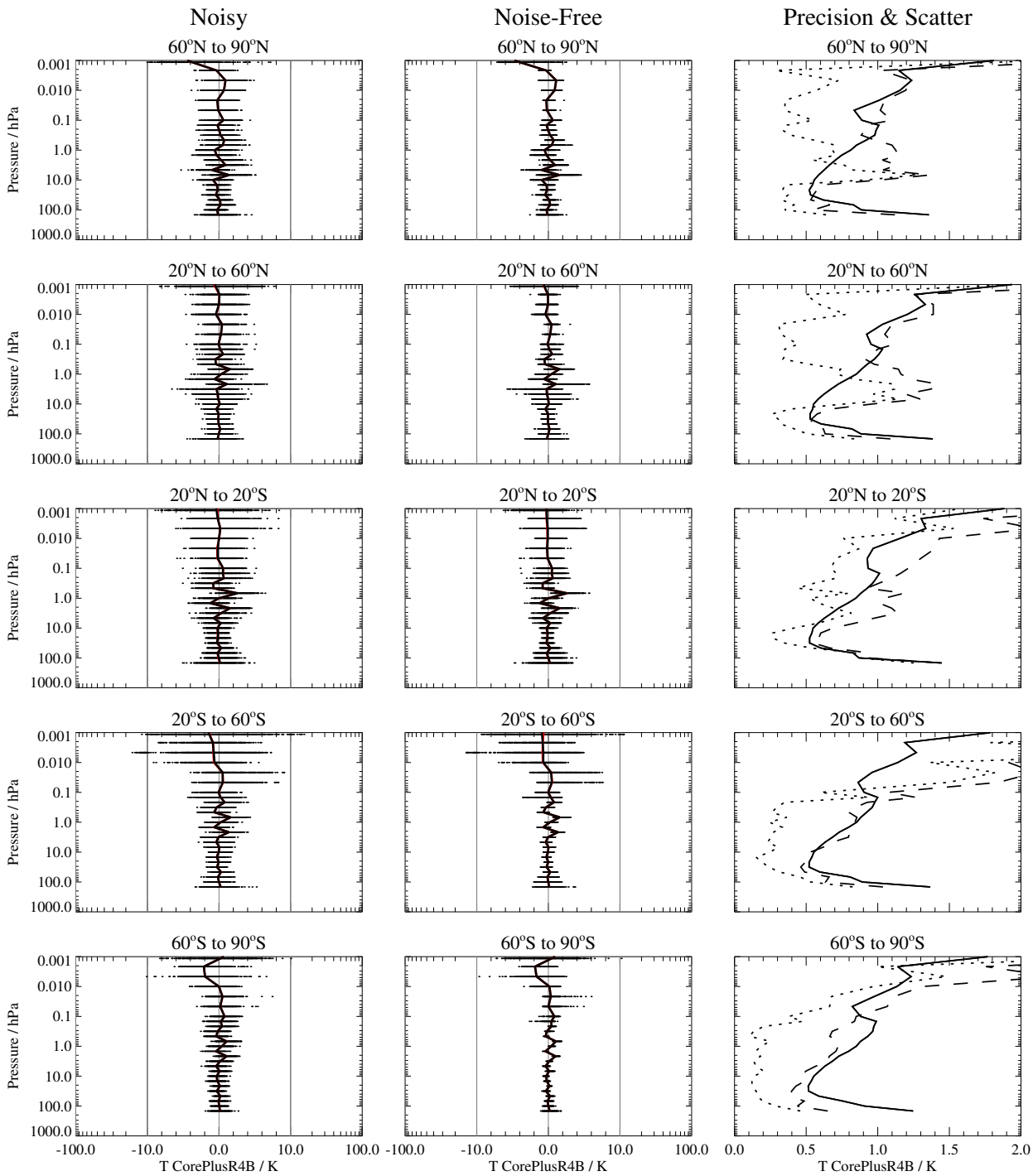

Figure A.45: A summary of the v1.5 data quality for Core+R4B Temperature for the `1996d051` test data set. Each row of panels represents a broad latitude bin. The first two columns show the differences between the retrieved Core+R4B Temperature and the true Temperature as a function of pressure, for the noisy and noise free case, along with a solid line which shows the median bias. The median bias of the `Status=0` profiles (i.e., those not significantly affected by clouds) is shown in red. The third column shows the mean estimated precision of Core+R4B Temperature (solid line), and the rms scatter about the mean bias in the noisy (broken line) and noise free (dotted line) cases.

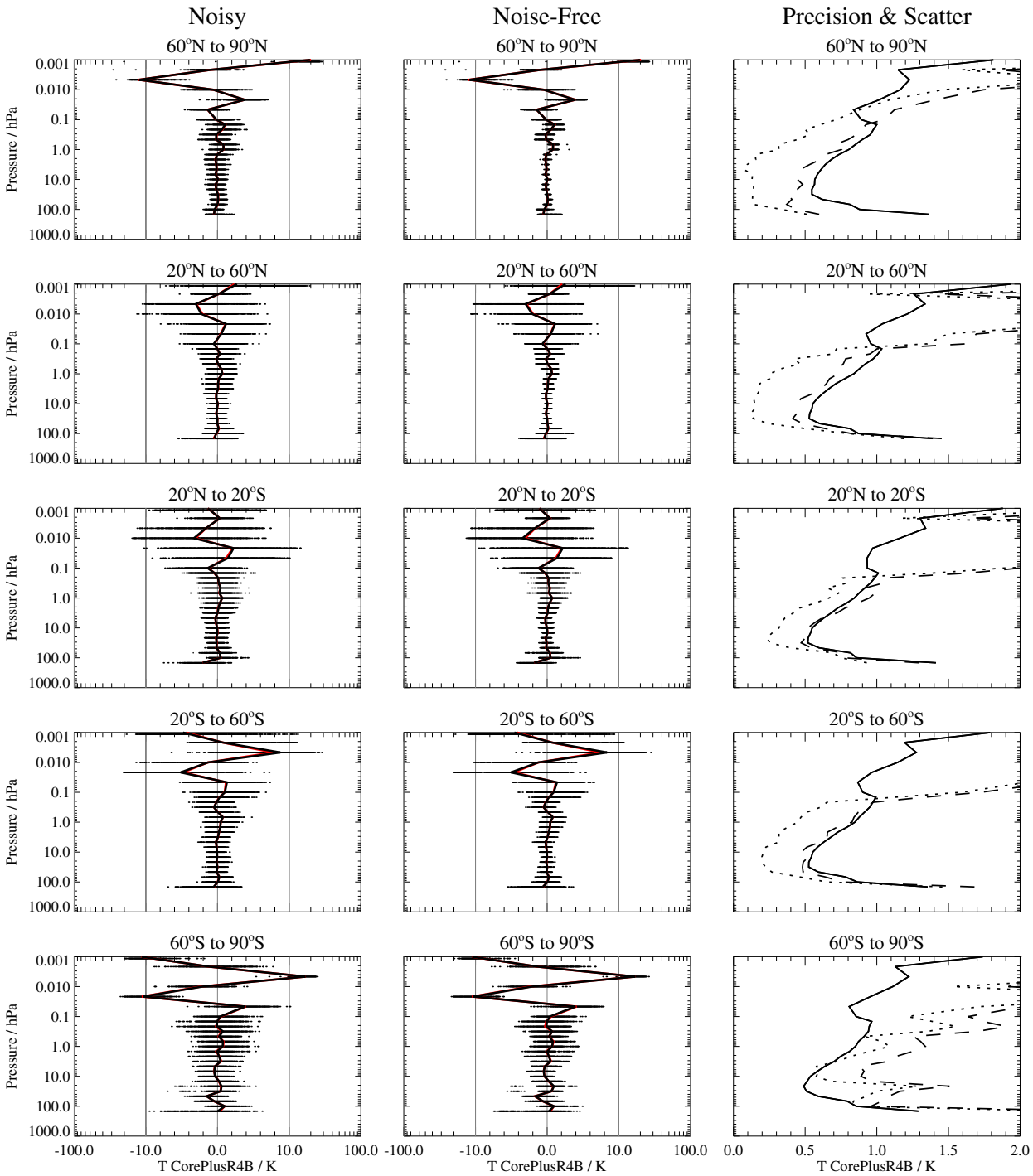

Figure A.46: A summary of the v1.3 data quality for Core+R4B Temperature, as for figure A.45 but for the `2000d276` test data set.

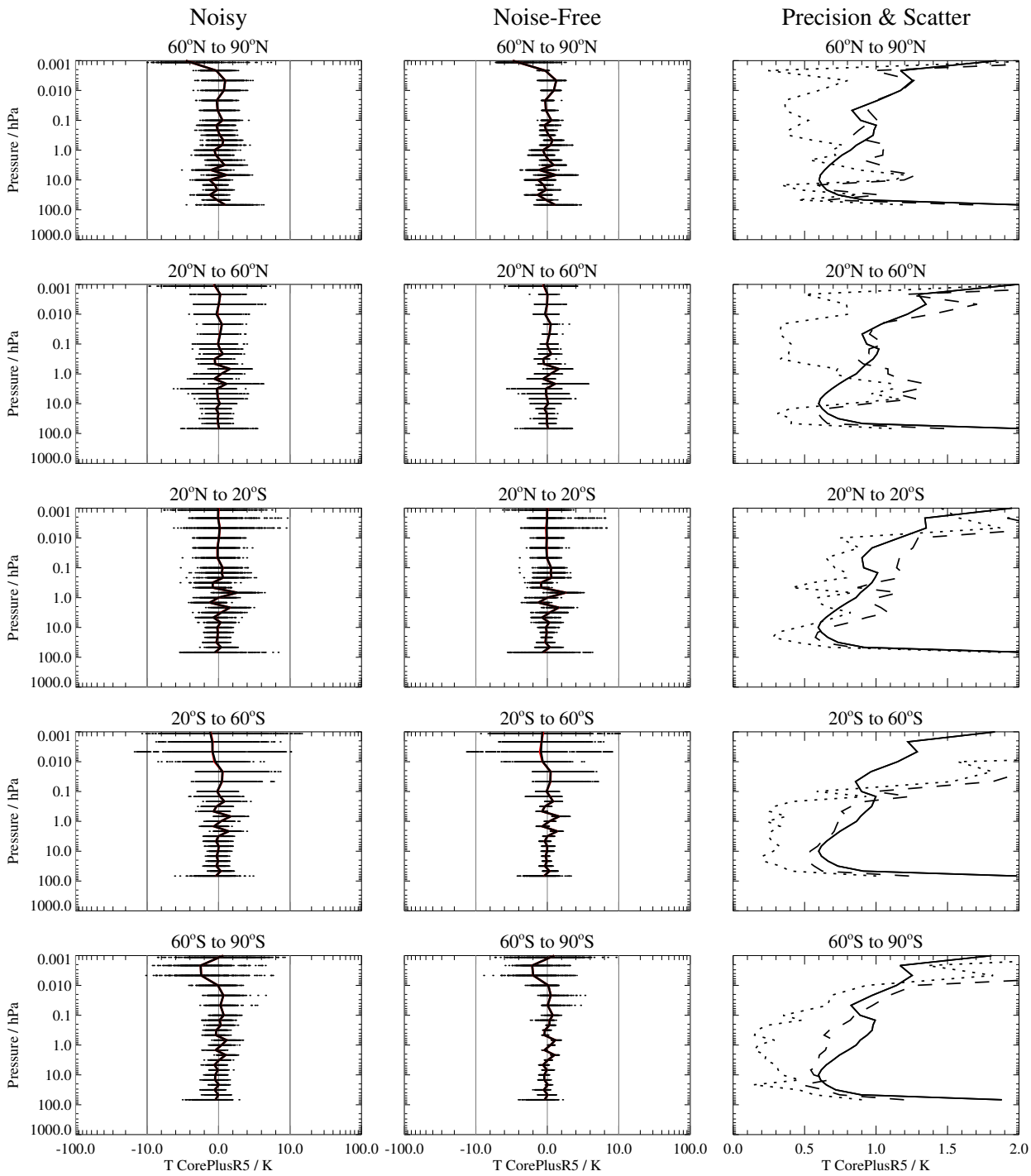

Figure A.47: A summary of the v1.5 data quality for Core+R5 Temperature for the `1996d051` test data set. Each row of panels represents a broad latitude bin. The first two columns show the differences between the retrieved Core+R5 Temperature and the true Temperature as a function of pressure, for the noisy and noise free case, along with a solid line which shows the median bias. The median bias of the `Status=0` profiles (i.e., those not significantly affected by clouds) is shown in red. The third column shows the mean estimated precision of Core+R5 Temperature (solid line), and the rms scatter about the mean bias in the noisy (broken line) and noise free (dotted line) cases.

T

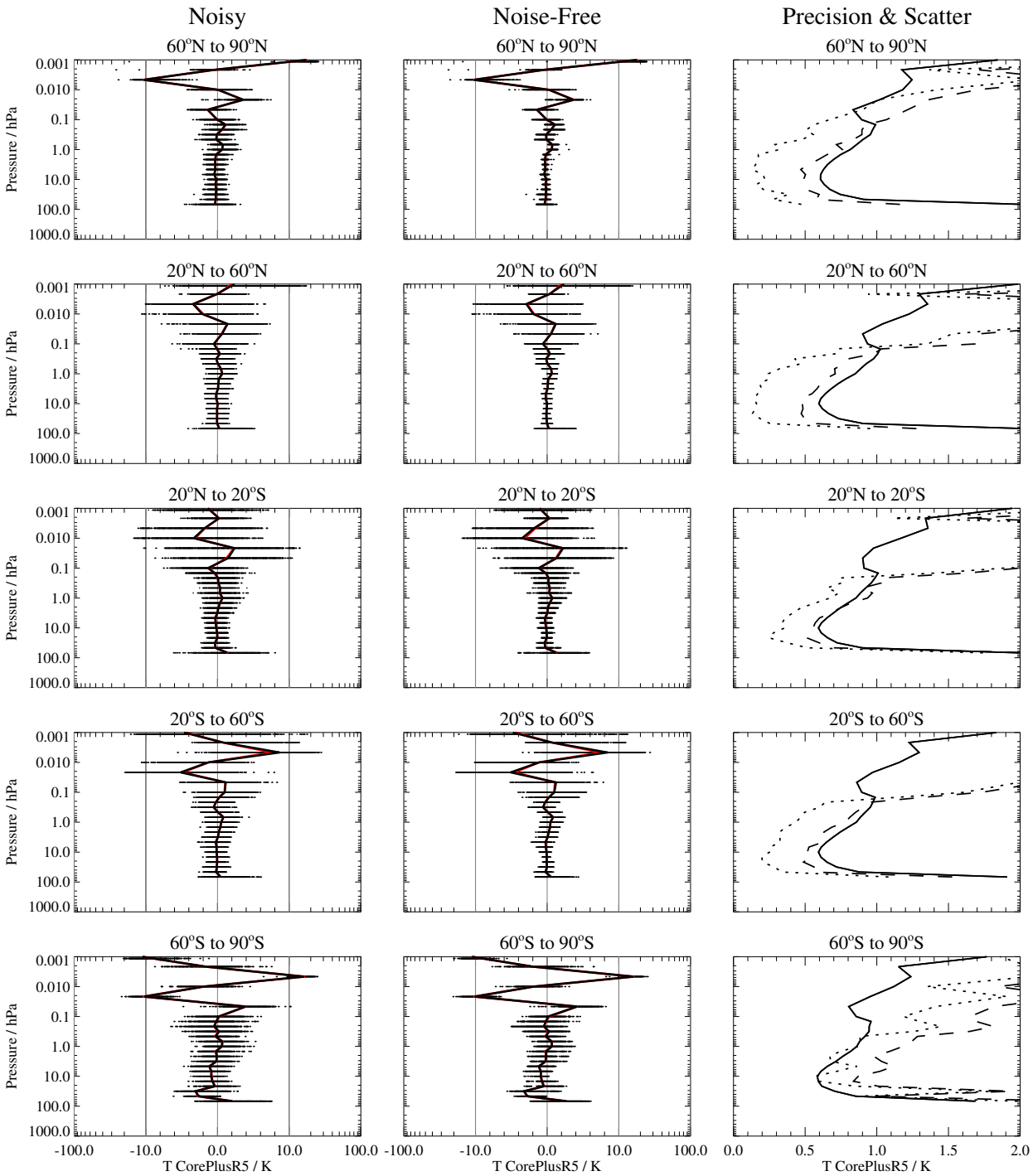

Figure A.48: A summary of the v1.3 data quality for Core+R5 Temperature, as for figure A.47 but for the `2000d276` test data set.

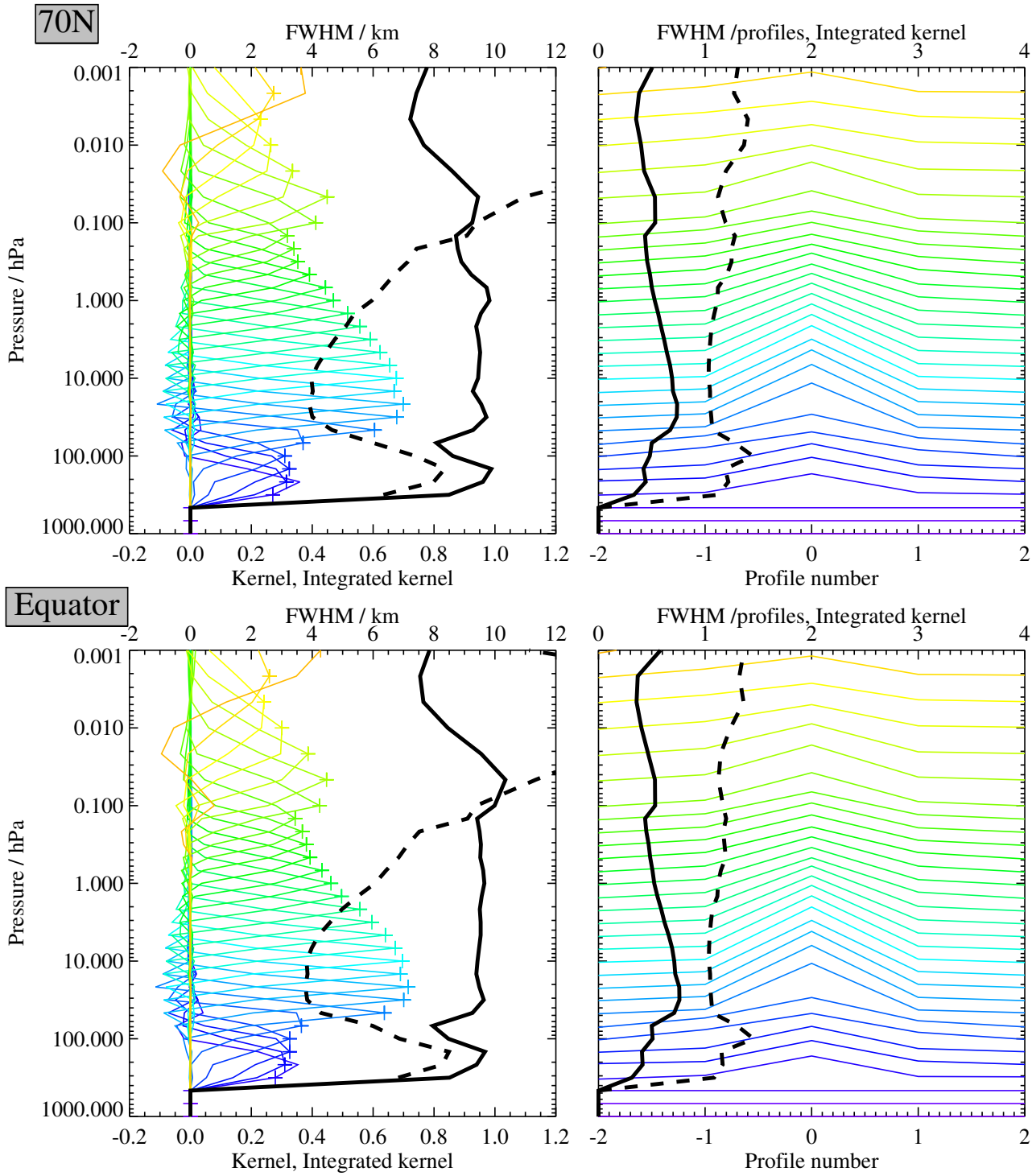

Figure A.49: The left hand plots show the vertical averaging kernel for Core Temperature for the `1996d051` test data set. The colored lines denote the averaging kernels for individual retrieved surfaces (denoted with the matching color + symbols). The thick solid black line shows the integrated area under each colored line. The thick dashed black line denotes the vertical resolution (full width at half maximum) approximately scaled into kilometers. The right hand plots show the horizontal averaging kernels in a similar manner, where the profiles are spaced at 1.5° great circle angle (approximately 165 km).

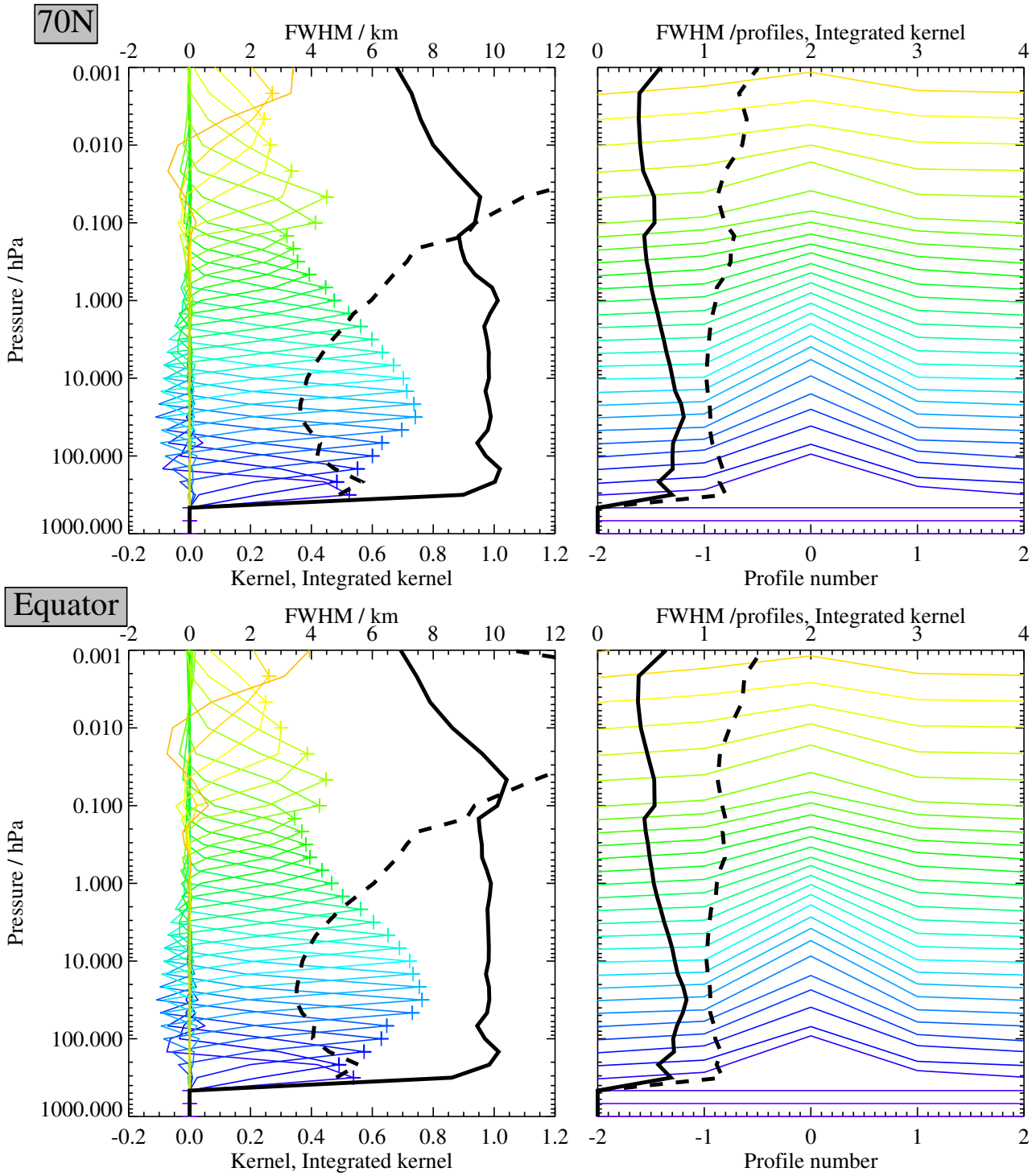

Figure A.50: The left hand plots show the vertical averaging kernel for Core+R2A Temperature for the `1996d051` test data set. The colored lines denote the averaging kernels for individual retrieved surfaces (denoted with the matching color + symbols). The thick solid black line shows the integrated area under each colored line. The thick dashed black line denotes the vertical resolution (full width at half maximum) approximately scaled into kilometers. The right hand plots show the horizontal averaging kernels in a similar manner, where the profiles are spaced at 1.5° great circle angle (approximately 165 km).

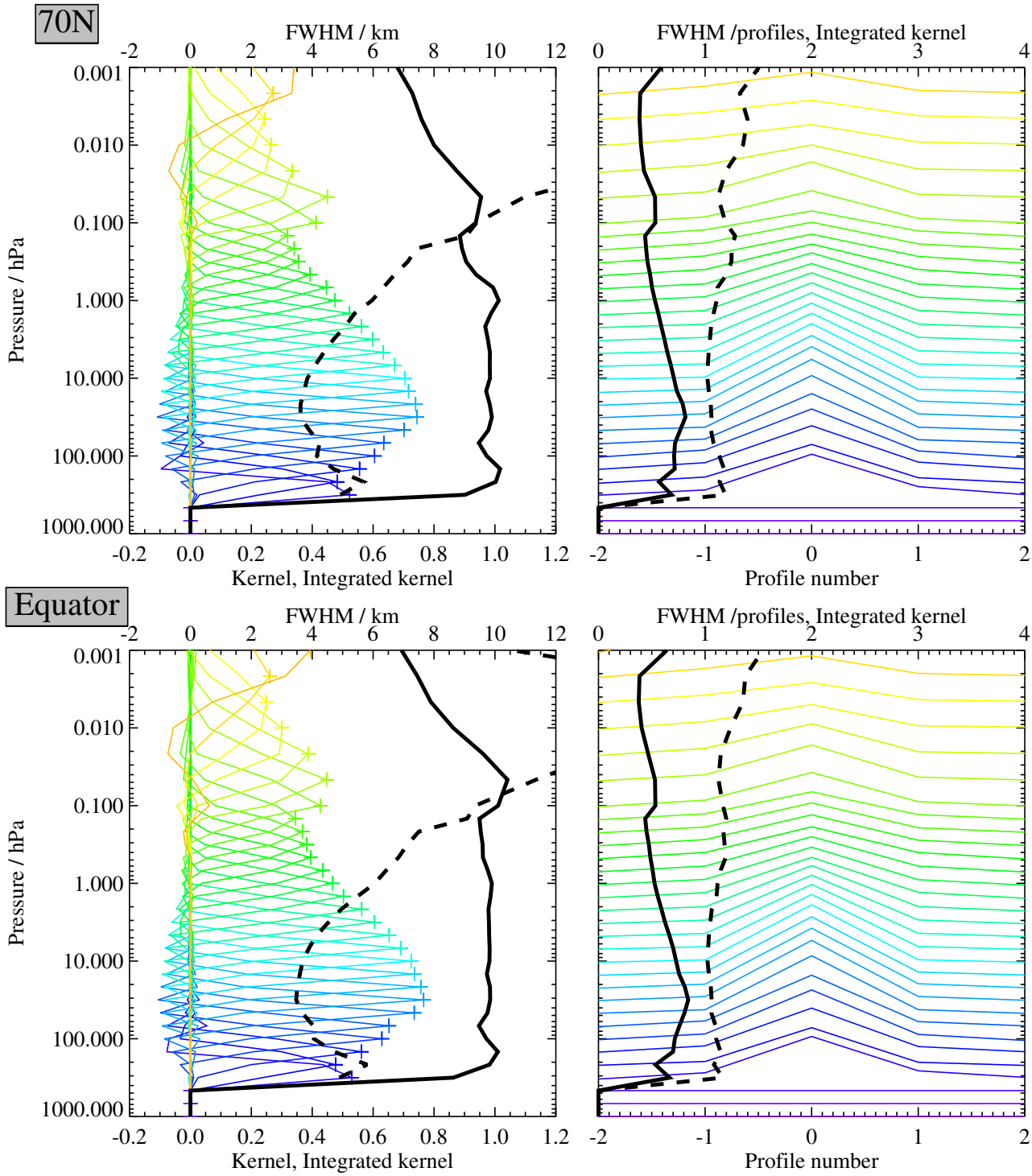

Figure A.51: The left hand plots show the vertical averaging kernel for Core+R2B Temperature for the `1996d051` test data set. The colored lines denote the averaging kernels for individual retrieved surfaces (denoted with the matching color + symbols). The thick solid black line shows the integrated area under each colored line. The thick dashed black line denotes the vertical resolution (full width at half maximum) approximately scaled into kilometers. The right hand plots show the horizontal averaging kernels in a similar manner, where the profiles are spaced at 1.5° great circle angle (approximately 165 km).

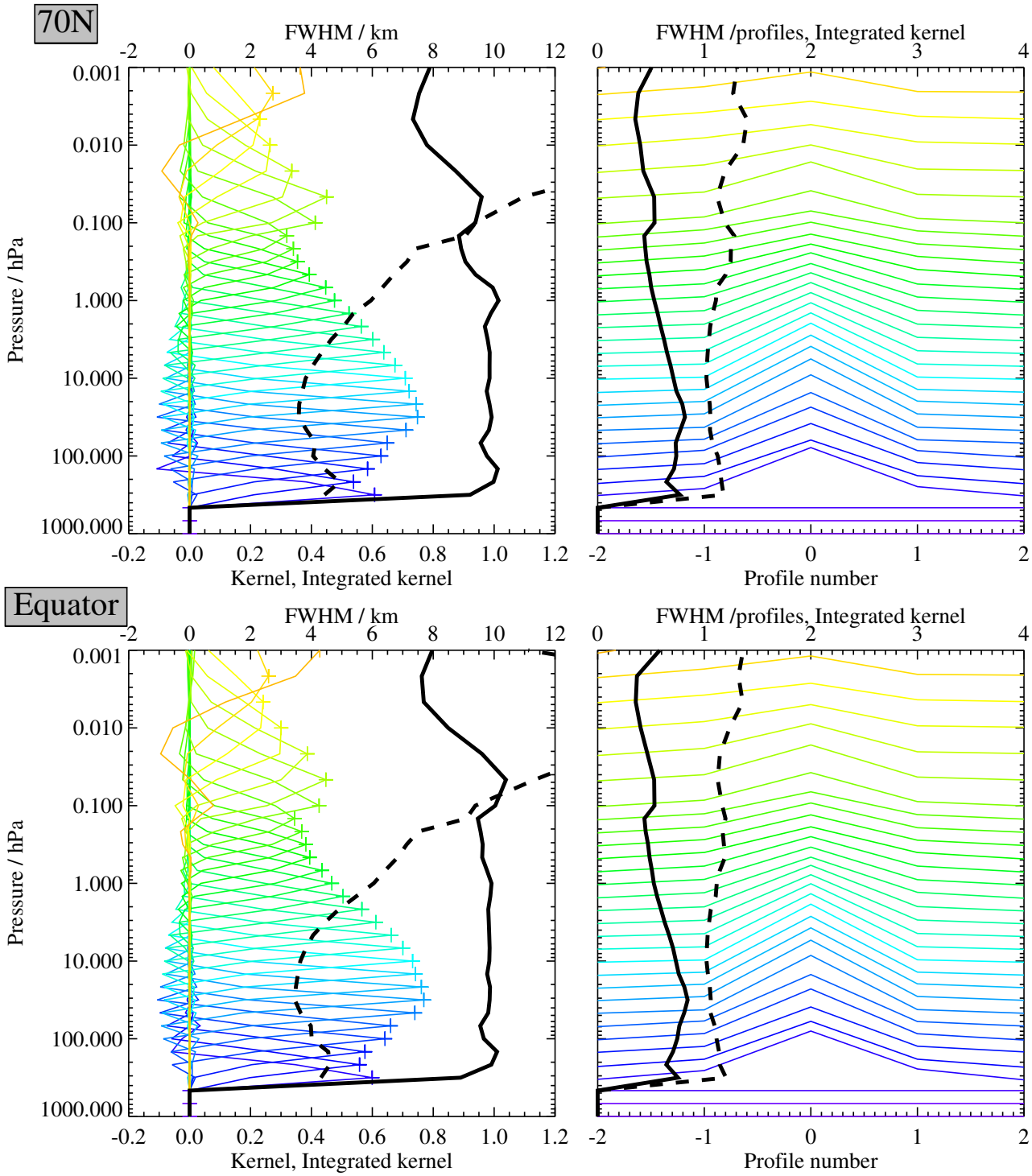

Figure A.52: The left hand plots show the vertical averaging kernel for Core+R3 Temperature for the `1996d051` test data set. The colored lines denote the averaging kernels for individual retrieved surfaces (denoted with the matching color + symbols). The thick solid black line shows the integrated area under each colored line. The thick dashed black line denotes the vertical resolution (full width at half maximum) approximately scaled into kilometers. The right hand plots show the horizontal averaging kernels in a similar manner, where the profiles are spaced at 1.5° great circle angle (approximately 165 km).

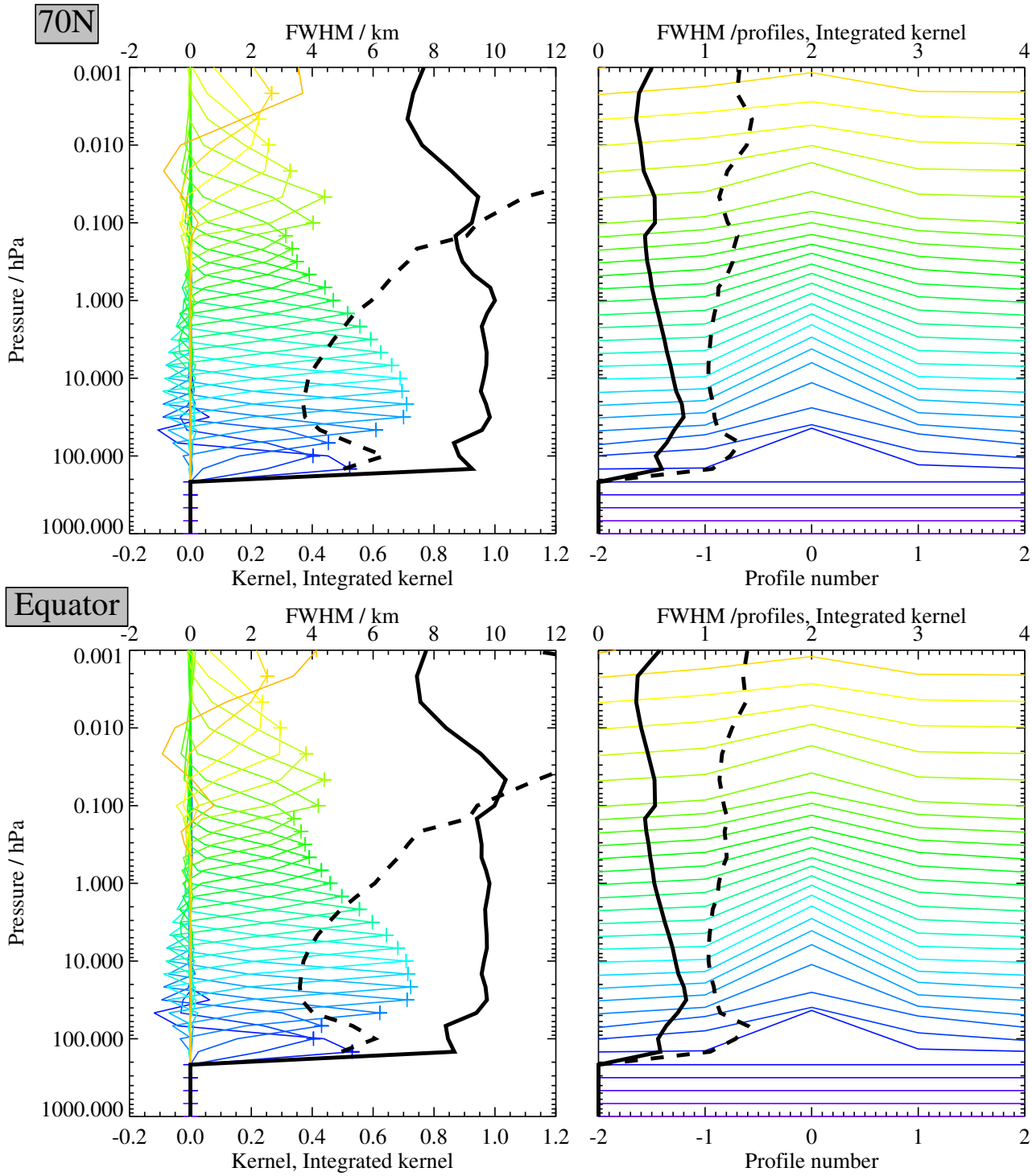

Figure A.53: The left hand plots show the vertical averaging kernel for Core+R4A Temperature for the `1996d051` test data set. The colored lines denote the averaging kernels for individual retrieved surfaces (denoted with the matching color + symbols). The thick solid black line shows the integrated area under each colored line. The thick dashed black line denotes the vertical resolution (full width at half maximum) approximately scaled into kilometers. The right hand plots show the horizontal averaging kernels in a similar manner, where the profiles are spaced at 1.5° great circle angle (approximately 165 km).

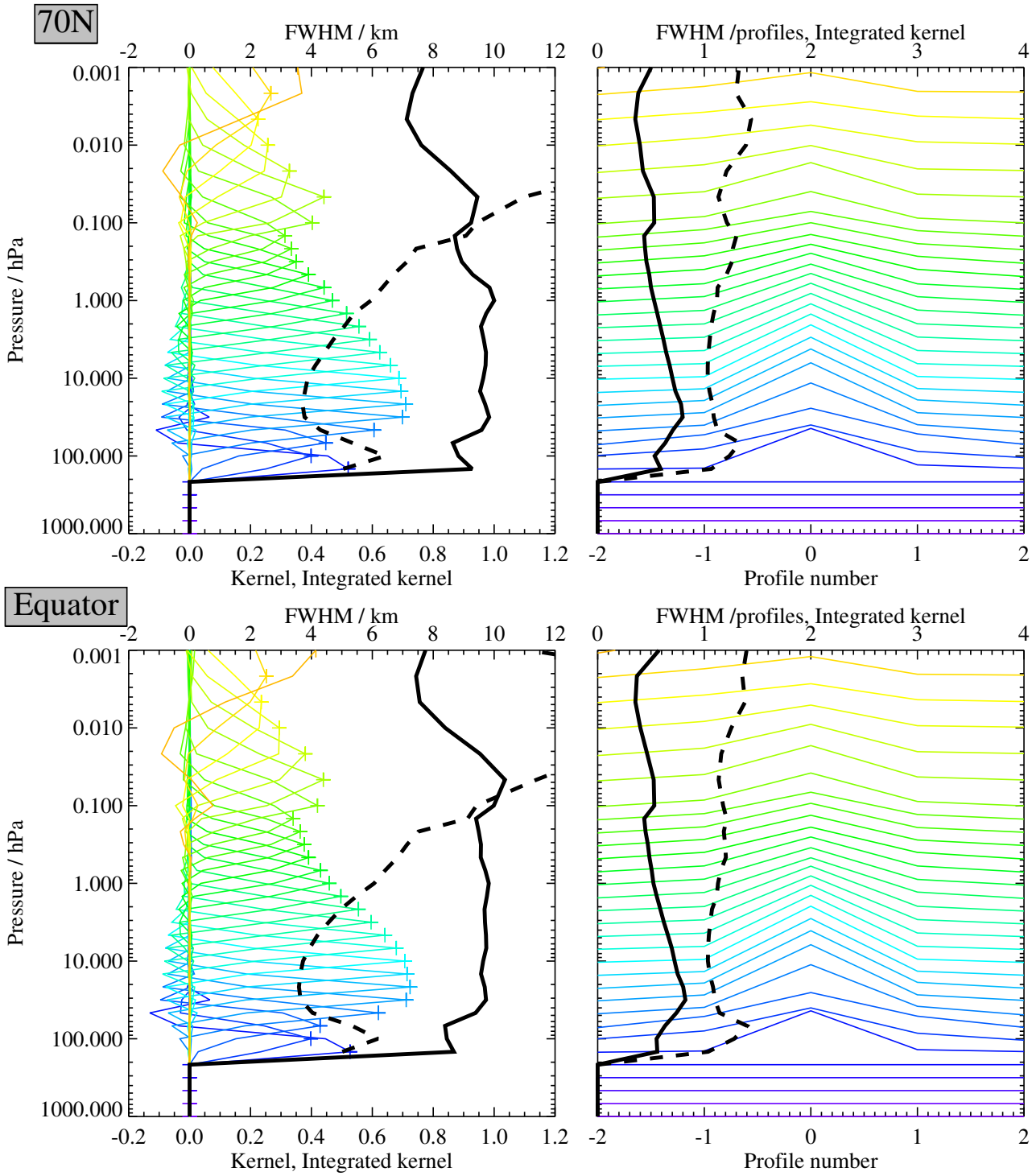

Figure A.54: The left hand plots show the vertical averaging kernel for Core+R4B Temperature for the `1996d051` test data set. The colored lines denote the averaging kernels for individual retrieved surfaces (denoted with the matching color + symbols). The thick solid black line shows the integrated area under each colored line. The thick dashed black line denotes the vertical resolution (full width at half maximum) approximately scaled into kilometers. The right hand plots show the horizontal averaging kernels in a similar manner, where the profiles are spaced at 1.5° great circle angle (approximately 165 km).

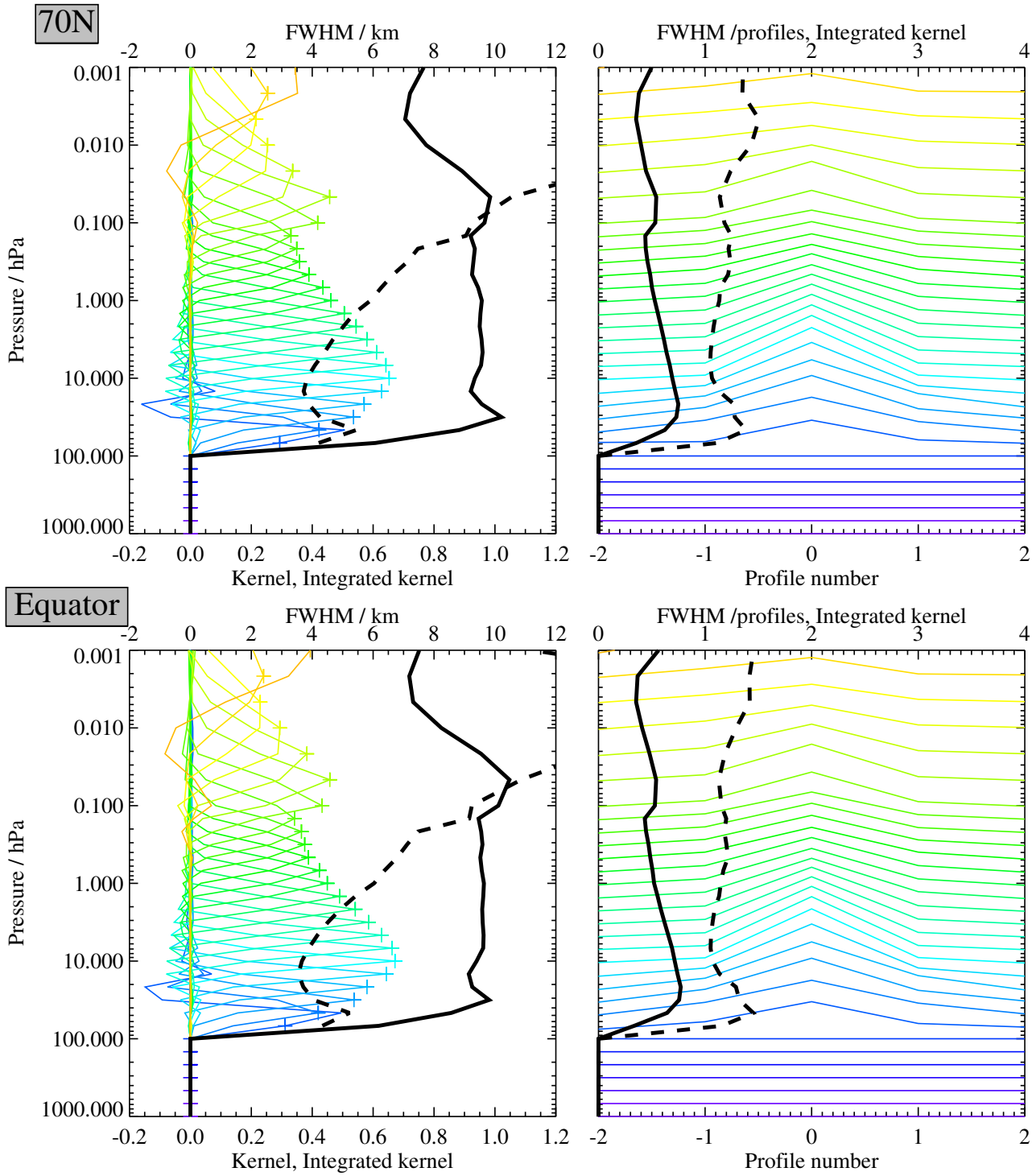

Figure A.55: The left hand plots show the vertical averaging kernel for Core+R5 Temperature for the `1996d051` test data set. The colored lines denote the averaging kernels for individual retrieved surfaces (denoted with the matching color + symbols). The thick solid black line shows the integrated area under each colored line. The thick dashed black line denotes the vertical resolution (full width at half maximum) approximately scaled into kilometers. The right hand plots show the horizontal averaging kernels in a similar manner, where the profiles are spaced at 1.5° great circle angle (approximately 165 km).

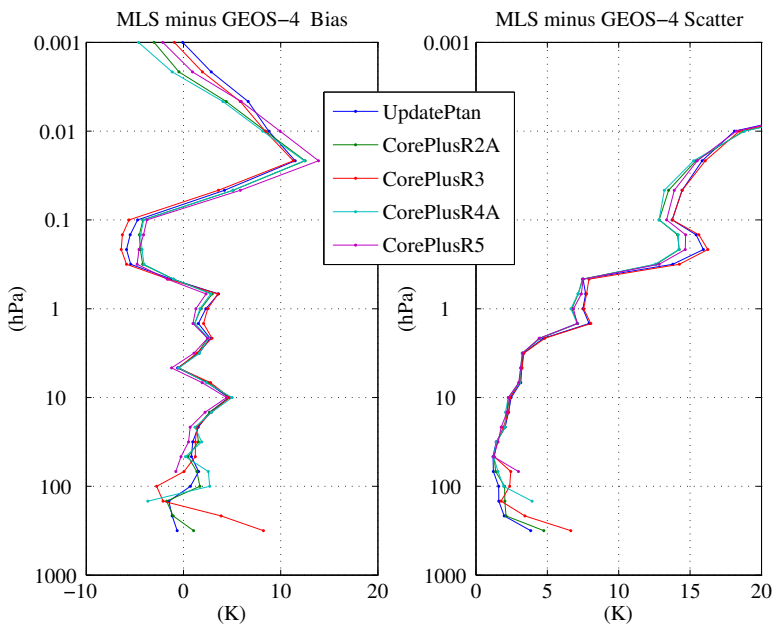

Figure A.56: Mean biases of five temperature phases relative to GEOS-4 for a typical day are shown in the left panel. In all phases, a warm bias in the MLS relative GEOS-4 of 1 – 2 K is evident in the stratosphere and there is a vertical oscillation near 10 hPa. A vertical oscillation at the 100 hPa level and lower is particularly apparent in Core+R3 temperature, and to a lesser extent in the other phases. This oscillation in Core+R3 is also apparent in the increased scatter shown in the right panel.